

Template/Pro forma for Submission

NMHS-Himalayan Institutional Project Grant
NMHS-FINAL TECHNICAL REPORT (FTR)
 Demand-Driven Action Research and Demonstrations

NMHS Grant Ref. No.:	GBPI/NMHS-2019-20/MG
-----------------------------	----------------------

Date of Submission:	3	1	0	7	2	0	2	3
	d	d	m	m	y	y	y	y

PROJECT TITLE (IN CAPITAL)

**PINE-OAK SYSTEM OF HIMALAYA: WATER CLIMATE
AND PLANT BIODIVERSITY**

Project Duration: *from* (30.09.2019) *to* (31.03.2023).

Submitted to:

Er. Kireet Kumar
 Scientist 'G' and Nodal Officer, NMHS-PMU
 National Mission on Himalayan Studies, GBP NIHE HQs
 Ministry of Environment, Forest & Climate Change (MoEF&CC), New Delhi
 E-mail: nmhspmu2016@gmail.com; kireet@gbpihed.nic.in; kodali.rk@gov.in

Submitted by:

[*Dr. Sandipan Mukherjee, Sc-D*]
 [Head: *Ladakh Regional Centre, G B Pant National Institute of Himalayan*]
 [Contact No.: +91-8859149537]
 [E-mail: *sandipan@gbpihed.nic.in*]

GENERAL INSTRUCTIONS:

1. The Final Technical Report (FTR) has to commence from the start date of the Project (as mentioned in the Sanction Order issued by NMHS-PMU) till completion of the project duration. Each detail has to comply with the NMHS Sanction Order.
2. The FTR should be neatly typed (in Arial with font size 11 with 1.5 spacing between the lines) with all details as per the enclosed format for direct reproduction by photo-offset printing. Colored Photographs (high resolution photographs), tables and graphs should be accommodated within the report or annexed with captions. Sketches and diagrammatic illustrations may also be given detailing about the step-by-step methodology adopted for technology development/ transfer and/ or dissemination. Any correction or rewriting should be avoided. Please provide all information under each head in serial order.
3. Any supporting materials like Training/ Capacity Building Manuals (with detailed contents about training programme, technical details and techniques involved) or any such display material related to project activities along with slides, charts, photographs should be brought at the venue of the Annual Monitoring & Evaluation (M&E) Workshop and submitted to the NMHS-PMU, GBP NIHE HQs, Kosi-Katarmal, Almora 263643, Uttarakhand. In all Knowledge Products, the Grant/ Fund support of the NMHS should be duly acknowledged.
4. The FTR Format is in sync with many other essential requirements and norms desired by the Govt. of India time-to-time, so each section of the NMHS-FTR needs to be duly filled by the proponent and verified by the Head of the Lead Implementing Organization/ Institution/ University.
5. Five (5) hard-bound copies of the Project Final Technical Report (FTR) and a soft copy of the same should be submitted to the **Nodal Officer, NMHS-PMU, GBP NIHE HQs, Kosi-Katarmal, Almora, Uttarakhand.**

The FTR is to be submitted into following two (02) parts:

Part A – Project Summary Report

Part B –Detailed Project Report

In addition, the Financial and other necessary documents/certificates need to be submitted along with the Final Technical Report (FTR) as follows:

Annexure I	Consolidated and Audited Utilization Certificate (UC) & Statement of Expenditure (SE) , including the interest earned for the last Fiscal year and the duly filled GFR-19A (with year-wise break-up).
Annexure II	Consolidated Interest Earned Certificate
Annexure III	Consolidated Assets Certificate showing the cost of the equipment in Foreign/ Indian currency, Date of Purchase, etc. (with break-up as per the NMHS Sanction Order and year wise).
Annexure IV	List of all the equipment, assets and peripherals purchased through the NMHS grant with current status of use, including location of deployment.
Annexure V	Transfer of Equipment through Letter of Head of Institution/Department confirming the final status of equipment purchased under the Project.
Annexure VI	Details, Declaration and Refund of any Unspent Balance transferred through Real-Time Gross System (RTGS)/ PFMS in favor of NMHS GIA General

NMHS-Final Technical Report (FTR)

Demand-Driven Action Research Project

DSL: Date of Sanction Letter

3	0	0	9	2	0	1	9
d	d	m	m	y	y	y	y

DPC: Date of Project Completion

3	1	0	3	2	0	2	3
d	d	m	m	y	y	y	y

Part A: Project Summary Report

1. Project Description

i.	Project Grant Ref. No.:	NMHS/MG/64					
ii.	Project Category:	Small Grant		Medium Grant	✓	Large Grant	
iii.	Project Title:	Pine - Oak system: Interactions with water, climate and plant biodiversity					
iv.	Project Sites (IHR States/ UTs covered) <i>(Location Maps attached):</i>	Uttarakhand and Himachal Pradesh (Location maps are attached as Annexure –A)					
v.	Scale of Project Operation:	Local		Regional	✓	Pan-Himalayan	
vi.	Total Budget:2.49.... (in Cr), As sanctioned.					
vii.	Lead Agency:	G B Pant National Institute of Himalayan, Environment (GBP-NIHE), Kosi- Katarmal, Almora, Uttarakhand.263643					
	Lead PI/ Proponent:	Dr. Sandipan Mukherjee, Sc-D, NIHE					
	Co-PI/ Proponent:	Dr. K. C. Sekar, Sc-F, NIHE Dr. Subimal Ghosh, Professor, IIT Bombay Dr. Sumit Sen, Associate Professor, IIT Roorkee Dr. Krishna Kishore Osuri, Associate Professor, NIT Rourkela Er. Vaibhav Gosavi, Sc-C, NIHE					
viii.	Implementing Partners:	IIT Bombay; IIT Roorkee; NIT Rourkela					
	Key Persons (Contact Details, Ph. No., E-mail):	Dr. Sandipan Mukherjee, Sc-D Head: Ladkah Regional Centre, NIHE, Leh, UT. Mob: +91-8859149537 Email: sandipan@gbphied.nic.in					

2. Project Outcomes

2.1. Abstract/ Summary (not more than 250-300 words)

The Pine (*Pinus* Spp.) and Oak (*Quercus* Spp.) systems of central Himalayan are known to provide substantial ecosystem services to the people of hill and near plains. However, sub-daily to annual scale interactions of Pine and Oak ecosystems with microclimatic and environmental parameters are not investigated in detail. Since quantification of ecosystem responses to micro-climatic fluctuation is expected to be beneficial for sustainable management of plant biodiversity, a detail ecosystem level assessment of plant-water-and microclimatic interactions are carried out in this project. With this broad overarching aim, this study also verifies the conjecture that “Oak forests are having higher ecosystem services than the Pine forests and, Pine stands may systematically be replaced with Oak forests, and subsequently the paradigm of water, climate and biodiversity is expected to change significantly from its current state.” The conjecture was primarily tested over the Kosi watershed area (~1800 km²) of Uttarakhand and only biodiversity assessment was carried out in Sainj watershed area (~780 km²) of Himachal Pradesh. The primary plant species distribution assessment indicates that out of total surveyed area under Kosi and Sainj-watersheds, Oak covers around 240 and 08 km² area, whereas Pine occupies around 750 and 44 km², respectively. In terms of ecosystem carbon exchange, both Pine (*P. roxburghii*) and Oak (*Q. leucotrichophora*) dominated ecosystems were found to be a sink of carbon (600-1000 gC/m² for Pine and 500-800 gC/m² for Oak). We have also identified a rainfall amount threshold for Pine and Oak-dominated ecosystems (10 ± 0.7 and 17 ± 1.2 mm, respectively) that resulted in highest ecosystem carbon assimilation in monsoon. Diurnal pattern of sap flux density of *P. roxburghii*, *Q. leucotrichophora*, and *Q. glauca* trees are calculated along with emphasis on Pine and Oak seasonal pattern of sap flux densities. The initial results indicated *P. roxburghii* has almost 1.5-2.0 times the sap flux densities than the other two *Quercus* species indicating higher water extraction by the *P. roxburghii* stands. When information network theory was used to identify micro-met controls effecting ecosystem carbon assimilation, we find that *P. roxburghii* dominated ecosystem is heat dominating while *Q. leucotrichophora* dominated ecosystem is moisture dominating at sub-daily scale. When plot scale water budget was estimated for *P. roxburghii* and *Q. leucotrichophora* dominated ecosystems, for an annual rainfall of 972 mm over Pine, the canopy interception loss is noted to be 199.9 mm whereas for a same amount rainfall over Oak, the interception loss was 182.9 mm indicating almost same interception loss. The surface runoff characteristics of Pine plots indicated runoff under Pine stands is primarily due to lateral subsurface flows whereas due to higher water holding capacity, runoff under Oak is primarily due to infiltration excess. Moreover, numerical simulations of land surface conditions using Noah-MP model for needle leaf trees over the Kosi-watershed could produce better land surface processes close to observations. The overall inference of this study indicates that *P. roxburghii* dominated ecosystems are better sink of carbon at the cost of higher loss of surface and ground water, consequently, *Q. leucotrichophora* dominated ecosystems are better for soil and water conservation as envisaged by the traditional knowledge.

2.2. Objective-wise Major Achievements

S#	Objectives	Major achievements (<i>in bullets points</i>)
1.	Assessment of Pine and Oak forest distribution under a warmer climate over Himalaya	<ul style="list-style-type: none"> • A thorough assessment of plant diversity over Kosi-watershed area is completed. • Similarly, plant diversity over Sainj watershed area is also completed. Method used and results are presented in Part-B. • In addition, identification of the species collected during field survey is also completed. Details are provided in Annexure-B. • Ecological integrity assessment is under process.
2.	Assessment of hydrological budget of Pine-Oak dominated watersheds and future scenarios under a warmer climate	<ul style="list-style-type: none"> • A thorough quantification of water yield of Pine and Oak ecosystem is completed. • Alongside, rainfall partitioning into throughfall and stemflow is also quantified to estimate interception loss from both Pine and Oak dominated micro-watershed. • In order to quantify the contributions of different LULCs to runoff generation in the upper Kosi River catchment, SWAT model is used to simulate the runoff in different sub-catchments. • Surface run-off, infiltration and leachate characteristics of Pine and Oak dominated micro-watersheds are compared using storm event based measurements. Associated methodologies and results are presented in Part-B. • Field survey for spring geo-tagging and instantaneous discharge measurement is completed at the Oak Forest Site (Shitlakheth). A total of 18 springs are geo-tagged. Details are provided in Annexure-C.

3.	<p>Assessment of microclimate variability of Pine-Oak dominated forests and future changes under a warmer climate and its societal implications.</p> <p>3.1. Comparison of Pine and Oak ecosystem exchange and transpiration using sap flow observations under limiting meteorological conditions for two sites of watersheds.</p> <p>3.2. Regional scale climate modeling for IHR including three sites of two watersheds including high resolution data assimilation.</p>	<ul style="list-style-type: none"> • A detailed comparison of daily to seasonal scale ecosystem fluxes is accomplished. Impact of different micro-meteorological parameters on net ecosystem carbon exchange is also identified on daily scale for Pine and Oak. • Impact of varying rainfall spells and amount on ecosystem carbon exchanges of Pine and Oak is also quantified. • Further, a Vegetation Photosynthesis and Respiration (VPRM) model is simulated during the period of 2011–2020 for Pine dominated ecosystem and calibrated with field observations. • Apart from the ecosystem carbon exchange measurement, a detailed assessment of stand level transpiration of <i>P. roxburghii</i>, <i>Q. leucotrichophora</i>, and <i>Q. glauca</i> trees is also completed. Furthermore, relationship between soil CO₂ efflux with varying rainfall spell and amount is also established for Pine and Oak dominated sites. Methodologies used and results are presented in Part-B. • Numerical simulations of land surface conditions using Noah-MP model for needle leaf trees over the Kosi-watershed could produce better land surface processes close to observations for the duration of 2011-2021. Detailed results are provided in Part-B.
4.	<p>Assessment of eco-hydro-climatological processes with information theory-based process network and understanding resilience under shock.</p>	<ul style="list-style-type: none"> • The networks of eco-hydro-meteorological variables obtained from in-situ flux tower observations of Pine and Oak dominated ecosystems are developed using the information theory-based Temporal Information Partitioning Network (TIPNet) approach. • The micro-meteorological drivers affecting carbon uptake of Oak and Pine ecosystems of the Himalayas with half-hour temporal resolution flux tower data are also identified. Detailed results are provided in Part-B.

Note: Further details may be summarized in DPR Part-B, Section-5. Supporting materials may be enclosed as annexure/ appendix separately to the FTR.

2.3. Outputs in terms of Quantifiable Deliverables*

S#	Quantifiable Deliverables*	Monitoring Indicators*	Quantified Output/ Outcome achieved	Deviations, if any, & Remarks thereof:
	<p>Assessment reports on Pine and Oak transpiration rates of Himalaya linking with water balance and recharge of ground water/springs (3 representative sites)</p>	<p>Database on Pine and Oak transpiration rates (Nos.)</p>	<p>Transpiration data for Pine (Particularly, <i>Pinus roxburghii</i>) and 2 Oak species (Particularly, <i>Quercus leucotrichophora</i> and <i>Quercus glauca</i>) is available from Nov, 2020 to 31st, March, 2023.</p>	<p>A manuscript on comparative estimates of transpiration and their links with micro-met parameters is under preparation.</p>

	New hydro-meteorological database of two (02) watersheds in three (03) IHR States in GIS format;	Hydro-meteorological database (No.) Number of spring Geo-tagged (nos.)	<ul style="list-style-type: none"> • 10 Hz carbon and water flux data is available for the duration of 1-Jan-2014 to dec, 2022 for Pine dominated forest. • 10 Hz carbon and water flux data is available for the duration of 22-April-2016 to till date for Oak dominated forest in Gangolihat, Pithoragarh, Uttarakhand with data gaps. • A total of 18 springs are geo-tagged at Shiltakhet region. 	Hydro-met watershed is developed for Kosi and Hat-Kalika watersheds.
	High-resolution land and climate model products (1970 - 2099);	Climate Model products (Nos.)	<ul style="list-style-type: none"> • Noah-MP, a new generation of LSM, simulations are generated for ST, SM, and energy fluxes and compared with the <i>in-situ</i> observations for 2011-2021. • High-resolution land data assimilation system (HRLDAS) derived land surface products, including SM and ST, are prepared, such data are not currently available for the Himalaya region. 	NA
	Technical reports on Ecological integrity of two dominant forests;		<ul style="list-style-type: none"> • Ecological integrity assessment for two dominant forest types is under progress. 	NA
	At least 08 Knowledge products: 04 quality research publications including journal articles, 02 book chapters, and 03 policy briefs.	Reports/Research articles/Policy documents prepared and published (Nos.)	<p>Journal articles:</p> <p>03-published; 02-submitted; 02- under preparation.</p> <p>Book chapters:</p> <p>01-published. 01- Conference abstract compendium.</p> <p>Conference publication:</p> <p>07 - National</p>	NA

			04 - International Policy briefs: Under preparation.
--	--	--	---

*As stated in the Sanction Letter issued by the NMHS-PMU.

2.4. Strategic Steps with respect to Outcomes (in bullets)

S#	Particulars	Number/ Brief Details	Remarks/ Attachment
1.	New Methodology/ Technology developed, <i>if any</i> :	<ul style="list-style-type: none"> 02-watersheds are investigated for current and future plant distribution 03-tree species investigated for sap flow / ET variability 02-Himalayan ecosystems investigated for soil CO₂ flux comparisons 02- Himalayan ecosystems investigated for surface run-off, leachate and infiltration characterization. 	NA
2.	New Ground Models/ Process/ Strategy developed, <i>if any</i> :	<ul style="list-style-type: none"> 02 ground models for measuring surface run-off from Pine and Oak dominated systems are established. 02 number of 1st order stream monitoring stations established over Pine and Oak dominated ecosystems. 	NA
3.	New Species identified, <i>if any</i> :	Nil	
4.	New Database established, <i>if any</i> :	4	-
5.	New Patent, <i>if any</i> :	Nil	-
	I. Filed (Indian/ International)	Nil	-
	II. Technology Transfer, <i>if any</i> :	Nil	-
6.	Others, <i>if any</i>	-	-

Note: Further details may be summarized in DPR Part-B, Section-5. Supporting materials may be enclosed as annexure/ appendix separately to the FTR.

3. New Data Generated over the Baseline Data

S#	New Data Details	Status of Existing Baseline	Addition and Utilisation New data
1.	Grid-wise (2 x 2 Km) vegetation and soil data produced for Kosi and Sainj watershed.	Pine-Oak distribution and dynamics over Himalayan region have been carried by targeting individual forest type (Singh and Singh, 1987). Moreover, soil dynamics have also been reported several times (Joshi et al., 1991, Pandey et al., 2018). However, stratified sampling using grid based approach is used for the first time in this study to assess plant diversity of Kosi and Sainj watersheds.	The baseline data on plant diversity and distribution over Kosi and Sainj watershed would work as primary database for further long-term monitoring and conservation of Oak forests under the climate change scenario.
2.	Sap flow derived transpiration data of Pine (<i>P. roxburghii</i>) and Oak (<i>Q. leucotrichophora</i> and <i>Q. glauca</i>)	Apart from the data generated from this project, no data is available on transpiration of Pine and Oak systems in India, as of now. However, a research was carried out in central Himalaya, Nepal where transpiration rate of <i>P. roxburghii</i> was reported (Ghimire et al., 2014).	Data on Pine-Oak stand level transpiration would work as baseline data to provide insights of water use pattern of Pine and Oak trees and are expected to highlight role of environmental conditions on governing the water cycles of Pine and Oak stands of Himalaya.
3.	Hydrological database (02 ground models for measuring surface run-off from Pine and Oak dominated systems are established; and 02 number of 1st order stream monitoring stations established over Pine and Oak dominated ecosystems of Uttarakhand)	Previous studies on natural forested watersheds are many, though these studies fail to provide much insight into hydrological processes (Negi 2002). However, a paired micro-watershed study between Oak-dominated and Pine-dominated forests in Central Himalayas reported the annual water yield of the Pine and Oak watershed (Kumar and Verma 1991). More recently, Qazi (2020) reported a micro-watershed study from a dense Oak watershed and a degraded Oak watershed. But studies comparing specific forest species (Pine and Oak) have not been replicated in recent decades. In this study, run-off plot experiments for understanding runoff generation mechanism and micro-watershed monitoring for hydrological assessment have been conducted in a paired micro watershed dominated by Pine and Oak forests of the upper Kosi river catchment in the Kumaon Himalayas in Uttarakhand.	The baseline data would be helpful in understanding of biophysical linkages between a warming climate and hydrologic regimes by development of a comprehensive data-based mechanistic water balance model. The study of eco-hydrological responses of two dominant land uses (Oak and Pine) would provide aid to decision making and devise state wide mitigation strategies towards soil, water and ecology conservation in the Indian Himalayan region.

4.	Soil efflux data (02-Himalayan ecosystems investigated for soil CO ₂ efflux comparisons in Uttarakhand)	Previous studies on soil efflux of Pine and Oak ecosystem are analysed individually. However, long term monitoring and comparison of ecosystem fluxes along with soil efflux are seldom evaluated for Pine and Oak ecosystem.	The generated data would be beneficial for predicting rate of CO ₂ emissions and sequestration of two contrasting forest type to suggest effective CO ₂ emissions reduction and mitigative measures under a rather warmer scenario.
-----------	--	---	---

Note: Further details may be summarized in DPR Part-B. Database files in the requisite formats (Excel) may be enclosed as annexure/ appendix separately to the soft copy of FTR.

4. Demonstrative Skill Development and Capacity Building/ Manpower Trained

S#	Type of Activities	Details with number	Activity Intended for	Participants/Trained			
				SC	ST	Women	Total
1.	Workshops	1. A webinar cum consultation meeting was organised with all PI/Co-PIs. The webinar was chaired by Prof. V.K. Gaur, Hon. Scientist, CSIR-4PI, Bengaluru.	The webinar was organised to provide information about the baseline data available and to discuss methodologies for implementation of the project.	-	-	02	12
		1. As a part of Azadi ka Amrit Mahotsav, a workshop entitled “Biosphere- atmosphere- extremely complex hydrosphere interaction. Status, challenges and way forward” was organised at GBP-NIHE in hybrid mode held on 14-Dec-2021.	The workshop was organized with the rationale that the topography along with heterogeneously distributed forests of Indian Himalayas results in non-linear interactions amongst biosphere – atmosphere – hydrosphere regimes which are further expected to change under a warmer climate.	-	-	05	35
2.	On-Field Trainings	1. A training cum demonstration programme was organised at GIS, Hawalbagh for school students on the occasion of world water day, 22 march, 2022.	The training was organised for on-field demonstration of augmented sensors for water budget estimation and transpiration calculation.	-	-	25	49
3.	Skill Development	NIL	-	-	-	-	
4.	Academic Supports	NIL	-	-	-	-	

Others (if any)	1. A lecture on “land-atmosphere interactions: An application to dynamic modelling” was delivered by Prof. Subimal Ghosh, IIT-Bombay, at GBP-NIHE on 20 th May, 2022.	To share the knowledge on land atmosphere interactions and to discuss how the stress from the global change have impacts on biosphere and affects the future trajectory using information theory based approach.	-	-	10	35
	1. A project end national conference entitled <i>Land-Atmosphere Interactions Controlling Weather & Climate: Applications of Numerical Models and Observations (LAI-2023)</i> was organized in NIT Rourkela during 9-12 January, 2023.	The conference was organised with the aim to bring together experts from various fields to discuss latest research and development in land-atmosphere interactions and their role in controlling weather and climate.			10	Total abstracts received - 70 Number of presentations - 61 Not participated - 9

Note: Further details may be summarized in DPR Part-B. Supporting materials may be enclosed as annexure/ appendix separately to the FTR.

5. Linkages with Regional & National Priorities (SDGs, INDC, etc.)/ Collaborations

S#	Linkages /collaborations	Detail of activities (No. of Events Held)*	No. of Beneficiaries
1.	Sustainable Development Goals (SDGs)/ Climate Change/INDC targets addressed	SDGs – 6 (Clean Water), 13 (Climate Action), and 15 (Life on Land) are addressed through 05 skill development and knowledge dissemination activities.	Total = 192
2.	Any other:	-	-

Note: Further details may be summarized in DPR Part-B, Section-6. Supporting materials may be enclosed as annexure/ appendix separately to the FTR.

6. Project Stakeholders/ Beneficiaries and Impacts

S#	Stakeholders	Support Activities	Impacts in terms of income generated/green skills built
1.	Line Agencies/ Gram Panchayats:	Shitlakhhet and Papoli Gram Panchayat, Almora, Uttarakhand	NA
2.	Govt Departments (Agriculture/ Forest/ Water):	Forest Department of Uttarakhand	NA
3.	Villagers/ Farmers:	-	-
4.	SC Community:	-	-

5.	ST Community:	-	-
6.	Women Group:	-	-
	Others, <i>if any</i> :	-	-

Note: Further details may be summarized in DPR Part-B, Section-6. Supporting materials may be enclosed as annexure/ appendix separately to the FTR.

7. Financial Summary (Cumulative)

The consolidated and audited Utilization Certificate (UC) and Year-wise Statement of Expenditure (SE) attached as **Annexure I**.

8. Major Equipment/ Peripherals Procured under the Project** (*if any*)

S#	Name of Equipment	Quantity	Cost (INR)	Utilisation of the Equipment after project
1.	Sap Flow Analyser (12) with accessories (GBPNIHE)	SF-L type sap flow analyser. (Ekomatic, Germany)	Rs. 25,34,414/- (with GST)	Three sap flow sensors installed in Pine trees at GBP-NIHE got destroyed in forest fire during 2022. Remaining 9 sap flow sensors would be dismantled from the sites and reinstalled in some other tree species.
2.	Soil CO ₂ analyser (02) (GBPNIHE)	EOS-FD, Eosense, Canada	Rs. 10,40,371.5/- (with GST)	Both the sensors would be reinstalled in some other location to estimate soil efflux of grassland.
3.	Plot Lysimeter setup Water Level Recorder: 0.5M and flume (IIT-R)	Local Fabricated with Xtream Capacitance Water Level Recorder	Rs. 1,81,200/- (without GST)	All the instruments installed for estimation of hydrological budget would be remained installed in Pine and Oak site till 2024 to provide support for Ph.D of Mr. Denzil Daniel.
4.	Two river/stream gauging with depth, conductivity and temperature sensors and accessories (IIT-R)	Local Fabricated with Odyssey sensors	Rs. 2,34,200/- (without GST)	
5.	Soil Moisture Sensors (6 sets of 3 sensors each.) with data loggers (IIT-R)	Acclima (TDR310H)	Rs. 9,45,000.00	
6.	Raingauge with logger (2) And PAR sensors(IIT-R)	Rainwise with Hobo pendant logger(Tipping bucket raingauge) and Apogee instruments (Quantum sensor)	Rs. 11,27,000/-	

7.	Throughfall collection system (troughs, supporting frames, tank)(10)(IIT-R)	Fabricated indigenously		
8.	Stemflow collection system (PVC collar, tubing, tank)(6) (IIT-R)	Fabricated indigenously		
9.	Field Laptop (IIT-R)	Lenovo(20RV (Lenovo Think Book 14-IML U))		
10.	One Laptop	Lenovo	Rs. 68500.00 /- (with GST)	Purchased at GBP-NIHE, Kosi-Katarmal Almora and Will be kept with PI.
11.	One PC (NIT-R)	--	Rs. 72,299/- (with GST)	Purchased at NIT, Rourkela for modelling and Will be kept with Co-PI.

Details should be provided in details (ref. **Annexure III & IV).

9. Quantification of Overall Project Progress

S. No.	Parameters	Total (Numeric)	Remarks/ Attachments/ Soft copies of documents
1.	IHR States/ UTs covered:	2	<i>Details are provided in Annexure-A.</i>
2.	Project Sites/ Field Stations Developed:	07	
3.	Scientific Manpower Developed (PhD/M.Sc./JRF/SRF/ RA):	05	
4.	Livelihood Options promoted	-	
5.	Technical/ Training Manuals prepared	02	01 – EC flux analysis manual 02- EC flux footprint analysis manual
6.	Processing Units established, if any	NA	NA
7.	No. of Species Collected, if any	110	<i>Detailed list is attached as Annexure-B.</i>
8.	No. of New Species identified, if any	NIL	NA
9.	New Database generated (Types):	4	<i>Under progress</i>
	Others (if any)	-	-

Note: Further details may be summarized in DPR Part-B. Supporting materials may be enclosed as annexure/ appendix separately to the FTR.

11. Knowledge Products and Publications:

S#	Publication/ Knowledge Products	Number		Total Impact Factor	Remarks/ Enclosures
		National	International		


S#	Publication/ Knowledge Products	Number		Total Impact Factor	Remarks/ Enclosures
		National	International		
1.	Journal – Research Articles/ Special Issue:	-	3- Published 2-submitted 2-under preparation	10.23 (Published)	<i>Copies of the manuscripts are attached as Annexure-D.</i>
2.	Book – Chapter(s)/ Monograph/ Contributed:	1- Conference abstract compendium	1-Book Chapter	-	<i>Copy of the book chapter is attached in Annexure-D.</i>
3.	Technical Reports:	01	NIL	-	Ecological Integrity Assessment under preparation
4.	Training Manual (Skill Development/ Capacity Building):	02	-	-	Under Preparation
5.	Papers presented in Conferences/Seminars:	7	4	-	
6.	Policy Drafts/Papers:	-	-	-	-
7.	Others, if any:		-	-	-

Note: Please append the list of KPs/ publications (with impact factor, DOI, and further details) with due Acknowledgement to NMHS. Supporting materials may be enclosed as annexure/ appendix separately to the FTR.

12. Recommendation on Utility of Project Findings, Replicability and Exit Strategy

Particulars	Recommendations
Utility of the Project Findings:	The initial findings of the project would be useful in providing scientific basis to the plantation and conservation strategies for Pine-Oak forests of central Himalaya.
Replicability of Project/ Way Forward:	The novel research insights would provide the baseline data to undertake qualitative/quantitative analyses of water-climate-biodiversity dynamics in the Central Himalayan Pine-Oak system. Furthermore, long term monitoring and conservations of identified Oak forests in near future would be useful in combating the climate change impact on carbon and water of the region.

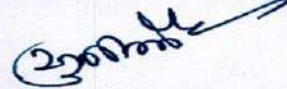
Exit Strategy:	Dissemination of the knowledge products (Research article and policy brief) generated from the project would be helpful in providing the scientific understanding on water use and carbon sequestration pattern of Himalayan Pine-Oak systems and their responses under changing climate scenario.
----------------	--


21/9/23

(PROJECT PROPONENT/ COORDINATOR)

(Signed and Stamped)

प्रमुख / Head
लद्दाख क्षेत्रीय केन्द्र / Ladakh Regional Centre
गो० ब० पंत राष्ट्रीय हिमालय पर्यावरण संस्थान
G.B. Pant National Institute of Himalayan Environment
लेह, लद्दाख (के०शा०ज०) / Leh, Ladakh (IT)



(HEAD OF THE INSTITUTION)

निदेशक / Director
(Signed and Stamped)
गो० ब० पंत राष्ट्रीय हिमालय पर्यावरण संस्थान
G.B. Pant National Institute of
Himalayan Environment (NIHE)
कोसी कटारमल, अल्मोड़ा-263643
Kosi Katarmal, Almora-263643

Place: ALMORA
Date: 26/07/2023

PART B: DETAILED PROJECT REPORT

The Detailed report should include an Executive Summary and it should have separate chapters on (i) **Introduction**, (ii) **Methodologies/Strategy/Approach**, (iii) **Key Findings and Results**, (iv) **Overall Achievements**, (v) **Project's Impacts in IHR** (vi) **Exit Strategy and Sustainability**, (vii) **References**, and (viii) **Acknowledgements** (acknowledging the financial grant from the NMHS, MoEF&CC, GoI).

Other necessary details/ Supporting Documents/ Dissemination Materials (*New Products/ Manuals/ Standard Operating Procedures (SOPs)/ Technology developed/Transferred, etc, if any*) may be attached as Appendix(ces).

1 INTRODUCTION

1.1 Background (max. 500 words)

The two dominant mid-elevation tree species of the central Himalaya are early succession, coniferous Chir-Pine (*Pinus roxburghii* Sarg.) and late succession, evergreen broad-leaf Oak (*Quercus Species*) which form pure and mixed forest patches. These two tree species are having difference in their anatomy and leaf structure (needle and broadleaf), provide substantial ecosystem services to the region and represent a significant forest cover with unique ecosystems (Joshi and Negi,2011). Having different characteristics and ecosystem services, *P. roxburghii* forests occur at elevations of 900-2200 m above mean sea level and naturally found on the driest and rockiest slopes, and has spread greatly under the influence of cutting and burning (Rawat et al,2011). On the other side, *Quercus* forests of central Himalaya are found between the elevations of 1000 - 3500 m above mean sea level (Rawat and Singh,1988). Oak forests are also important to the subsistence agricultural economy of the hill people (Singh and Singh,1987). In Uttarakhand state of India around 5.24% (1284 km²) of the total forest area is occupied by the Banj-Oak (Oak Spp.) (Dhyani and Dhyani,2016); whereas 16% is occupied by Chir-Pine (Pine Spp.) (Rawat et al, 2011). Since *P. roxburghii* and *Quercus* dominated ecosystems are highly responsive to micro-climate, particularly with respect to temperature and rainfall (Singh and Singh,1987), and the central Himalayan region is significantly experiencing climate and anthropogenic changes, quantification of physiological and ecosystem changes of these dominant forest types to microclimatic fluctuations are of paramount importance. Moreover, a comprehensive knowledge of these forest ecosystems functioning as a response to changes in the microclimate is necessary to frame forest adaptive measures and conservation policies.

1.2 Overview of the major issues addressed (max. 500 words)

Long-term changes in the air temperature and rainfall can be responsible for vegetation migration and changes in the phenology (Huntely,1991). Under the changing climate of western and central Himalayan region (Mukherjee et al, 2015, 2019; Mukherjee, 2021; Ballav et al, 2021), the forest ecosystems are also expected to respond heterogeneously, and it is now being reported that different vegetations of the Himalayan region are strongly responding to these climatic fluctuations and changes (Schickhoff et al,2016). Moreover, during the recent concentration of human settlements in the Oak forest area, lopping and felling, and occasional fire spreading from pine forest, and encroachment of Oak forests by Pine stands have reduced the area under Oak forest. However, the cause-effect relationships between interactions of climate-water and biodiversity changes are not quantified over central Himalaya. In addition to this, there is an increasing common perception that Pine stands may systematically be replaced with Oak forests, and subsequently the paradigm of water, climate and biodiversity is expected to change significantly from its current state. Therefore, a thorough assessment of differences in hydro-meteorological properties, hydrological budgets and ecosystem exchanges of carbon and water over these forests including their anticipated changes in a warmer climate are carried out.

1.3 Baseline Data and Project Scope (max. 500 words)

Very brief baseline information was available of the study area including Kosi basin in Kumaon region and Sainj watershed, H.P. (partly) developed through in-house and externally funded projects. Moreover, eddy covariance data of net ecosystem exchange of Pine and Oak dominated forests of Himalaya were available at GBPNIHE, Almora through NMSHE and other projects. Few background data on interactions between climate-water-biodiversity were already in the repository of the PI and Co-PIs of this project. The overarching aim of the project was to provide a comprehensive assessment of water-climate-biodiversity interactions of Pine and Oak dominated watershed over the Himalaya. This study was proposed to bring three different dimensions, climate-water-biodiversity, of Pine and Oak watersheds in to one frame and to quantify their interaction numerically. In view of the current unavailability of clear policy directives on plantation or selective lopping of pine and oak trees of Himalaya, such study is highly anticipated by researchers and policy makers

Therefore, this study would be expected to highlight science based recommendations on selected plantation of Pine and Oak patches over Himalaya.

1.4 Project Objectives and Target Deliverables (as per the NMHS-Sanction Order)

Project Objectives	Quantifiable Deliverables*	Monitoring Indicators*
Assessment of Pine and Oak forest distribution under a warmer climate over Himalaya	Assessment reports on Pine and Oak transpiration rates of Himalaya linking with water balance and recharge of ground water/springs (3 representative sites)	Database on Pine and Oak transpiration rates (Nos.)
Assessment of hydrological budget of Pine-Oak dominated watersheds and future scenarios under a warmer climate	New hydro-meteorological database of two (02) watersheds in three (03) IHR States in GIS format;	Hydro-meteorological database (No.)
Assessment of microclimate variability of Pine-Oak dominated forests and future changes under a warmer climate and its societal implications	High-resolution land and climate model products (1970 - 2099);	Number of spring Geo-tagged (nos.)
Assessment of eco-hydro-climatological processes with information theory based process network and understanding resilience under shock	Technical reports on Ecological integrity of two dominant forests;	Climate Model products (Nos.)
	At least 08 Knowledge products: 04 quality research publications including journal articles, 02 book chapters, and 03 policy briefs.	Reports/Research articles/Policy documents prepared and published (Nos.)

2 **METHODOLOGIES/STARTEGY/ APPROACH** – supporting documents to be attached.

2.1 **Methodologies used (max. 500 words)**

In order to address objective 1, grid-based approach was used for uniform sampling and documentation of plant diversity where the targeted watershed (Kosi and Sainj) was divided in to 10 x 10 km grids. Each grid was further sub-divided in to 2 x 2 km grids wherein 100 x 100 m quadrates laid down to sample biodiversity and soil parameters. The grid based approach used in this study is the first time implementation of this method to assess plant biodiversity of the Himalayan region. To address objective 2, plot scale run-off analysis was carried out to identify water yield of Pine and Oak micro-watersheds. Furthermore, in order to compare hydrological budget of a Pine and an Oak dominated micro-watershed, stemflow and throughfall have estimated for both the watershed. Apart from this, the roles of different LULCs to runoff generation in the upper Kosi River catchment was identified using SWAT model and simulated the runoff in different sub-catchments. Objective 3 was divided into two sub-objectives in which the first sub-objective was to Comparison of Pine and Oak ecosystem exchange and transpiration using sap flow observations under limiting meteorological conditions for two sites of a watershed. In order to estimate transpiration rate of Pine-Oak trees, sap flow based measurements were used where 6 sensors were installed in *P.roxburghii* trees, however, in case of Oak 3 sensors were installed in *Quercus leucotrichophora* whereas 3 sensors were installed in *Quercus glauca*. Subsequently, sapwood area of the identified species was estimated in order to calculate stand level transpiration. Similarly, the second part of this sub-objective was implemented by using daily scale ecosystem exchange data from the already established sites Pine and Oak system at Kosi and Gangolihat, Kali watershed under varying meteorological conditions. The second part of the objective 3 was regional scale climate modeling for IHR including three sites of two watersheds including high resolution data assimilation. Land Surface characteristics for three sites in the Himalaya were quantified based on uncoupled Noah-MP LSM. Subsequently, regional land surface conditions were developed using the High-Resolution Land Data Assimilation System over base Himalayan Uttarakhand region. The last objective was addressed using the information theory approach to investigate the hydro-meteorological controls affecting the carbon uptake variability of the Oak and Pine ecosystems of the Himalayas. The process networks are generated with the Temporal

Information Partitioning Network (TIPNet) framework proposed by Goodwell and Kumar (2017a,2017b). The carbon uptake potentials of the Oak and Pine ecosystems of the Himalayas and their linkages to micro-meteorological variables were assessed by generating process networks using half-hourly flux tower data considering the maximum memory of 06 hours. We considered the memory of 6 hours to account for the four different phases of the diurnal cycle.

Descriptive file

2.1.1. Assessment of Pine and Oak forest distribution under a warmer climate over Himalaya

The distribution of plant diversity (Angiosperms and Gymnosperms) in Kosi watershed studied and analysed on the basis of grid approach (Fig. 1a). In view of better coverage, we have prepared 10 x 10 km grid map (1000 Km²) of Kosi watershed which was divided into total 33 grids. Out of 33 grids, Almora region covers 21 grids with a total area of 1094.32 sq. km. and Nainital covers 12 grids with a total area of 773.68 km² (Fig.1b).

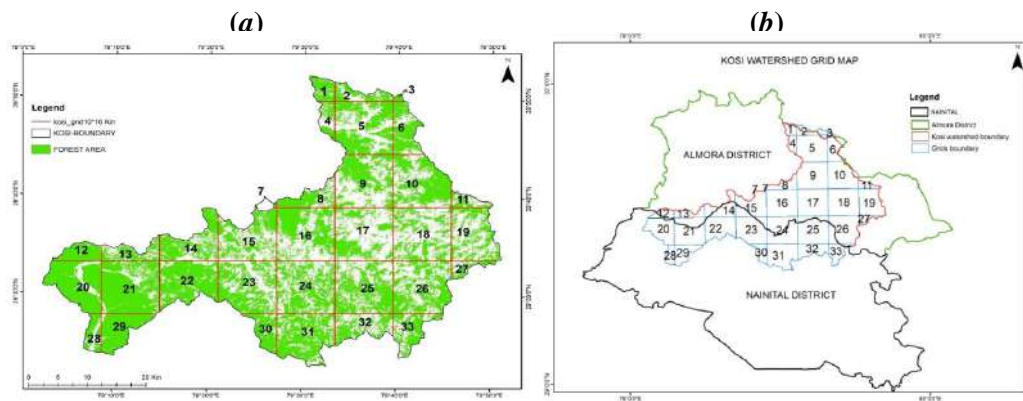


Fig. 1: Subplot (a) showing distribution of Kosi watershed into grids and subplot (b) area covered by Kosi watershed in Almora and Nainital District, respectively.

Each 10x10 km grid was divided into 2x2 km for refining the documentation on plant diversity and soil characteristics. Initially, the analysis was carried out for Almora district for which vegetation analysis, soil sample collection and analysis was done from centre point of each grid.

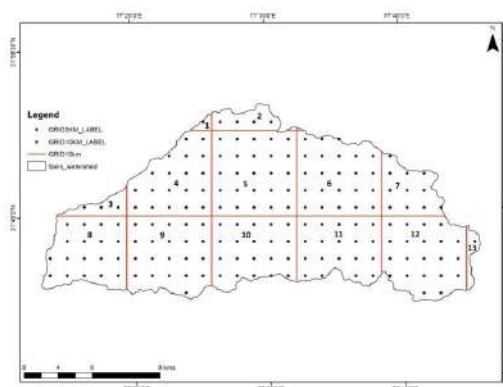


Fig. 2: Grid map of Sainj watershed for systematic diversity and distribution analysis.

Vegetation analysis: Systematic sampling method was used in order to document the vegetation analysis of Kosi and Sainj watershed area. Quadrates of different sizes were laid down for different life forms within different grids.

Quadrat size:

- **For Trees:** 10 x 10 m
- **For Shrubs:** 5x5 m
- **For Herbs :** 1x1 m

Thus, in each 2x2 km grid, a total of 4 sample plots of 10m×10m size for trees, 8 sample plots of 5m×5m for sapling and shrub and 20 sample plots of 1m×1m for seedling were laid systematically over different grids. For trees, the number of individuals and Circumference at Breast Height (CBH) was measured following standard ecological approaches. The total number of shrubs and herbs found in each quadrat were counted. The ecological characteristic, such as density, frequency, etc. were analysed as per Misra (1968), Shannon and Weaver (1963) and Muller-Dombois & Ellenberg (1974).

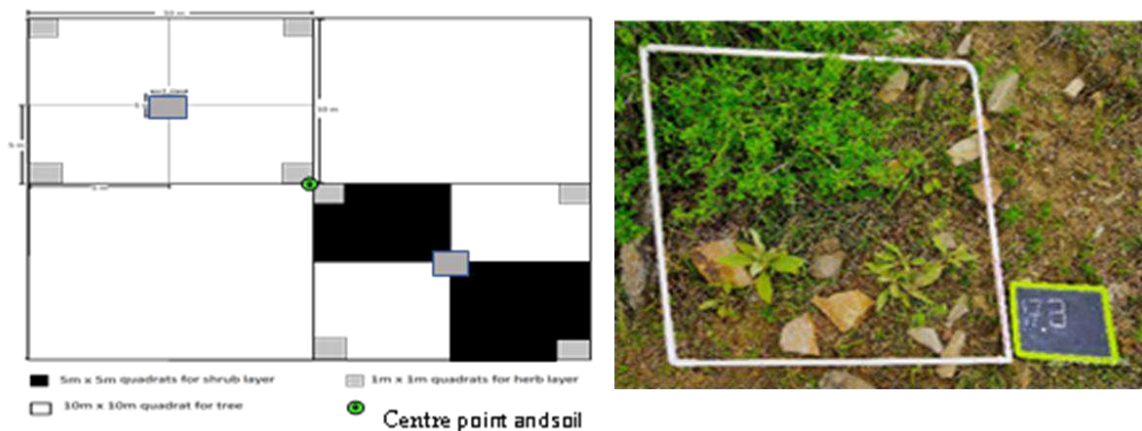


Fig. 3: Subplot (a) showing Quadrat design for 4 km Grid (2 x 2 km) and subplot (b) showing 1x1 m for herb vegetation

Analysis of data

Frequency, density, abundance and IVI of tree species was calculated based on the formulae (Sharma et al., 2013) given below-

Frequency: It refers to the degree of dispersion of individual species in an area and usually expressed in terms of percentage occurrence. It is calculated by equation:

$$\text{Frequency} = \frac{\text{No. of quadrats in which a spp. occurred}}{\text{Total number of quadrats studied}} \times 100$$

Density: It represents the number of individuals of the species in any unit area. It is expressed as the numerical strength of the species in the community.

$$\text{Density} = \frac{\text{Total no. of individuals of a spp. in all quadrats}}{\text{Total number of quadrats studied}}$$

Abundance: It represents the number of individuals of any species per sampling unit of occurrence. It is the ratio of the total number of individuals of species in all quadrats and the total number of quadrats in which species occurred.

$$\text{Abundance} = \frac{\text{Total no. of individuals of a spp. in all quadrats}}{\text{Total number of quadrats in which species occurred}}$$

Basal Area: Basal area refers to ground actually penetrated by the stems and is used to calculate dominance of tree species. It is considered as good indicator of size, volume, or weight of tree. It provides information on the proportion or dominance of larger and smaller tree in a community. It is one of the most important parameter in estimating the standard biomass in an area that in turn used as a measure of productivity. The basal area is calculated by using following formulae:

Basal Area = $(CBH)^2/4\pi$, Where, CBH is circumference at the breast height

Importance Value Index (IVI): Importance value index of a species in the community gives the idea of relative importance of the species as compared to other species. For calculating the importance value index of species, the absolute values recorded were converted to relative values. It thus incorporates following three parameters:

Relative Frequency: as the proportion of frequency of a species to the stand as a whole and calculated as:

$$\text{Relative Frequency} = \frac{\text{Frequency of the species}}{\text{Total Frequency of all the species}} \times 100$$

Relative Density: as the proportion of density of a species to the stand as a whole and calculated as:

$$\text{Relative Density} = \frac{\text{Density of the species}}{\text{Total Density of all the species}} \times 100$$

Relative Dominance: as the proportion of dominance of a species to the stand as a whole and calculated as:

$$\text{Relative Dominance} = \frac{\text{Basal area of the species}}{\text{Total Basal area of all the species}} \times 100$$

In calculating the importance value index, the percentage value of relative frequency, relative density, and relative dominance are summed together and this value is designated as importance value index or IVI of species (Curtis, 1959) which determines vegetation status and importance of component species within a stratum stand.

IVI = Relative density + Relative Frequency + Relative density

Soil collection and analysis: The soil sample was collected from 10-15 cm depth of soil in each centre point of 4 km² grid (2 x 2 km) of the study area. Total Nitrogen, Organic Carbon, Total Potassium, Total Phosphorus, Water Holding capacity, pH, porosity, etc. were analysed using standard procedure (Okalebo *et al.*, 2012; Osman, 2013) at Centre for land water and resource management (GBPNI Kosi- Katarmal).

Analysing Resource utilization pattern: The nearest village was selected for resource use survey in Pine-Oak dominated grid. Selection criteria of village depend upon the distance of the village from the grid and approachable grids. Questionnaire survey including basic information such as the total population of the village, total household information fuelwood collection trend annual fuelwood collection was obtained. About 50 % of total population of the village < 25 years was selected following random sampling method for the questionnaire survey. Different parameters such as the resource use patterns, annual mean collection, use value, Resource Use index of Pine and Oak grids were calculated basis of Samant *et al.* (2000).

Ecological integrity rating matrix of Kosi-watershed

Ecological integrity generally provides valuable information for assessing ecosystem conditions and management effectiveness, and is an important component of ecologically based monitoring. Ecological integrity assessment (EIA) is to provide a succinct assessment of the current status of the composition, structure, processes, and connectivity of a particular occurrence of an ecosystem type. Assessing the current ecological condition or integrity of an ecosystem requires developing measures of the structure, composition and function of an ecosystem as compared to reference or benchmark ecosystems operating within the bounds of natural or historic disturbance regimes (Lindenmayer and Franklin 2002, Young and Sanzone 2002).

Methodology: The ecological integrity assessment would be made for the Kosi-watershed using the method proposed by Faber-Langendoen et al. (2006) and Brown and Williams (2016). Particularly, level-I and level-II approach (i.e. Remote Assessment and Rapid Assessment) of ecological integrity assessment, as indicated by Brooks et al. (2004) would be considered.

Major ecological factors to be considered for the EIA would be

- a) Landscape (land use index, natural land cover)
- b) Vegetation (native, invasive, structure, regeneration)
- c) Hydrometeorology (water source, rainfall distribution)
- d) Soil

Finally, a rating matrix, indicating current status, would be generated for natural vegetations. Till now, grid-wise vegetation assessment indices have calculated for EIA. Additionally, various index such as species richness, species diversity, stem count, are also calculated for each 2x2 km grid area along with this soil parameters such as pH, Porosity, WHC, Organic Carbon, N, P, K.. Further, hydro-meteorological parameters for each grid needs to be extracted for module formulation.

2.1.2. Assessment of hydrological budget of Pine-Oak dominated watersheds and future scenarios under a warmer climate

The study area region belongs to the upper Kosi River catchment. It is mainly located in the Kumaon region of Uttarakhand, ranging from Longitude 29°22'38" N to 29°51'11" N and Latitude 79°18'17" E to 79°52'4" E. The elevation range lies between 194 to 2757 m. The total area of the upper Kosi River catchment comes to around 1469 km². In addition to satisfying other primary hydrological roles, it also provides water for drinking purposes for Almora. Two forest patches within two headwater watersheds, respectively, of the upper Kosi river catchment in the Kumaon Himalayas were instrumented for watershed scale water budget studies. The head watersheds, called Sithlakheth (91.2 hectares) and Papoli (90.8 hectares), have a mean elevation of 2015 m and 1470 m, a relief of 244 m and 254 m, and both having North aspects (Fig. 1). Stratified soil samples in both locations, 1 each per location have been sampled for textural analysis.

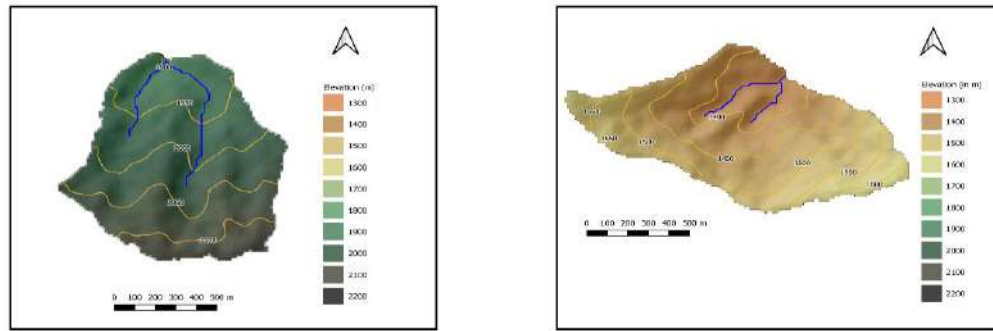


Fig. 1. Watershed boundary and DEM of (left) Sitlakheth and (right) Papoli watersheds. The blue line represents streams. Contour lines at 50m interval are also provided.

The watershed delineation was done on ALOS PALSAR Radiometric Terrain Corrected high-resolution (RT1) product of pixel size 12.5m. The DEM was processed using SAGA 7.8.2 and maps were produced using free and open source QGIS 3.16. During field survey conducted in 2021, Sitlakheth was identified as an Oak dominated watershed with two dominant Oak species – *Quercus leucotrichophora* (common name Banj Oak) and *Quercus glauca*. The Papoli watershed was identified as a Pine dominated watershed with Pine stands of *Pinus roxburghii*. LULC maps for both watersheds were generated using supervised classification on 10 m resolution Sentinel-2 (S2 Multispectral Instrument) images. Level-2A orthorectified atmospherically corrected surface reflectance images from 31-October-2021 to 30-April-2022 were organized according to cloudy pixel percentage, and the image for 01-April-2022 was selected for LULC classification. Based on knowledge gained from field visits, sample regions were identified for supervised classification into 5 classes – forest, agricultural, barren, settlement and water bodies. The supervised classification was done using the Random Forest classifier on Google Earth Engine (Gorelick 2017). Based on the LULC classification (Fig. 3), Sitlakheth has 57.6 % forest cover while Papoli has 64 % forest cover. Extensive road construction during 2021 has resulted in reduction in forest cover in Sitlakheth.

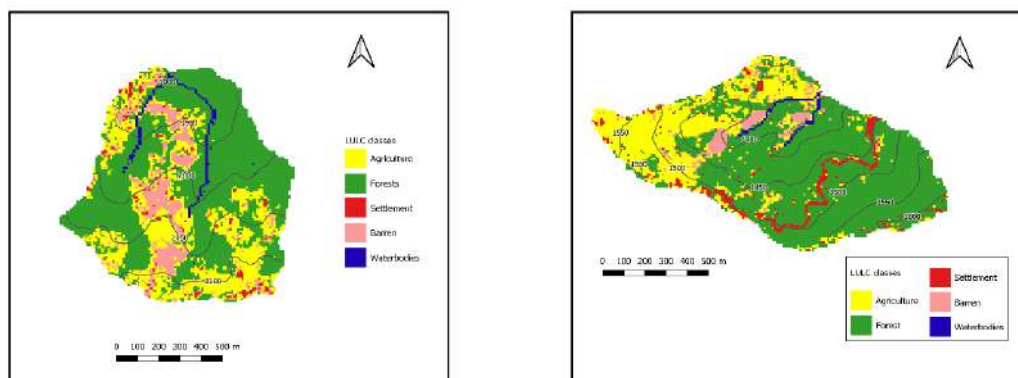


Fig. 2. LULC maps of (left) Sitlakheth and (right) Papoli watersheds. (LULC classification was done on Google Earth Engine and final maps were produced using free and open source QGIS 3.16).

A monitoring programme was initiated in January 2021 and surface runoff processes were monitored at three 3m x 1.5m plots each under Oak and Pine forest canopies, respectively. The surface runoff plots (Fig. 3-A and 3-E) were bounded by stainless steel sheets and water directed through a 0.6 feet HS-flume instrumented with a

capacitance-based water level sensor with datalogger (Odyssey Dataflow Systems Limited, New Zealand). Apart from this, streamflow was also gauged with a capacitance-based water level sensor placed in a 6 inch PVC pipe stilling well at Shitlakheth (Fig. 3-C). A stage-discharge relationship is developed for the location by taking 10 discharge measurements in the monsoon and winter season (June to December 2022). Similarly, at Papoli, a 3 feet steel H flume was installed across the stream and instrumented with a capacitance-based water level sensor (Fig. 3-F). The relationship between stage and discharge was estimated from standard tables.

Continuous record of rainfall was taken from GB Pant NIHE 30 m eddy covariance instrumented tower. Along with this, two rain gauges were instrumented during June, 2022 at Shitlakheth and Papoli site for continuous measurement of the rainfall at both sites.

Soil pits were dug adjacent to the central plots of each forest type, and six tunnels of size $75 \times 60 \times 45$ cm were made beneath the plots (Fig.3 -A and 3-E). Tunnels were prepared for lysimeter installation. Zero tension pan lysimeters were made of metal trays tapered by an angle of 0.094° towards the wire mesh covered outlet. The metal trays were then filled with crystal beads and glass marbles. The lysimeters were installed into the tunnels with the support of a pair of screw jack, and the outlet of the lysimeters was attached with carboys by PVC pipes for leachate collection.

Initially, disturbed soil samples were collected using an auger hole sampler at three depths (0-10 cm, 10-20 cm and 20-30 cm) for each plot outside the plot boundary so that the plot area remains natural and undisturbed. These soil samples were used for soil chemical analysis and soil moisture laboratory experiments. Undisturbed soil samples (11) were also collected in Eijkelkamp soil sample rings for the analysis of other soil physical properties such as bulk density and permeability. Handheld mini-disk infiltrometer (Decagon Devices, Inc.) experiments were performed inside the plots to calculate soil hydraulic conductivity and sorptivity. The infiltrometer experiments were performed for each ecosystem plot in triplicates to estimate these soil hydraulic properties. As unsaturated hydraulic conductivity and sorptivity are the functions of soil water content so, just after the infiltrometer test top layer of soil samples were collected for gravimetric soil moisture measurement.

Soil moisture measurement was monitored at 2 vertical profiles, 1 each in close proximity to the surface runoff plots. Moisture content was monitored at 15 min intervals with TDR probes (Acclima Digital True TDR-310N Sensor). In each soil moisture profile, TDR probes were inserted at 3 depths (Fig. 4-D and 4-H). In the Pine forest, the depths are 5cm, 15cm and 30 cm below which bed rock was encountered. In the Oak site, the soil was sufficiently deep. Soil moisture probe was placed at 15 cm, 40 cm and 70 cm. Below 80 cm parent materials in the form of small rock pieces was encountered. Fresh road cutting confirmed the soil depth at Shitlakheth ranging from 80 cm to 120 cm.

In order to calculate interception loss at each site, stemflow and throughfall collection systems were designed and installed at both locations (Fig. 3-B and 3-F). For stemflow collection, each sample tree was fitted with a spiral collar made of PVC ribbed suction hose split longitudinally for the entire length except the last 60 cm. The unsplit portion of the hose was then guided into 70 litre drums for stemflow collection. The throughfall was collected on troughs made of 4 inch PVC pipes split in half longitudinally. Three troughs of length approximately 3m were installed in each site. Water samples were being collected from the throughfall and stemflow drums, zero tension pan lysimeters under the plots, and from the stream. Installation was completed in the month of October 2021.



Fig. 3. Photographs of field installations at Pine site (A, B, C, D) and Oak site (E, F, G, H); A & D are surface runoff plots with a view of the collection system for soil leachate; B & E are stem flow and throughfall collection systems; C is the stilling well at the outlet of Sitlakh watershed while F is the 3 feet flume at the outlet of Papoli watershed; D & H are installation pictures of soil moisture sensors.

First, soil samples moisture was extracted at pressure 0.1 bar and 15 bar by pressure plate experiment unit. For that, both the vessels were set up at the required pressure. The pressure was supplied in the vessels through an air compressor. At particular pressure, the experiment was conducted till moisture extraction stops from the soil. Then the pressure was released slowly from the vessels by using the valve unit of experiment set-up i.e., exhaust valve, lower valve, upper valve, and isolation valve. Then those vessels were opened and plates were taken out. Then instantly soil samples were weighed by a weighing machine and put into the oven dryer for 24 h at a temperature of 105 °C for measuring soil moisture. The next day samples were collected from the oven dryer and the dry weight of the samples was measured for the calculation of gravimetric soil moisture content. By the same process pressure plate experiments were performed at different pairs of pressures such as 0.1 bar – 15 bar, 0.5 bar – 5 bar, 0.33 bar – 10 bar, and 0.7 bar – 3 bar, and gravimetric soil moisture was determined (Fig. 4). The bulk density of soil samples at different depths was measured by tapped cylinder method in the Environment Hydrology Lab at IIT Roorkee. A weighed sample of soil was filled into a 100 ml measuring cylinder. Three sets of twenty mechanical taps were given to the cylinder by raising and tapping of the cylinder on the lab counter. After that tapped volume of soil in the measuring cylinder was observed and bulk density determined as a ration of weight of soil and volume of soil.



Fig. 4. Laboratory pressure plate soil moisture experiment set-up: (left) Saturated soil samples placed on the ceramic pressure plates; (right) Pressure plate apparatus consisting of two pressure vessels, two pressure measurement unit, and pressure generator.

Chemical analysis

The soil samples collected from both ecosystems were prepared to analyzed for nutrients, pH, electrical conductivity, base cation, and base anions at Department of Hydrology, IIT, Roorkee, Environment Hydrology Laboratory. For that soils were dried in the oven drier at 105°C for 24 hours then sieved through a 5 mm sieve before analysis. Then for further process, 5 gm soil and 50 ml distilled water was mixed in a conical flask by providing a handshake to each soil sample. After that prepared samples were first filtered by ordinary filter paper followed by a syringe filter of 0.2 μm . pH and EC were measured by multiparameter sensor electrode instrument by dipping the probe into the sample flask. Runoff and leachate samples from the plots were collected in the sample bottle after the rainfall event and stored in the refrigerator. For further analysis stored samples of runoff and leachate were filtered by ordinary filter paper and analyzed in the “Central Laboratory” of GBPNIHE, Almora. pH and EC were analyzed by the multiparameter sensor electrode. Sodium and potassium were measured by flame photometer and sulphate measured by spectrophotometer. Other chemical parameters such as total hardness (TH), calcium hardness, and calcium were measured by the titration method. Further soil and water samples were analysed at DOH, IIT R and NIH Roorkee. Throughfall, stemflow and leachate samples (monsoon 2021) were digested in the microwave digester (EPA Method 3015A) and then analysed for micro- and macro-nutrients using Microwave Plasma Atomic Emission Spectroscopy (MPAES; Agilent 4210-MP-AES) at the Institute Instrumentation Center in IIT Roorkee. Textural analysis of soil samples from soil moisture pits was done in the Soil and Water Lab at NIH Roorkee using wet sieving and Soil Particle Size Analyzer.

Watershed scale hydrological modelling

Objectives

The primary goal of this modelling study was to understand the contributions of different LULCs to runoff generation in the upper Kosi River catchment. Hydrological modelling of the catchment was carried out using SWAT model to simulate the runoff in different sub-catchments. The specific objectives of the study were:

- i. To collect and pre-process geospatial and climatic datasets for the catchment.
- ii. To setup the SWAT model and simulate the hydrological responses.
- iii. To calibrate and validate the SWAT model using SWAT-CUP.
- iv. To understand the role of different LULCs in runoff generation through SWAT simulations.

Reasons for selecting the SWAT model

- i. The SWAT model has been widely used universally in different catchments and climate zones worldwide for several hydrological studies. Therefore, the model is widely accepted by hydrologic community for its performance in simulating different hydrological processes in different types of catchments.
- ii. It is freely available for use.
- iii. It can be used on a different scale and a single watershed, and multiple connected watersheds.
- iv. The SWAT model breaks each watershed into different hydrological response units (HRUs), which enable us to understand the hydrological processes at finer scale.

SWAT model

Soil and Water Assessment Tool (SWAT) is a river basin or watershed scale model developed by USDA Agricultural Research Services (ARS). It was developed to study the effect of land management practices on river basin functions like water yield and sediment and nutrient transport and so is suited for studying the effect of LULC changes on the watershed. SWAT is a continuous time model, and is not suited for single event flood routing, but for long term yield studies. For modelling purposes, the study area can be divided into sub-basins or sub-watersheds. The input data for each sub-basin can be divided into climate, hydrological response units (which are a unique combination of soil type, slope and LULC), surface storage, ground water and main reach or river. The model simulates the hydrological processes in two distinct phases – the land phase and the water or routing phase. The land phase simulation governs the amount of water, sediment and nutrient loading in to the main stream. The water phase routes the water, sediment and nutrient through the channel network to the outlet of the river basin.

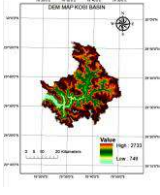
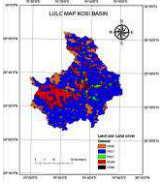
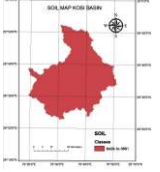
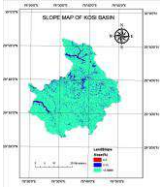
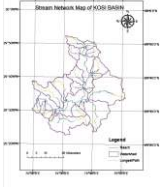
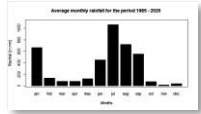
SWAT model data requirements

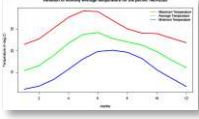
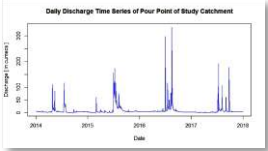
For the setup of the SWAT model, two types of input data are required.

1. Spatial data
2. Hydro-climatologically data

Kosi river catchment has 21 sub-basins and 75 HRUs. Hydrological data available for the Kosi Catchment is only four years, from 2014-to 2017. Two years of rainfall data 2012-13 is obtained from the Indian Metrological Department (IMD) website and was used for the warmup period. Next two years' data (2014-15) was used for the calibration period and remaining two years (2016-17) were used for the validation period. Before calibration and validation, sensitivity analysis was also carried out to determine the most sensitive parameters. Uncertainty analysis is done by “The Sequential Uncertainty Fitting procedure version 2 (SUFI-2)” using the SWAT-CUP interface

The data used in setting up the SWAT model for the upper Kosi basin is summarized in the following table.

Sl. No.	Data description	Data source/ preparation	<i>Snapshot of dataset</i>
Spatial Data			
1.	Digital Elevation Model	SRTM 30m x 30m	 <p>DEM MAP OF KOSI BASIN</p> <p>Value High: 1750 Low: 744</p>
2.	Land Use Land Cover map	Terra and Aqua Combined Moderate Resolution Imaging Spectroradiometer (MODIS) Land cover Type (MCD12Q1) map. The map identifies five LULC classes in upper Kosi – forests evergreen, forests mixed, agricultural land row crops, pasture and residential.	 <p>LULC MAP OF KOSI BASIN</p>
3.	Soil map.	FAO Digital Soil Map of the World. The entire river basin was identified as having Clay-Loam type soil.	 <p>SOIL MAP OF KOSI BASIN</p> <p>SOIL Clay-Loam</p>
4.	Slope distribution	The catchment slope is divided in to 3 categories – 0 to 3 %, 3 to 15 %, and >15%. A majority of the catchment (92%) was identified within the 3 to 15% slope class.	 <p>SLOPE MAP OF KOSI BASIN</p> <p>SLOPE 0-3% 3-15% >15%</p>
5	Stream network map	Generated in the ArcSWAT tool based on the SRTM DEM.	 <p>Stream Network Map of KOSI BASIN</p> <p>Legend Stream Catchment</p>
Hydroclimatological data			
6	Rainfall data	IMD data from 2012 – 2017. Climatology data from 1985 – 2020 was freely downloaded from NASA to understand the seasonality of rainfall in the region.	 <p>Average monthly rainfall for the period 1985 - 2020</p> <p>mm</p>

7	Temperature data	From NASA.	
8	Relative humidity data, Solar radiation data, and wind speed	For this study, simulated data generated in the SWAT model was used.	
9	Discharge	Discharge data was obtained from GB Pant NIHE from the gauging location maintained at 29°33'23" N and 79°20'44" E for four years – 2014 to 2017.	

Model setup

The model setup proceeds through three stages – the watershed delineation, HRU analysis and weather data input summarized in Figure 6.

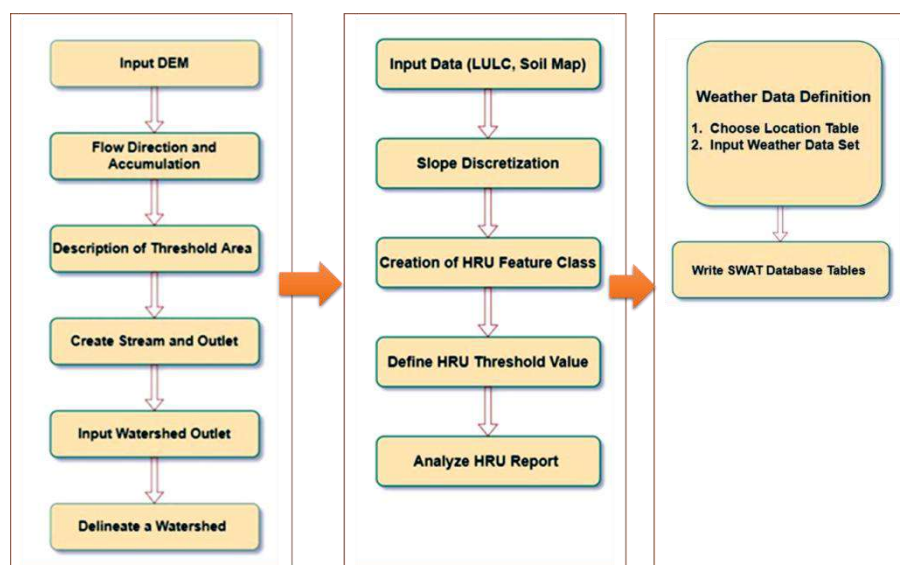


Fig. 5 Summary of SWAT model setup

2.1.3. Assessment of microclimate variability of Pine-Oak dominated forests and future changes under a warmer climate and its societal implications.

2.1.3.1. Comparison of Pine and Oak transpiration using sap flow observations under limiting meteorological conditions for two sites of a watershed (*stand level transpiration study. Manuscript is under preparation, 2032*)

Sap flow measurement is a precise technique to study the tree water relations and to quantify whole-plant water use. Total plant volumetric sap flow (Q) is the movement of fluid within xylem and is functionally correlated with transpiration, stem refilling and transport of solutes. The water use linked evaporative loss of vegetation

consists of two components, first one is plant transpiration (T) and the second one is direct evaporation from the soil and surface of other organic matter (E). The measurement of whole plant water use especially in woody plants is rather difficult considering the huge canopy and complex environmental responses. The quantum of water loss in a tree depends on canopy size, physiological condition and soil and atmospheric factors. There is also an increasing interest in water and carbon fluxes at the canopy atmosphere interface in the perspective of global climate change scenario. Moreover, sap flow measurements are useful to assess the physiological response of trees to environmental factors and changing climate. Estimation of transpirational water loss is a direct method for accounting the water use of individual tree. Granier (1985) developed a dual-probe sap-flow measuring system which is known as thermal dissipation probes (TDP). The TDP probe method has been popular among tree physiologists as it is simple and more reliable. So far, there are not enough published experimental data on water use of Pine and Oak trees and hence worthy to study it thoroughly with an advanced sap flow measurement technology.

Data collection: Data were collected from sap flow analysers installed in 6 trees of mature Pine and 6 trees of Oak (3- *Quercus leucotrichophora* and 3- *Quercus glauca*) in two different forest patches. SF-L type sensors were used in each site having thermal dissipation probe and reference thermocouple to continuously record background temperature. Data used in this study was for the period of November, 2020 to Aug, 2021. Meteorological data used (as aerial distance is around 9.5 km from the Oak site) in the analysis was obtained from a field station at Kosi-Katarmal, Almora, India (29°3'N, 79°3'E), at an elevation of 1217 m above mean sea level and falls within *Cwa* category. The field station is situated in the upper Kosi-watershed and within the campus of GB Pant National Institute of Himalayan Environment, Kosi-Katarmal, Almora. The average crown height of surrounding mixed vegetation was 12 m. A 3-D sonic anemometer (CSAT3, Campbell Scientific Inc., Utah, USA) and an infrared CO₂/H₂O gas analyzer (EC150, Campbell Scientific Inc., Utah, USA), installed at 30 m height ($z_m = 30$ m, where z_m is the uncorrected measurement height) having a measuring frequency of 10 Hz, were operational with a net radiation sensor (CNR 4, Kipp and Zonnen, Netherlands) and an automatic rain gauge (TE525, Campbell Scientific, Utah, USA). Wind speed and direction sensors (HMP45, Vaisala) along with atmospheric temperature and relative humidity sensors were installed at 2, 20 and 32 m heights of the flux tower.

Details of the needle size and DBH are given below:

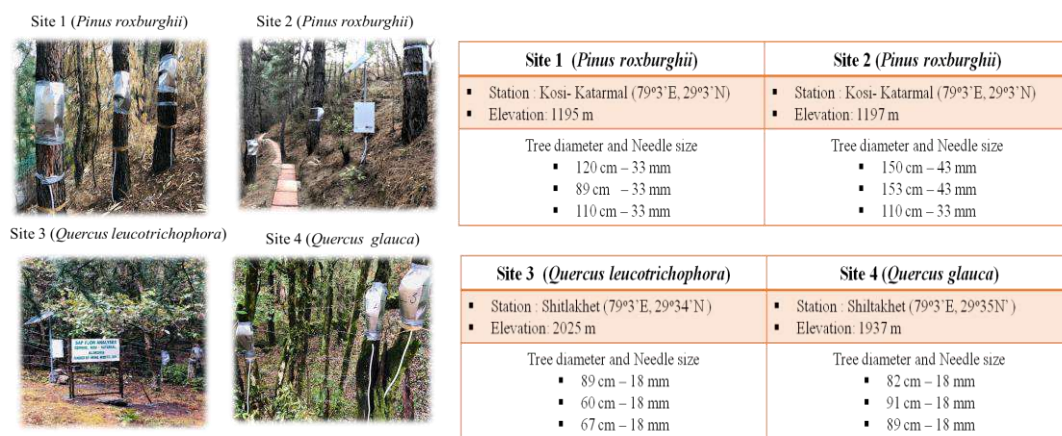


Fig. 1: Sap flow analyser installed in *Pinus roxburghii* (a and b), *Quercus leucotrichophora* (c) and *Quercus glauca* (d).

In order to calculate the sap flow of the tree, data measured are processed in three steps:

- **Step 1: Data correction**

$$\Delta TC = \Delta T - (\Delta T_{R1} + \Delta T_{R2}) / 2$$

Where ΔTC is the corrected temperature difference in μ , ΔT is the voltage or temperature signal in μV , ΔT_{R1} is voltage and temperature in μV and ΔT_{R2} is voltage and temperature in μV

- **Step 2: Calculating the Sap flow density**

$$U = 0.714 * ((\Delta TC_{max} - \Delta TC) / \Delta TC)^{1.231}$$

Estimation of sapwood area:

Tree transpiration can be estimated from whole sap flow Q_t , by multiplying sap flux density J_p ($ml.cm^{-2}.min^{-1}$) to sapwood area A_x as there is no direct method to estimate Q_t . Equation is given below:

$$Q_t = J_p * A_x$$

In order to estimate sapwood area, increment borer was used to extract the tree core sample from selected Pine and Oak trees. 15 samples were collected in case *Pinus roxburghii* and *Quercus leucotrichophora*. However, in case *Quercus glauca* only 10 samples were collected because most of the trees were found near the stream and were unreachable to collect samples.



Fig. 2: Sapwood depth calculations using tree core samples taken from in *Pinus roxburghii* (a), *Quercus leucotrichophora* (b) and *Quercus glauca* (c).

2.1.3.2. Comparison of Pine and Oak ecosystem fluxes under limiting meteorological conditions for two sites (particularly, rainfall. A manuscript highlighting ecosystem interaction is published in *Environment Monitoring and Assessment*, 2023)

Pine-Oak ecosystem flux measurements and instrumentation: The ecosystem fluxes and meteorological parameters were measured from two different field stations. The first site, referred to as “Pine site” is already highlighted in the above section. The second site, referred to as “Oak site”, situated in the Gangolihat block, Pithoragarh, Uttarakhand, (80.02°E, 29.39°N) at an elevation of 1650 m. The site falls under Koppen climate classification of C_{wb} with average monsoon season rainfall of around 704 mm with average heavy rainy days of 2.48 per season (Mukherjee et al 2014, Mukherjee 2021). The land-cover assessment of the watershed shows that out of the 37 km^2 of total watershed area 54.5% is under forest, of which 38.4% area had dominant *Q. leucotrichophora* trees. The flux tower was surrounded by *Q. leucotrichophora*, maintaining a dense canopy throughout the year. Associated dominant tree species within the forest cover include *Pyrus pashia*, *Cedrus deodara* and *Juglans regia* (Joshi et al 2020). The average height of the canopy was around 8 m. The eddy covariance tower had a 3-D sonic anemometer (CSAT3, Campbell Scientific Inc, Utah, USA) along with an

infra red CO₂/H₂O gas analyzer (EC150, Campbell Scientific, Utah, USA), installed at 10 m height having a working frequency of 10 Hz measuring 3-D wind vectors, CO₂/H₂O flux and sonic temperature. Furthermore, net radiation sensor (NR Lite, Kipp and Zonnen, Netherlands), rainguage (TE525, Campbell Scientific, Utah, USA) and relative humidity - air temperature sensors were also installed. The raw data files were produced at 30 min interval.

(a) Impact of monsoon season rainfall spells on the ecosystem carbon exchanges of Himalayan Chir-Pine and Banj-Oak dominated forest

The Chir-Pine and Banj-Oak site data presented in this study were considered only for monsoon seasons of 2016-2017, i.e. for the period of 00:00 Hrs of 1 June, 2016 to 23:30 Hrs, 30 Sep., 2016 and 00:00 Hrs of 1 June, 2017 to 23:30 Hrs, 30 Sep., 2017. Therefore, a total of 244 days of data were used. The rationale for considering the monsoon season is two-folds, (i) both the study sites received around 70% of the total annual rainfall during monsoon, and (ii) both Chir-Pine and Banj-Oak dominated ecosystems had highest growth during the monsoon. The 10 Hz raw data quality assessment for both sites was performed using the EddyPro software (v6.0, LiCor-Bioscience, USA) and following similar approaches presented in Mukherjee et al (2018,2020), Lohani and Mukherjee (2021) and Deb Burman et al (2021). However, a brief description of the quality assessment procedures used in the flux data is provided here. The general quality check assessments were made as per Vickers and Mahrt (1997); the sonic temperature corrections were made following Schotanus et al (1983); the WPL corrections were made following Webb et al (1980); the low and high-pass filtering was made using Moncrieff et al (1997,2004); the tilt correction was made using Wilczak et al (2001). Additionally, displacement height was computed using the average canopy height at both sites and following the numerical model of Foken and Nappo (2008).

Quantification of the amplitude of rainfall and ecosystem exchange: To quantify amplitude of rainfall, triggering the highest change in the ecosystem fluxes, temporal variability of the daily total rainfall and NEE, GPP, RE was investigated using wavelet spectra. Initially, the continuous wavelet spectra of NEE, GPP, and RE were produced for Chir-Pine and Banj-Oak systems as they provide information in the frequency domain having many overlapping time scales (Torrence and Compo,1998; Grinsted et al,2004; Domingues et al,2005; Salmond,2005). Furthermore, cross wavelet spectra between rainfall and NEE, GPP, RE were produced for Chir-Pine and Banj-Oak ecosystems and compared. The rationale for using the cross-wavelet spectra was to compare phase relationships and local correlations between the ecosystem fluxes and rainfall during the monsoon period. A brief description of the wavelet spectral method used in this study could be found in Mukherjee et al (2018) with description of the axes and colour used in the scalograms.

Quantification of the impact of rainfall spell on net ecosystem exchanges: Impact of rainfall spells on NEE was estimated based on the successive rainfall events where '0-day' and the 'rainfall event + 01-day' had no rainfall. Consequently, successive rainy days of a monsoon season were considered upto 10-day from 0-day of initiation where 0-day and 11-day implied no rain (length of rainfall spell, hereafter). The analysis was carried out till 10-day from 0th day of rainfall initiation due to the fact that the maximum successive rainy day for both the monsoon seasons of 2016-2017 was 10-day for Chir-Pine site and 9-day for Banj-Oak site. The analysis steps were as follows:

- Counted rainy days (i.e. any day having rainfall greater than 0 mm) of monsoon season based on length of rainfall spell (continuous rainfall spell upto 10-day from 0-day of initiation), i.e. counted all those days having 1-day, 2-day, 3-day,....., 10-day continuous rainfall.
- The 0-day and 'rainfall event + 01-day' of counting initiation was represented with no rainfall. For example, a 1-day spell indicated no rain on 0-day and 2-day.
- Seasonal total rainfalls of all such rainfall spells (1-10-day) were counted for 2016-2017. Subsequently, average rainfall amount and NEE (for both Chir-Pine and Banj-Oak ecosystems) was computed for all such rainfall spells of 2016-2017.

Scatter diagram of the average NEE and associated length of rainfall spell was produced to identify the impact of rainfall spell on carbon assimilation by each ecosystem. Consequently the average NEE was modeled with rainfall spell using a power-law equation: $NEE = aS^b$, where, S is spell duration, a and b are constants for optimization. A non-linear least square curve fitting method that uses 'trust-region-reflective' algorithm (Coleman and Li, 1996) were used to find the actual values of a and b . The curve fitting method was initiated with the set input of [1 1]. The final coefficients were then used to construct the model $NEE = aS^b$ and correlation coefficients (CC) were computed at a p-value <0.005.

Quantifying the impact of rainfall amount on the net ecosystem exchanges: It is reported by Yuhui et al (2018) that the amount of precipitation within a rainfall spell can also be a significant stimulator to ecosystem growth. Subsequently, two approaches were opted to evaluate the impact of rainfall amount on the carbon assimilation by the ecosystems of this study. In the first approach, effort was made to assess the impact of maximum rainfall within a rainfall spell on carbon assimilation. Subsequently, the following steps were adopted:

- Identification of maximum rainfall within the length of rainfall spell was initiated starting from 2-day rainfall spell. It was assumed that the maximum rainfall amount was observed within a rainfall spell at the r_d day.
- To check the impact of maximum rainfall of a spell on the NEE of subsequent days, prepared an array of all the NEE values during r_d , r_d+1 , r_d+2 and r_d+3 days of each rainfall spell duration.
- Next, to find the duration of highest carbon assimilation by each ecosystem after a maximum rainfall within a spell, irrespective of spell duration, box plots of all the NEEs were produced for each r_d , r_d+1 , r_d+2 and r_d+3 days.

Finally, the boxplots were used to identify the highest carbon assimilation by an ecosystem after the maximum rainfall irrespective of rainfall spells. In the second approach, the impact of rainfall amount on carbon assimilation was estimated by quantifying rainfall threshold that had maximum carbon assimilation for Chir-Pine and Banj-Oak dominated ecosystems. However, only successive rainfall events upto 5-day rainfall were considered for the analysis under the assumption that a rainfall spell greater than 5-day is generally categorized as 'heavy rainfall spell' Qing et al (2015) and Tang et al (2018). The analysis was carried out as per the following steps:

- Selected rainy days (i.e. any day having rainfall greater than 0 mm) of monsoon season based on continuous rainfall spell upto 5-day from 0-day of initiation, i.e. counted all those days having 1-day, 2-day, 3-day,.....,5-day continuous rainfall.

- Average rainfall of all such rainfall spells (1 to 5-day) was identified for 2016-2017. Subsequently, average NEE for both Chir-Pine and Banj-Oak dominated ecosystems, was computed for all such rainfall spells of 2016-2017.
- Scatter diagram of the average NEE and associated rainfall amount, irrespective of the rainfall spell, was produced to identify the rainfall amount that has highest carbon assimilation by each ecosystem.

Finally to model the rainfall amount with NEE, a quadratic equation (i.e. $NEE = aR_m^2 + bR_m + c$, where R_m is the rainfall amount) was fitted to each scatter plot, and the Y-axis minimum of each plot was identified as the optimum rainfall amount resulting highest carbon assimilation. The quadratic equation model was also evaluated with respect to observations, and r^2 values were computed.

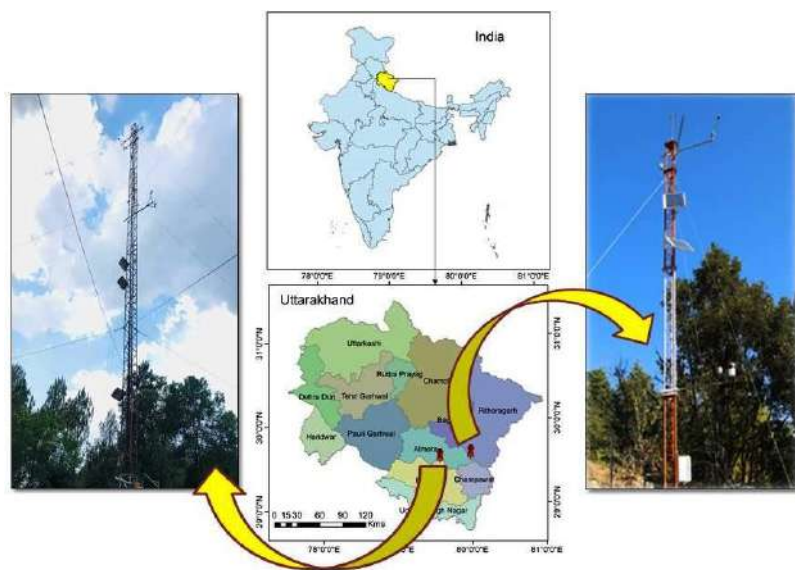


Fig. 3 Location of the eddy covariance towers for Chir-Pine (left) and Banj-Oak (right) dominated ecosystems.

(b) Impact of monsoon season net radiation on the ecosystem carbon exchanges of Himalayan Chir-Pine and Banj-Oak dominated forest

In order to quantify the impact of net radiation on Pine Oak ecosystem exchange two different analysis were carried out. In the first analysis, light use efficiency of both Pine and Oak dominated ecosystems were quantified and subsequently tested the conjecture “on more rainy and cloudy days, light use efficiency (GPP/PPFD) would be lower, hence GPP would be lower”. LUE is defined as the amount of carbon fixed per incoming light and can be calculated as

$$LUE = \frac{Sum(GPP)}{Sum(PPFD)}$$

Where GPP is gross primary productivity in $\mu\text{mol.CO}_2.\text{m}^{-2}.\text{s}^{-1}$ and PPFD is Photosynthetic photon flux density ($\mu\text{mol. quanta m}^{-2} \text{ s}^{-1}$). It is dimensionless quantity which expresses the amount of radiation required per unit

amount of carbon fixation. The Light use efficiency for varying length of rainfall spell (LRS) was quantified and plotted to comprehend the role of radiation in plant productivity. In order get more clarity on this, a separate analysis was carried out by segregating Light use efficiency of rainy days and rain free days for the period of the study (Figure:2). Almost identical pattern of light use efficiencies during rain free and rainy days were observed for the period of the study.

(c) Comparative assessment of water use efficiency at ecosystem level (*Presented in Asia Oceania Geosciences Society , 2022*)

Carbon fluxes are tightly coupled to water cycle in terrestrial ecosystem. Ecosystem water and carbon exchange are considerably affected by climate variability through a set of coupled physical and physiological processes. Understanding this coupling process and the factors that interact with the changing social demands and climate variability is important for mitigation strategies. Water use efficiency (WUE) is an indicator of the trade-off between carbon uptake and water loss to the atmosphere at the plant or ecosystem level. Assessment of temporal dynamics and the response of WUE to climatic variability is an essential part of land degradation assessments in water-limited systems. Moreover, Water use efficiency (WUE), which integrates ecosystem carbon and water cycles, is an important index for evaluating ecosystem sensitivity to climate change. However, the WUEs of two dominant tree species of central Himalaya, i.e. coniferous Chir-Pine (*Pinus roxburghii*) and evergreen broad-leaf Banj-Oak (*Quercus leucotrichophora*), having differences in their anatomy and leaf types, and providing substantial ecosystem services to region, were not evaluated at multiple temporal scale. Pine-Oak forests of Himalayas are also known to have many tangible and intangible benefits in terms of ecosystem productivity and significantly contribute to store large amount carbon which plays vital role in global carbon cycle. There are four factors changing in the climate that will affect water use by plants. These factors are: increasing carbon dioxide (CO₂) concentrations, increasing temperatures, more variable precipitation, and variations in humidity. The present study aims to evaluate and compare WUE at ecosystem level for two most dominant species of central Himalaya and establish a relationship of WUE efficiency with changing environmental conditions. As described above four factors: Vapor pressure deficit, precipitation, PPFD (Photon flux density) and air-temperature are used to show the impact of changing environmental conditions to water use efficiency.

Data description: Pine-Oak measurements and instrumentation is already discussed in **section-C-1**. Data in this study were analyzed for the period of April, 2016 to December, 2017 with special emphasis to pre-monsoon (April-June), monsoon (July-September) and post monsoon (October-December) seasons. The global radiation was used to compute 30 min photosynthetic photon flux density (PPFD) values ($\mu\text{mol.m}^{-2}.\text{s}^{-1}$) However, the additional amount of CO₂ which do not take part in exchange processes assumed to be stored in canopy, left unmeasured by eddy covariance system.

(d) The impact of limiting meteorological conditions on ecosystem fluxes (*Ecosystem level study. Book chapter highlighting Oak ecosystem variation is Published, 2023.*)

Data in this study were analyzed for the period of 1 March, 2020 to 30 November, 2020 with special emphasis to pre-monsoon (March-May), monsoon (June-September) and post monsoon (October-November) seasons.

The primary eddy covariance data assessment was carried out using the EddyPro software (v6.0, LiCor-Bioscience, USA). After Eddypro processing, the eddy covariance data were used for flux partitioning and 30 min values of NEE, GPP and RE values in $\mu\text{mol.m}^{-2}.\text{s}^{-1}$ were produced using the methods of Lasslop et al (2010) of REddyProc (v1.1.3). The ambient water vapour mass densities were used to compute 30 min VPD values (kPa). The global radiation was used to compute 30 min photosynthetic photon flux density (PPFD) values ($\mu\text{mol.m}^{-2}.\text{s}^{-1}$). At last, daily averages of NEE, GPP, RE, VPD and PPFD were computed along with daily averages of wind speed (ms^{-1}), air temperature ($^{\circ}\text{C}$), relative humidity (%), and daily total rainfall (mm). Here, a negative NEE implies carbon assimilation by the ecosystem. The flux variability assessments were carried out for the pre-monsoon (March-May), monsoon (June-September), and post-monsoon (October-November) seasons. The NEE - VPD relationships were quantified for each season using the power law relationships $\text{NEE} = a\text{VPD}^b$ and a , b were optimised.

2.1.3.3. Rainfall Induced Changes in the Soil CO₂ Effluxes of Chir-Pine and Banj-Oak Dominated Ecosystems of Central Himalaya

Soil efflux is one of the major contributors of CO₂ to the atmosphere, and natural drying and rewetting of the soil through rainfall can significantly modulate the efflux amount of an ecosystem. Although the central Himalayan region is occupied with two dominant ecosystems, Chir-Pine (*Pinus roxburghii*) and Banj-Oak (*Quercus leucotrichophora*), differences in their soil efflux dynamics and responses of effluxes to varying rainfall are not examined in detail. Therefore, this study presents a comparative assessment of seasonal variation of the soil efflux of Chir-Pine and Banj-Oak dominated ecosystems. Efforts are made to quantify the changes in soil effluxes from these ecosystems due to varying rainfall spells amount. Data used in this study were collected from eosense carbon dioxide forced diffusion chamber (eosFD-CO₂) sensors installed under a Chir-Pine dominated ecosystem (29°3'N, 79°3'E), at Kosi-Katarmal, Almora, India and a Banj-Oak dominated ecosystem (29°34'N, 79°3'E), at Shitlakheth, Almora, India for a total of 3655 days of summer (March-May), monsoon (June-September) and winter (November-February) seasons during 2021-2022.



Fig.4 Soil CO₂ efflux installed at Oak and Pine site.

Soil CO₂ analysers are installed in *Pinus roxburghii* and *Quercus leucotrichophora* forest . Forced Diffusion Chamber type sensors are used for Soil CO₂ measurement which contains single NDIR for flux computation. Soil CO₂ data for both sites are available from March, 2021 to till date.

2.1.4. Regional scale climate modeling for IHR including three sites of two watersheds including high resolution.

(a) Future precipitation extremes over base Himalayan Uttarakhand region: analysis using the statistically downscaled, bias-corrected high-resolution NEX-GDDP datasets

The current study considers the Uttarakhand state to offer a better understanding of the varying rainfall patterns in the region (Figure. 1). Uttarakhand, previously known as Uttaranchal, is one of the northern states in India. The state lies between the latitudes of 28°N to 31.5°N and the longitudes of 77.5°E to 81.4°E. This state is located in the Himalayas' foothills, mainly a hilly state. Uttarakhand state's total geographical area of 51,125 km², of which 93% are mountains, in which 65% are covered by forest, glaciers are at the high elevation regions and coolest weather, at lower elevations there is dense forest (Banerjee et al. 2020). This state is abundant natural resources like glaciers, lush forests, perennial rivers, and snow-capped mountain peaks that can also be found across the state. Uttarakhand state receives 80 % rainfall in the SW-monsoon season, and the annual average rainfall is 1494.7 mm (Banerjee et al. 2020).

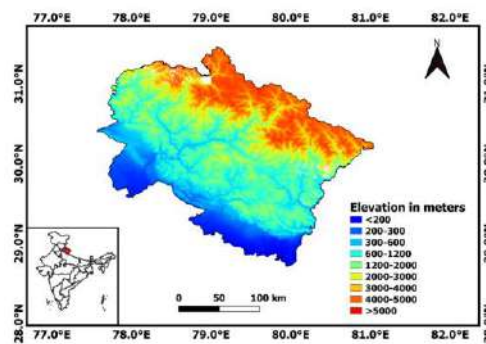


Figure 1: Topography map of Uttarakhand state, India, the study region.

NASA Earth Exchange (NEX)-Global daily downscaled projections (GDDP) dataset provides a suite of 20 statistically downscaled models from a set of CMIP5 models for two scenarios RCP 4.5, and RCP 8.5 (representative concentration pathways 4.5 and 8.5). This data was used to generate future climate projections (Wood et al. 2004). More information is available at <https://cds.nccs.nasa.gov/nex-gddp/>. The Bias Correction Spatial Disaggregation (BCSD) statistical downscaling method has been applied to generate these data products (Wood et al., 2004). The NEX-GDDP model output is evaluated against high resolution gridded precipitation data (0.25° x 0.25°) from APHRODITE for the baseline period (1976-2005) for monthly means, seasonal means; and extreme precipitation indices. The APHRODITE data have been widely used for trend and extreme analysis of rainfall in several regions, including India (Banerjee et al. 2020).

(b) Projected changes in precipitation and temperature extremes using bias corrected NEX-GDDP6 simulations over Hindu Kush Himalaya

The present study examines the changes in precipitation and temperatures over the Hindu Kush Himalayan region over two warming scenarios. The cryosphere of the Hindu Kush Himalayan region acts as one of the sensitive indicators of accelerated climate change. Coupled Model Intercomparison Project Phase 6 (CMIP6)

model simulations are now considered a better alternative to studying anthropogenic forcings' impacts than previous versions (Kumar et al., 2023). CMIP6 models capture regional features better (Gusain et al., 2020; Kumar & Sarthi, 2021), and many studies have noted that they offer improved simulations of precipitation extremes (Luo et al., 2021; Chen et al., 2021). Given these circumstances, we have used the NASA Earth Exchange Global Daily Downscaled Projections (NEX-GDDP6) dataset for the present study. The NEX-GDDP6 dataset consists of downscaled data from CMIP6 under two greenhouse gas emissions scenarios known as Shared Socioeconomic Pathways (SSPs) (Thrasher et al., 2022). Downscaled datasets capture extreme climate events better as they represent small-scale topographic features better (Gutowski et al., 2010). This study aims to shed light on significant changes in temperature and precipitation extremes over the HKH region and hopes to help policymakers prepare for major climatic changes under a future warming climate.

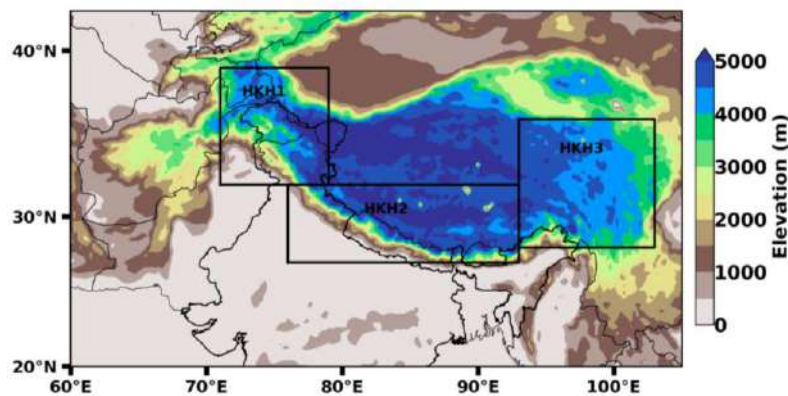


Figure 2: Hindu Kush Himalayan (HKH) region and the three sub-regions (rectangular black box) of the northwest Himalaya and Karakoram (HKH1), central Himalaya (HKH2), and southeast Himalaya and Tibetan Plateau (HKH3).

The study region separately analyzed the area-averaged summary of three sub-regions of Hindu Kush Himalaya (HKH) in the Himalayas and Tibetan Plateau, namely the northwest Himalaya and Karakoram (HKH1; 71°-79°E, 32°-39°N), the central Himalaya (HKH2; 76°-93 °E, 27°- 32°N), and the southeast Himalaya and Tibetan Plateau (HKH3; 93°-103°E, 28°-36°N) (Figure 2).

(c) Land Surface characteristics based on uncoupled Noah-MP LSM for three sites in the Himalayas: sensitivity to vegetation and Evaluation with ground, satellite, and global analysis. (Under Review: JGR Atmospheres)

The study uses different global and regional analyses to identify suitable atmospheric forcing to the Noah-MP LSM. For this purpose, the analysis from the European Centre for Medium-Range Weather Forecasts (ECMWF) Re-Analysis version 5 (ERA5)-Land data (Muñoz-Sabater et al., 2021), Indian Monsoon Data Assimilation and Analysis (IMDAA, Rani et al., 2021), the Global Land Data Assimilation System (GLDAS, Rodell et al., 2004), the Modern-Era Retrospective analysis for Research and Application Version 2 (MERRA-2; Gelaro et al., 2017), and FiNaL (FNL) analysis of the Global Forecasting System (GFS) of the National Centers for Environment Prediction (NCEP; NOAA/NCEP, 2000) are considered. These analyses are widely

used and identified to be better over different parts of the globe. The details about these products have been summarized in Table 1. The ERA5-Land, IMDAA, GLDAS and MERRA2 data are interpolated to the station location by nearest neighbor method. The temperature, RH, and winds from ERA5-Land, IMDAA, GLDAS, NCEP FNL, and MERRA2 are validated at Kosi-Katarmal, Kantali and Gangolihat stations. Integrated Multi-satellitE4 Retrievals for Global Precipitation Measurement Mission (IMERG) precipitation half hourly data with $0.1^\circ \times 0.1^\circ$ resolution (Huffman et al., 2015) is also used to force the land surface model.

Noah-MP Model

Noah-MP is a new generation of LSM which is developed to improve the efficiency of the Noah LSM (Chen and Dudhia, 2001; Ek et al., 2003). Noah-MP simulates the momentum, land atmospheric energy, SHF, LHF, carbon exchanges, surface runoff, water equivalent, SM, snow depth, terrestrial water storage in mountain Asia (Xue et al., 2019). For this study, Noah-MP v1.1 in an offline stand-alone 1-D model is used at the observatory locations of Kosi- Katarmal, Kantali and Gangolihat (Figure 3).

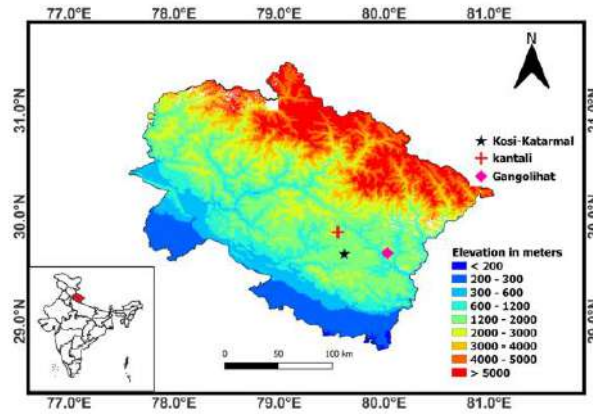


Figure 3. Topography map of the Uttarakhand state and location of observational sites, Kosi-Katarmal (29.46° N, 79.624° E) marked by black star, Kantali (29.85° N, 79.56° E) marked Red Cross, and Gangolihat (29.65° N, 80.033° E) marked by orange diamond.

ERA5-Land analysis could be a better forcing to the LSM than the other analyses. These results are consistent with other global studies. For instance, ERA5-Land has been widely used for studying land-atmosphere interactions, meteorology, and hydrology (Li et al., 2022). The Temperature, pressure and V wind, short and long wave radiation data obtained from the European Centre for Medium-Range Weather Forecasts (ECMWF) Re-Analysis version 5 (ERA5)-Land and precipitation from the Integrated Multi-satellitE Retrievals for Global Precipitation Measurement Mission (IMERG) forcing to the land surface modelling (LSM) than the other analyses during the period of 2011-2021.

Table 1: Different vegetation experiments

Exp1	Vegetation
Exp2	Deciduous Needle leaf

Exp3	Evergreen broad lea
Exp4	Barren/Sparsely vegetated

The sensitive experiment is conducted using different vegetation types (following USGS classification) in Table 1. The Noah-MP was integrated at three locations (Figure 1) from 2011 to 2021 in the different vegetation type experiments. These sites cover EXP2 vegetation in Kosi- Katarmal, and Kantali, as well as Gangolihat in EXP3. The first year 2011 is considered for spinup time (Charusombat et al., 2011). data assimilation.

Table 1: Details of data sets used in this study

Data sets	Temporal resolution	Spatial resolution	Data and time period
CPC	Daily	0.5° x 0.5°	1985-2014
NEX-GDDP6	Daily	0.5° x 0.5°	1985-2014 (Historical) SSP245 & SSP585 from 2015-2100

Table 2: List of NEX-GDDP6 models

NEX-GDDP6 models				
ACCESS-CM2	CNRM-CM6-1	GFDL-CM4_gr2	KACE-1-0-G	MPI-ESM 1-2-LR
ACCESS-ESM1-5	CNRM-ESM2-1	GISS-E2-1-G	MIROC-ES2L	MRI-ESM2-0
BCC-CSM2-MR	EC-Earth3	HadGEM3-GC31-LL	MIROC6	NESM3
CanESM5	EC-Earth3-Veg-LR	INM-CM4-8	KIOST-ESM	NorESM2-LM
CMCC-CM2-SR5	FGOALS-g3	INM-CM5-0	MPI-ESM 1-2-HR	NorESM2-MM
CMCC-ESM2	GFDL-CM4	IPSL-CM6A-LR	MPI-ESM 1-2-LR	UKESM1-0-LL

Table 3: List of extreme climate indices analyzed in the study

Indices	Name	Units
CDD	Consecutive dry days	days
CWD	Consecutive wet days	days
Rainy days	Rainy days	days
RX1 Day	Maximum 1-day precipitation	mm
RX5 Day	Maximum consecutive 5-day precipitation	mm
TX10p	Cold days	days
TX90p	Warm days	days
TN10p	Cold nights	days
TN90p	Warm nights	days

SU	Summer days	days
----	-------------	------

2.1.5. Assessment of eco-hydro-climatological processes with information theory-based process network and understanding resilience under shock.

Micrometeorological drivers affecting the variability of carbon uptake in the Himalayan Oak and Pine dominated ecosystems: An assessment of causal relationships (Under review, Journal of hydrology)

Table 1. Comprises ecosystem characteristics, flux tower details, datasets, and TIPNet configuration.

(A) ECOSYSTEMS CHARACTERISTICS (Naudiyal and Schmerbeck, 2017)		
Characteristics	Oak ecosystem (Banj-Oak/ <i>Quercus leucotrichophora</i>)	Pine ecosystem (Chir-Pine/ <i>Pinus roxburghii</i>)
Leaf longevity	Mostly evergreen with a one-year leaf span	With almost one year of leaf longevity, the deciduous tendency during spring
Light requirement	Shade tolerant in the early years of formation	Strong light-demanding species
Soil quality tolerance	Needs well-drained, relatively fertile soil	Demands coarse-grained dry soils.
Fire tolerance	Not fire-resistant. (Mature trees may survive low-intensity fires)	Mature trees can survive surface fires
(B) FLUX TOWER DETAILS (Mukherjee et al., 2018; Deb Burman et al., 2021; Lohani et al., 2023)		
Locations	Gangolihat, Pithoragarh, Uttarakhand, India (29 39'22.99 N, 80 03'38.93 E)	Kosi-Katarmal, Almora, Uttarakhand, India (29°38'22" N, 79°37'26" E)
Co-dominant species in the locality	<i>Cedrus deodara</i> , <i>Juglans regia</i> , and <i>Pyrus pashia</i>	<i>Quercus leucotrichophora</i> , <i>Pyracantha crenulata</i> , and <i>Cymbopogon iwarancusa</i>
EC height	10 m	30 m
Elevation	1650 m	1217 m
Canopy height	8 m	12-15 m
Variables (at half-hourly scale)	Net Ecosystem Exchange (NEE), Net Solar Radiation (NSR), Air Temperature (TA), Vapor Pressure Deficient (VPD), Sensible Heat (SH), Latent Heat (LH), Wind Speed (WS), Relative Humidity (RH), Precipitation (P)	Net Ecosystem Exchange (NEE), Net Solar Radiation (NSR), Air Temperature (TA), Vapor Pressure Deficient (VPD), Sensible Heat (SH), Latent Heat (LH), Wind Speed (WS), Relative Humidity (RH), Precipitation (P)

(C) TIPNET CONFIGURATION		
Study duration (7 weeks/season)	JJA: 17 Jun - 4 Aug 2016 (49 days) SO: 3 Sept - 21 Oct 2017 (49 days)	JJA: 17 Jun - 4 Aug 2016 (49 days) SO: 3 Sept - 21 Oct 2017 (49 days)
Statistical significance test	100 (Method of Shuffled Surrogates)	100 (Method of Shuffled Surrogates)
Bin scheme	Local Binning	Local Binning
PDF estimation	Fixed method	Fixed method
Number of bins	100	100
Number of lags	12 (06 hrs)	12 (06 hrs)

The present study uses the information theory approach to investigate the hydrometeorological controls on the carbon uptake variability of the Oak and Pine ecosystems of the Himalayas. The process networks are generated with the Temporal Information Partitioning Network (TIPNet) framework proposed by Goodwell and Kumar (2017a,2017b). The process network consists of nodes representing the variables, and the connections between these variables are termed links (Ruddell and Kumar 2009a, 2009b). The TIPNet is a multivariate system characterized based on Shannon’s entropy (Shannon 1948) which measures the uncertainty that occurs and detects the nonlinear and weak dependencies in the system. The Shannon’s entropy $H(Y)$ of the given discrete time series in the system is provided as (Shannon 1948):

$$H(Y) = -\sum p(y) \log_2(p(y)) \dots\dots\dots (1)$$

Entropy-based statistics such as mutual information (MI) and transfer entropy (TE) indicate the connections that appear in the networks. MI shows the real-time links between two variables without considering the direction of information flow (Kaiser and Schreiber 2002). It indicates the information exchange among the system variables and does not associate with the direction of information flow (Kaiser and Schreiber, 2002). In the system of two source variables, the total flow of information is as follows (Goodwell and Kumar 2017a; 2017b):

$$I(Y_{s1}, Y_{s2}; Z_{tar}) = \sum p(Y_{s1}, Y_{s2}, Z_{tar}) \log_2 \left\{ \frac{p(Y_{s1}, Y_{s2}, Z_{tar})}{p(Y_{s1}, Y_{s2}) p(Z_{tar})} \right\} \dots\dots\dots (2)$$

The indicator of causality, TE, represents the strength of information transferred from the memory of the system variable to the target variable at the present state and is associated with the direction of information flow (Schreiber 2000). It is a measure of uncertainty present in the system and a strong indicator of causality. In this, the target uncertainty can be reduced by calculating the conditional MI, which signifies the TE of the multivariate system (Goodwell and Kumar 2017a; 2017b):

$$I(Y_{s1}, Z_{tar} | Y_{s2}) = I(Y_{s1}, Y_{s2}; Z_{tar}) - I(Y_{s2}; Z_{tar}) \dots\dots\dots (3)$$

Where the Y_{s2} is received from the target history and adapted as $Z_{tar}(t - \tau)$. Therefore, the TE indicates the MI amongst the target variable at $(t - \tau)'$ which conditioned on the target variable in past

$(t - \tau)'$. TE estimation follows the probability density function (pdf) for lagged sources and targets. The study duration details and the TIPNet configuration used during the development of networks are shown in Table 1C.

2.2 Data collected and Equipments utilized (max. 500 words)

- Data collected through stratified sampling using grid based approach is the first time implementation of the approach to assess plant diversity of Kosi and Sainj watersheds. Data collected would be helpful to provide conservation strategies.
- Apart from the data generated from this project using sap flow sensors, no data is available on transpiration of Pine and Oak systems in India, as of now. However, a research was carried out in central Himalaya, Nepal where transpiration rate of *P. roxburghii* was reported (Ghimire et al., 2014). Data collected through sap flow would provide species specific information of water use.
- In this study, run-off plot experiments for understanding runoff generation mechanism and micro-watershed monitoring for hydrological assessment have been conducted in a paired micro watershed dominated by Pine and Oak forests of the upper Kosi river catchment in the Kumaon Himalayas in Uttarakhand.
- Soil CO₂ efflux using generated data is beneficial for predicting rate of CO₂ emissions and sequestration of two contrasting forest type to suggest effective CO₂ emissions reduction and mitigative measures under a rather warmer scenario.

2.3 Details of Field Survey conducted, if any (max 500 words)

Extensive field survey was conducted in order to assess grid-wise plant diversity under the Kosi- and Sainj watersheds area. Similarly, field surveys were conducted to identify the resource utilization pattern of Pine and Oak under the Kosi-watershed area using a questionnaire survey method. Apart from this, a field survey was conducted in the Shitlakhhet region for spring geo-tagging. A project end field visit was organized by GBP-NIHE, Almora for the entire research team in order to get the idea of the augmented instrumentation and Pine-Oak distribution over the Kosi-watershed area.

2.4 Strategic Planning for each activity with time frame (max. 200 words)

Each activity of the project had a pre-defined methodology to follow. However, due to country wide lockdown during 2020, the instrumentation procurement and installation got delayed.

Activity	Y1				Y2				Y3			
	Q1	Q2	Q3	Q4	Q1	Q2	Q3	Q4	Q1	Q2	Q3	Q4
Field survey for Phytosociology, EIA @ U.K.			■	■			■	■				
Field survey for Phytosociology, EIA @ H.P.							■	■	■	■		
Echo-Hydrological instrumentation and installation @ U.K.					■	■	■	■				
Sap flow sensor installation			■	■								

3 KEY FINDINGS AND RESULTS – supporting documents to be attached.

3.1 Major Activities/ Findings (max. 500 words)

The study aimed at verifying the conjecture that “Oak forests are having higher ecosystem services than the Pine forests and, Pine stands may systematically be replaced with Oak forests, and subsequently the paradigm of water, climate and biodiversity is expected to change significantly from its current state.” The conjecture was primarily tested over the Kosi watershed area (~1800 km²) of Uttarakhand and only biodiversity assessment was carried out in Sainj watershed area (~780 km²) of Himachal Pradesh. The primary plant species distribution assessment indicates that out of total surveyed area under Kosi and Sainj-watersheds, Oak covers around 240 and 08 km² area, whereas Pine occupies around 750 and 44 km², respectively. In terms of ecosystem carbon exchange, both Pine (*P. roxburghii*) and Oak (*Q. leucotrichophora*) dominated ecosystems were found to be a sink of carbon (600-1000 gC/m² for Pine and 500-800 gC/m² for Oak). We have also identified a rainfall amount threshold for Pine and Oak-dominated ecosystems (10 ± 0.7 and 17 ± 1.2 mm, respectively) that resulted in highest ecosystem carbon assimilation in monsoon. Diurnal pattern of sap flux density of *P. roxburghii*, *Q. leucotrichophora*, and *Q. glauca* trees are calculated along with emphasis on Pine and Oak seasonal pattern of sap flux densities. The initial results indicated *P. roxburghii* has almost 1.5-2.0 times the sap flux densities than the other two *Quercus* species indicating higher water extraction by the *P. roxburghii* stands. When information network theory was used to identify micro-met controls effecting ecosystem carbon assimilation, we find that *P. roxburghii* dominated ecosystem is heat dominating while *Q. leucotrichophora* dominated ecosystem is moisture dominating at sub-daily scale. When plot scale water budget was estimated for *P.*

roxburghii and *Q. leucotrichophora* dominated ecosystems, for an annual rainfall of 972 mm over Pine, the canopy interception loss is noted to be 199.9 mm whereas for a same amount rainfall over Oak, the interception loss was 182.9 mm indicating almost same interception loss. The surface run off characteristics of Pine plots indicated runoff under Pine stands is primarily due to lateral subsurface flows whereas due to higher water holding capacity, runoff under Oak is primarily due to infiltration excess. Moreover, numerical simulations of land surface conditions using Noah-MP model for needle leaf trees over the Kosi-watershed could produce better land surface processes close to observations. The overall inference of this study indicates that *P. roxburghii* dominated ecosystems are better sink of carbon at the cost of higher loss of surface and ground water, consequently, *Q. leucotrichophora* dominated ecosystems are better for soil and water conservation as envisaged by the traditional knowledge.

3.2 Key Results (max. 500 words in bullets covering all activities)

- The primary plant species distribution assessment indicates that out of total surveyed area under Kosi and Sainj-watersheds, Oak covers around 240 and 08 km² area, whereas Pine occupies around 750 and 44 km², respectively.
- The total rainfall received was 972 mm of which the total annual discharge from the Pine watershed was 131 mm while that from the Oak watershed was 348 mm which is approximately 13.5% and 36% respectively. The higher rainfall runoff conversion rate of the Oak watershed is indicative of lesser losses from precipitation in the Oak watershed.
- From the SWAT modelling, LULC impact on water yield was found that urban area contributes more to the surface runoff followed by agricultural and forest area. The contribution of mixed forest and Evergreen areas to surface runoff is approximately same.
- In the Pine forest, during high intensity spells, the rain drops penetrate the canopy more easily resulting in higher throughfall %. Moreover, during winter and pre-monsoon months, the throughfall % recorded in the Pine forest was as low as 34% while during monsoon, it was as high as 96.7%. Furthermore, for the Oak forest stand, because of the dense canopy structure of the Oak forest, a constant throughfall % across rainfall totals, and rainfall intensities was observed.
- In terms of ecosystem carbon exchange, both Pine (*P. roxburghii*) and Oak (*Q. leucotrichophora*) dominated ecosystems were found to be a sink of carbon (600-

1000 gC/m² for Pine and 500-800 gC/m² for Oak). We have also identified a rainfall amount threshold for Pine and Oak-dominated ecosystems (10 ± 0.7 and 17 ± 1.2 mm, respectively) that resulted in highest ecosystem carbon assimilation in monsoon.

- The initial results indicated *P. roxburghii* has almost 1.5-2.0 times the sap flux densities than the other two *Quercus* species indicating higher water extraction by the *P. roxburghii* stands.
- The Noah-MP LSM could reproduce the diurnal, monthly, and seasonal evolution of land conditions such as ST, SM, heat fluxes, and ET and reasonably agrees with the *in-situ* observations. Moreover, Noah-MP products appear to be better than the global analysis datasets most of the time in different seasons.
- Moreover, numerical simulations of land surface conditions using Noah-MP model for needle leaf trees over the Kosi-watershed could produce better land surface processes close to observations.
- When information network theory was used to identify micro-met controls effecting ecosystem carbon assimilation, we find that *P. roxburghii* dominated ecosystem is heat dominating while *Q. leucotrichophora* dominated ecosystem is moisture dominating at sub-daily scale.

Descriptive file

3.2.1. Assessment of Pine and Oak forest distribution under a warmer climate over Himalaya

3.2.1.1: Assessment of Pine and Oak forest distribution over Kosi-watershed area

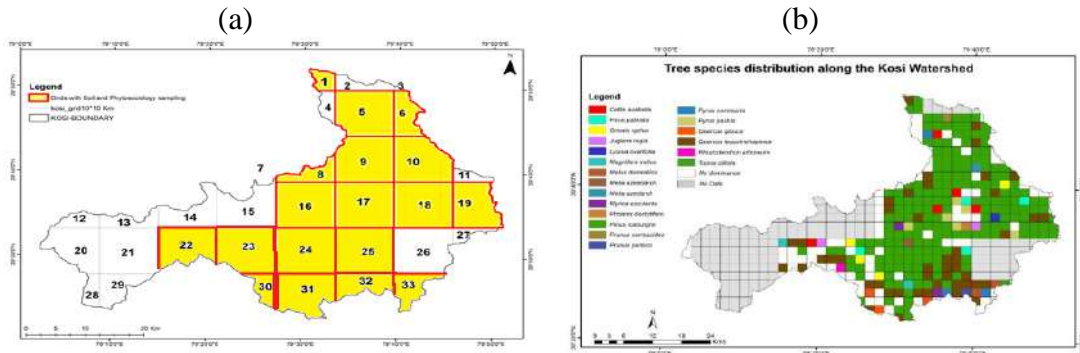


Fig 1: (a) shows the total covered grids for Phytosociology and soil data. Subplot (b) shows the species distribution over Kosi-watershed area.

A total of 18 grids (10 x 10 km) under Kosi-watershed are completed along with Phytosociology and soil data.

Vegetation analysis

The total area under watershed is 1867.6 km². Total area assessed was 1288 km² however for the remaining area was lying under Corbett National Park thus we didn't get the permission from PCCF was field activities in the respective area. Total 10 x 10 km grids completed = 18, total 2 x 2 km grids completed were = 322. Out of which in 188 (2x 2 km) grids i.e., 752km² of area *Pinus* was found to be the dominant species which is about 58 % of total covered area, however *Oak* was found dominant in 60 (2x 2 km) grids i.e., 240 km² which is about of 18.66 % of total covered area, in 36 grids species such as *Pyrus pashia*, *Celtis australis*, *Pyrus communis*, *Rhododendron arboreum*, *Ficus palmata*, *Grewia optiva*, *Ficus palmata*, *Juglans regia*, *Lyonia ovalifolia*, *Magnifera indica*, *Malus domestica*, *Melia azedarach*, *Myrica esculenta*, *Phoenix dactylifera*, *Prunus cerasoides*, *Prunus persica*, *Quercus glauca*, *Toona ciliate* were other species found to be dominant in remaining grids. Around 152km² area was under agriculture land /construction.

Species Richness along the Kosi-watershed area

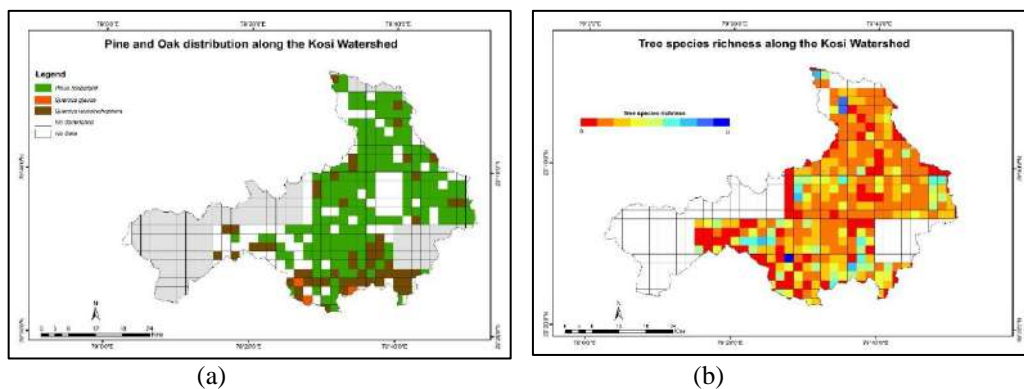


Fig 2. (a) Showing Pine and Oak dominance over the watershed area (b) showing species richness of the area

About 33.54 % of total covered area was found to be Pure Pine Forest and only 1.24 % area is Pure Oak Forest (with no other associated species), about 24.84 % area was dominated by Pine out of which 13.35 % area was co-dominated by Oak and 11.49 % by other species like *Pyrus pashia*, *Myrica esculenta* etc. Focusing on Oak Forest cover 18.63 % area was dominated by Oak out of which in 6.21 % area the co-dominant species was Pine and rest 12.42% the area was co-dominated by other species like *Myrica esculenta*, *Rhododendron arboreum* etc.) Species richness in the area was recorded between low to moderate (0-5) however in some grids it was found to be high (5-7). Results indicate that Oak forests were found to have high species richness as compared to Pine Forest.

Regeneration status of the area

Regeneration status of the area shows that the survival of Oak seedling is very less. Some of the sub-grids indicate good regeneration of *Quercus leucotrichophora* having good number of seedlings but at sapling stage the survival rate was found very less concluding a major threat to Oak Forest cover in future. However, in case of Pine good to fair regeneration was observed in the area.

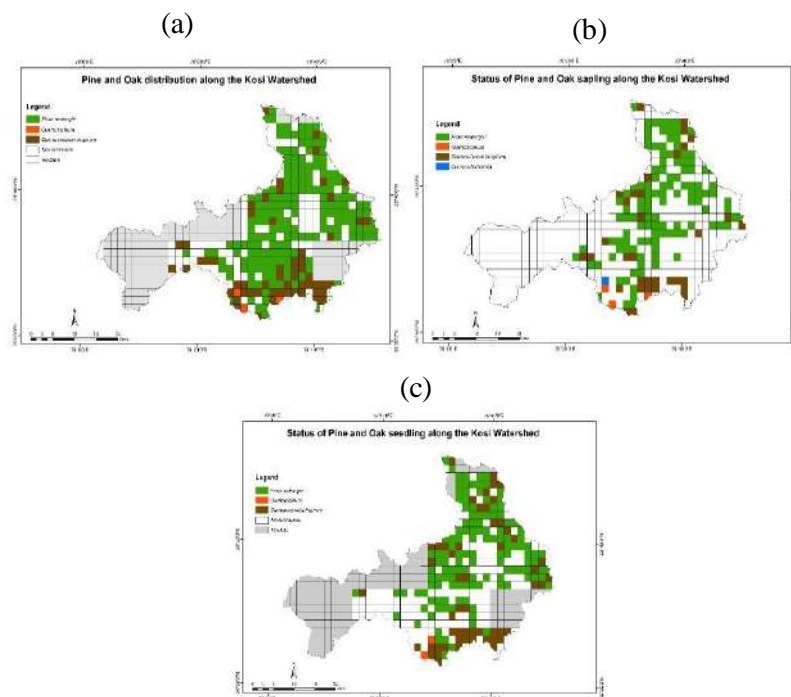


Fig.3. Showing status of Pine and Oak distribution at (a) Tree (b) Sapling and (c) Seedling stage.

Soil Analysis: Physical Characteristics: pH influences the availability of plant nutrient and it is a good indicator of soil fertility. In this study soil pH was varied from 4.3 to 7.85 for Pine dominated forest type, while for Oak dominated it ranges from 4.5 to 7.05, there was no distinct variation in soil pH among the forest type, however in some Oak dominated forest type the value of pH was recorded somewhat low or towards acidic because of the co-dominance of Pine in that region, the values for both Pine and Oak were found low and comparable with the value of Joshi et al., 2021 (6.66 for Pine forest type and 5.9 for Oak forest type) and Pandey et al., 2019 (6.8 for Pine forest type and 5.66 for Oak forest type).

Soil texture play key role in the determination of water holding capacity in the soil. It shows how much of water hold by particular soil particle. Clay soil has highest and sandy soil has lowest WHC. In the present study the values of WHC for Pine Forest ranged between (19 – 84.80) and for Oak Forest type it ranges from (17- 77.08). The values of WHC of some grids are comparable with that of Pandey et al.,2019 (49.23 for Pine – 69.27 for Oak) however some values are higher than that are earlier recorded.

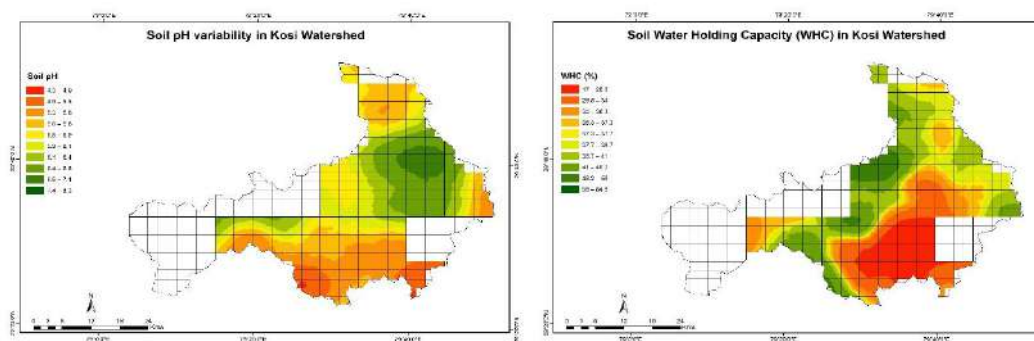


Fig.4. Representing Soil pH data in the Kosi-watershed area

Soil Analysis: Chemical Characteristics: Soil organic carbon is a key factor of carbon cycle and the variations of its accumulation affect global carbon balance of ecosystem directly as well as indirectly. In the present examination soil organic carbon (%) varied from 0.19 -7.80 for *Pinus roxburghii* forest type and 0.69% to 6.63 % for *Quercus leucotrichophora* dominant forest. The value of organic carbon of present study slightly higher as compare (value=2.08 for pine - 4.21% for Oak) with Joshi et al., 2021 also higher than Pandey et al., 2019 (value – 2.78% for Pine and 3.34% for Oak). The high value of SOC can be attributed to higher litter decomposition in Oak forest.

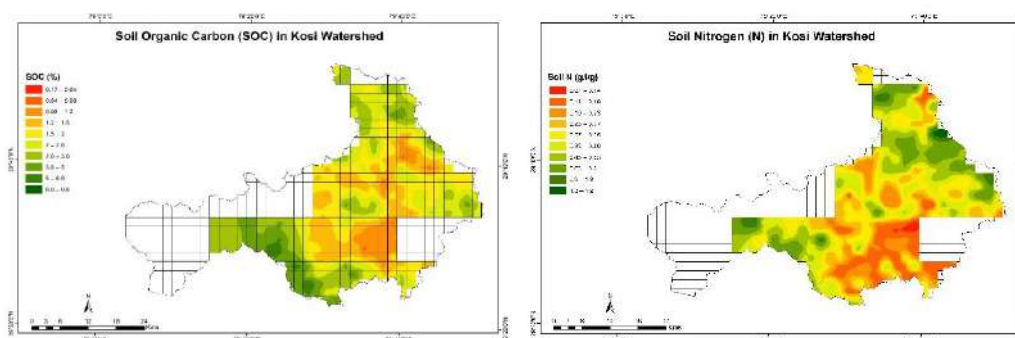


Fig.5. Soil Organic carbon and Nitrogen in Kosi-watershed area

In addition, soil nitrogen is also an important element for plant growth. The nitrogen concentration generally decreased with the increasing soil depth. In the present study, total nitrogen was ranging between (0.07 to 1.83%) for Pine dominated forest, (0.13 – 1.23%) for Oak dominated forest. The value of total nitrogen in present study was comparable (0.26 % for Pine and 0.42% for Oak) with Joshi et al., 2021 also with Pandey et al., (0.23 for Pine and 0.35 for Oak) and the minimum value for total N (0.07%) is comparable with that of Khera et al., 2001 (0.04 and 0.11%). Similarly, The value of K ranges between 0.02 to 1.57 for Pine dominated forest and 0.03 – 1.02 for Oak dominated forest. The value of K was found to be lower in Nainital region as compared to Almora as due to the change in vegetation type. In general, Potassium content can be

found in soluble form and in all parts of plants and responsible for the formation of carbohydrate and protein. Soil analysis for phosphorus indicated percentage of phosphorus was recorded ranging between 0.007 to 0.48 for Pine dominated forest and 0.017 to 0.64 for Oak dominated Forest. The minimum value of P for both Pine and Oak dominated forest was found to be low as compared with Joshi et al.,2021 (0.11 for Pine and 0.031 for Oak).

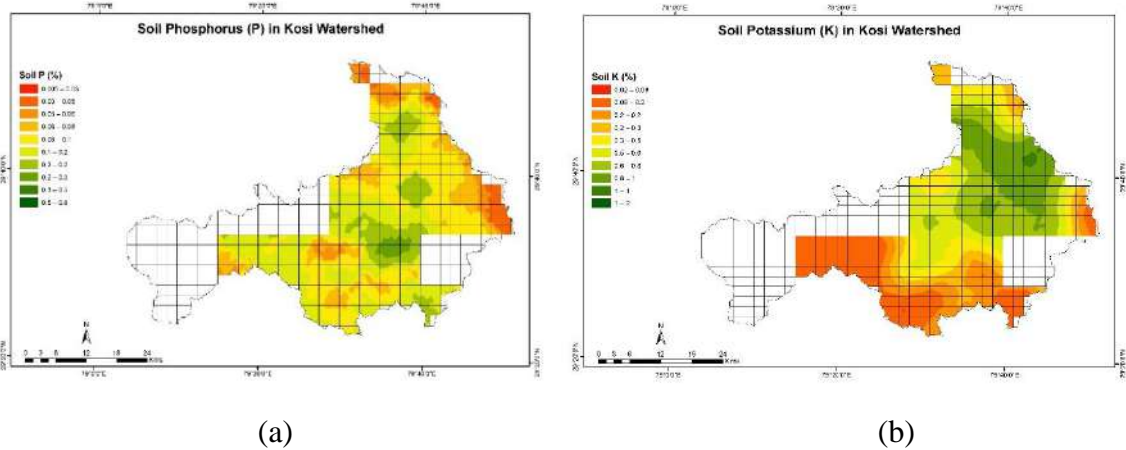


Fig. 6 (a) – Total Phosphorus ; (b) - Total Potassium in Kosi- watershed area

Species diversity along the altitude gradient over Kosi-watershed area

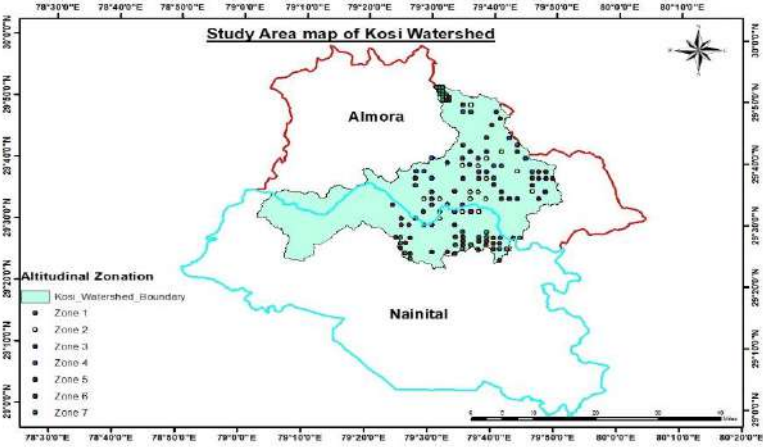


Fig.7 Zones Distribution map of area

For evaluating the impact of altitude on species diversity. The total covered grids were categorized into different gradient in 20 0m scale over Kosi - watershed. Further we have randomly selected 20 (2x2 km) i.e 80 sqkm area at each altitude gradient for analysis of plant diversity. Based on the altitudinal gradient of the study area, it was divided into 7 altitudinal zones for detailed vegetation analysis Zone 1(1000-1200m), Zone 2 (1200-1400m), Zone 3 (1400-1600m), Zone 4 (1600-1800m), Zone 5(1800-2000m), Zone 6(2000-2200m) and Zone 7 (2200-2400m).

Species diversity along altitude zones: In the present study total of 32 tree species belonging to 23 Genera and 18 families were recorded over different altitudinal gradient. The species richness ranged from 20 to 11 across the altitude gradient 1000- 2400 m. However, at highest elevation the species richness (11) and Margalef's index (1.55) was found minimum while the maximum species richness (20 species) and Margalef's index (2.93) were recorded for altitude range 2000-2200 m. Menheink's index ranged between 0.94 to 0.44, the minimum value (0.44) was recorded for the highest elevation 2200 – 2400 m asl (Table 2), significantly correlating with value of Sharma et al (2009) that was (0.272) for the highest elevation 2800-2700 m asl, whereas the maximum value (1.76) was noted for 1200- 1400 m asl, followed by (0.84) for 1000- 1200 m asl altitude range. This shows an uneven distribution of species in different altitudinal zones over Kosi-watershed area. Species richness was found highest in the mid-altitudinal ranges are also reported in Garhwal Himalaya (Grytness and Vetaas (2002) and Grytness (2003) in other temperate forests. The lower species richness at lower altitude can be due to the fact that major part of lower areas was disturbed due to construction of resorts, dams, agriculture etc. Compared with other zones the highest density (807 trees ha) was recorded for the altitude zone 2000-2200m followed by the altitude zone 2200- 2400 (776 trees ha⁻¹) while the lowest density was observed for 1200-1400 m (201 trees ha) (Table 1).

Altitude (m asl)	SR	H' diversity	CD	MI	MeI	Density(ind/ha)
1000-1200	13	1.47	0.58	2.19	0.84	296.25
1200-1400	12	1.76	0.75	2.16	0.94	201.25
1400-1600	11	1.35	0.64	1.67	0.56	481.25
1600-1800	18	1.66	0.68	2.67	0.75	720
1800-2000	14	1.39	0.37	2.07	0.61	648.75
2000-2200	20	2.07	0.81	2.93	0.78	807.5
2200-2400	11	1.52	0.70	1.55	0.44	763.75

Table. 1 Total species richness and diversity parameters of trees species along different altitudinal gradients. SR= Species richness, MI= Margalef's index, MeI = Menheink's index, H' = Shannon Diversity, Cd= Concentration of Dominance (Simpson's Index).

All the zones were found to be Pine dominated except Zone 7(2000-2200m) that was found to be Oak dominated. Zone 2 was found to be dominated with Pine with highest IVI values (Table 2).

Zone	Altitudinal Range (m asl)	Dominant Tree species	IVI Values
Zone 1	1000-1200	Pine dominant	120.68
Zone 2	1200-1400	Pine dominant	155.50
Zone 3	1400-1600	Pine dominant	94.51
Zone 4	1600-1800	Pine dominant	90.34

Zone 5	1800-2000	Pine dominant	94.77
Zone 6	2000-2200	Quercus dominant	61.26
Zone 7	2200-2400	Pine dominant	94.56

Table 2: Species dominance Based on IVI values

Diversity parameters and indices: Tree species diversity along altitudinal gradient showed differences in species diversity indices. In general, the Shannon diversity index (H') showed a linear trend along with altitudinal gradient with maximum diversity at Zone 6 (2000-2200m). The difference in species diversity at different altitude were reported in the analysis. The overall maximum species diversity (Shannon-Weiner diversity) (2.07) was reported for Zone 6 (2000-2200m). However, the second maximum species diversity (1.76) was reported for altitude zone, whereas the minimum value of Shannon-Weiner diversity (1.35) was observed for altitude range 1400-1600 m. The value of species diversity of the study area was ranging between 1.35 to 2.07 which shows that Kosi- watershed has low to moderate species diversity which are comparable with those of Sharma et al (2009; 0.99-2.37), Bhat et al (2020; 2.097-3.373), Singh. S. et al (2016; 1.27-1.86) in different regions of Uttarakhand.

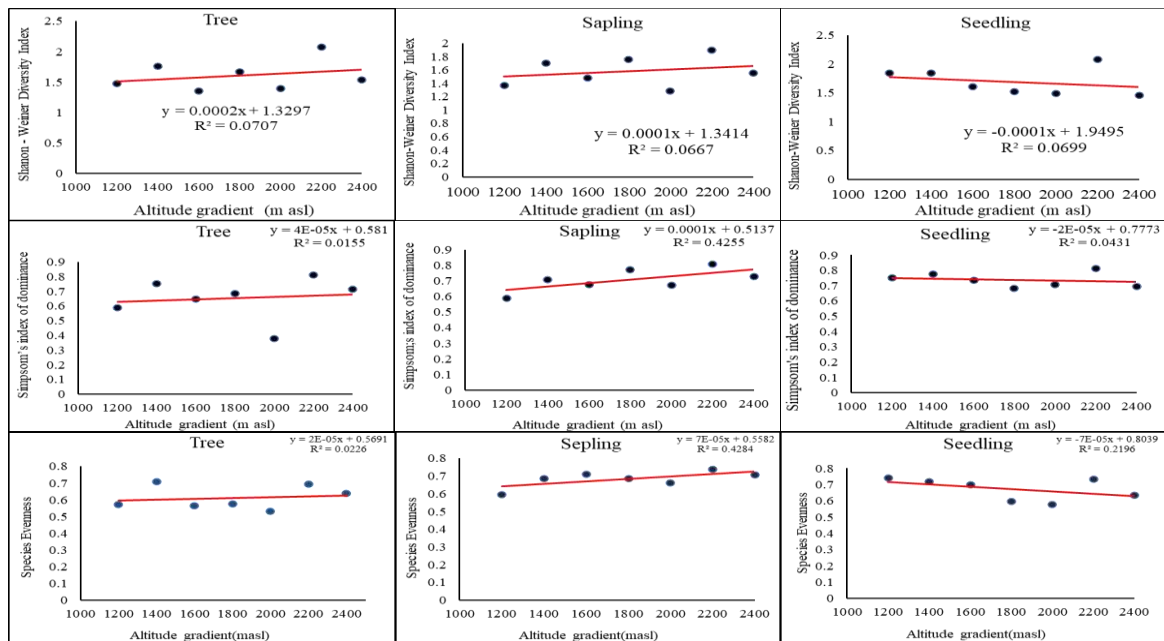


Fig.8. Species diversity parameters along the altitude gradient

Simpson's index or Concentration of Dominance

The Simpson's index or Concentration of Dominance (CD) was reported between 0.37 to 0.81 however same values was reported by Sharma et al. (2009) in a study on temperate mixed forest were 0.237, 0.246, 0.349. 0.56 for Oak, Oak-pine, Oak- scrub and Chir Pine dominated forests. The maximum value of Simpson's diversity index (0.81) was recorded for the altitude zone 2000-2200 m, followed by Zone 1200-

1400m (0.75), whereas the minimum Simpson's diversity index (0.37) was observed for 1800-2000m altitude range.

Evenness Index

The highest evenness index value was recorded for the altitude zone 1200-1400m which was (0.70) which represents a unstable community but somehow tending towards a stable community as the value is near 0.75 and the lowest evenness index values was for altitude 2000-2200m altitude (0.53) which represents a highly unstable community however it was noted that the highest species diversity value (2.07) was recorded highest for the same altitude zone as this altitude zone was only *Quercus* dominant altitude zone as compared with other zones.

Beta-diversity

β - diversity is showing an decreasing trend with altitude which signifies that species composition is changing with increasing altitude indicating low level of similarity .

	Zone 1	Zone 2	Zone 3	Zone 4	Zone 5	Zone 6	Zone 7
Zone 1							
Zone 2	0.6						
Zone 3	0.41667	0.65217					
Zone 4	0.54839	0.53333	0.31034				
Zone 5	0.55556	0.69231	0.28	0.25			
Zone 6	0.69697	0.625	0.48387	0.31579	0.29412		
Zone 7	0.75	0.47826	0.45455	0.37931	0.36	0.35484	

Fig.8. Showing beta-diversity along altitudinal gradient

Biomass and Carbon stock

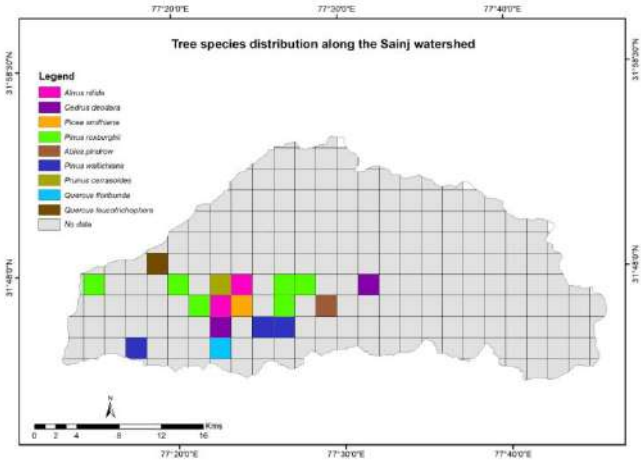
The study reveals that the highest ABG (162.03) value was recorded for Zone 6 (2000-2200m) having the highest species richness (20) and the only *Quercus*. dominated zone as it was observed for Zone 4 that despite of having high density (ind/ha) the biomass value was recorded low (73.76 t/ha) it is also observed from the results that despite of having *Pinus roxburghii* as dominant species at Zone 4, Zone 5, Zone 7 the biomass value was found to be more for *Quercus leucotrichophora* for the respective three zones, as it can be due to tree characteristics like DBH as reported by (Feldpausch et al.,2012) that lower values of DBH results into lower biomass and Carbon sequestration.

Altitude Zone	Density(ind/ha)	Total ABG Biomass (Megagram per hectare)	Total Carbon Stock
Zone 1	296.25	45.74	21.72
Zone 2	163.75	22.80	10.83

Zone 3	481.25	84.24	40.01
Zone 4	720	73.76	35.03
Zone 5	648.75	126.78	60.22
Zone 6	807.5	162.03	76.96
Zone 7	776.25	148.65	70.61

3.2.1.2: Assessment of Pine and Oak forest distribution over Sainj-watershed area

Only plant diversity assessment has been carried out for Sainj watershed area. A total of 80 km² area has been assessed for plant diversity till now. A total of 22 tree species were recorded belonging to 20 genera and 15 family. 2 species of Pine that are *Pinus roxburghii* and *Pinus wallichiana* were recorded and 2 species of Oak *Quercus leucotrichophora* and *Quercus floribunda* were recorded. Out of total covered area Pine was dominated in 44 km² area and Oak was also dominated in 8 km² area. Remaining 28 km² area was dominated by other species such as *Alnus nitida*, *Prunus cerasoides*, *Picea smithiana*, *Cedrus deodara*, *Abies pindrow*,



Conclusion

Around 58.38% of total covered area of watershed is dominated by *Pinus roxburghii* and 18.63 % area is dominated by *Quercus spp.* vegetation which signifies the pine dominance over the area. Some of the grids indicate maximum dominance of *Pinus roxburghii* and co-dominance of *Quercus leucotrichophora*. Similarly, in some sub-grids we found dominance of *Pinus roxburghii* at tree stage but *Quercus leucotrichophora* was found dominant at sapling and seedling stage which can further replace the *Pinus roxburghii* if the forest can be protected from forest fire. The species composition of both the watersheds is different.

References

Bhuyan, P., Khan, M.L. and Tripathi, R.S. (2003). Tree diversity and population structure in undisturbed and human impacted stands of tropical wet evergreen forest in Arunachal Pradesh, Eastern Himalayas, India. *Biodiversity and Conservation*, 12:1753–1773.

Curtis, J. T. (1959). *The Vegetation of Wisconsin, An Ordination of Plant Communities*. University Wisconsin. Press, Madison, Wisconsin.

JOSHI, V. C., BISHT, D., Sundriyal, R. C., CHANDRA, N., & ARYA, D. (2021). PHYSICO-CHEMICAL PROPERTIES OF SOIL IN RELATION TO SPECIES COMPOSITION AND DIVERSITY OF SUBTROPICAL AND TEMPERATE FOREST STANDS IN THE WESTERN HIMALAYA. *Asian Journal of Plant and Soil Sciences*, 6(2), 37-45

Khan, M.L., Rai, J.P.N. and Tripathi, R.S. (1987) Population structure of some tree species in disturbed and protected sub-tropical forests of north-east India. *Acta Oecologica-Oecologia Applicata*, 8: 247–255.

Misra, R. (1968). *Ecology Work Book*. Oxford and IBH publishing Co., New Delhi.

Muller-Dombois, D and Ellenberg, H. (1974). *Aims and Methods of Vegetation Ecology*. John Wiley and sons, New York.

Negi, G. C. S., Rikhari, H. C., & Garkoti, S. C. (1998). The hydrology of three high-altitude forests in Central Himalaya, India: a reconnaissance study. *Hydrological processes*, 12(2) :343-350.

Okalebo, J. R., Gathua, K. W., & Woome, P. L. (2002). Laboratory methods of soil and plant analysis: a working manual second edition. *Sacred Africa, Nairobi*, 21.

Osman, K. T. (2013). Plant nutrients and soil fertility management. In *Soils* (129-159). Springer, Dordrecht.

Ralhan, P. K., Saxena, A. K. and Singh, J. S. (1982). Analysis of forest vegetation at and around Naini Tal in Kumaun Himalaya. *Proceedings of the Indian National Science Academy-Part B: Biological Sciences*, 48(1) :121-137.

Rawat, Y. S., & Singh, J. S. (1988). Structure and function of oak forests in central Himalaya. I. Dry matter dynamics. *Annals of Botany*, 62(4) : 397-411.

Saxena, A. K. and Singh, J. S. (1984). Tree population structure of certain Himalayan Forest associations and implications concerning their future composition. *Vegetatio*, 58(2) :61-69.

Semwal, R. L. and Mehta, J. P. (1996). Ecology of forest fires in chir pine (*Pinus roxburghii* Sarg.) forests of Garhwal Himalaya. *Current Science*, 70(6) :426-427.

Shankar U (2001) A case of high tree diversity in a sal (*Shorea robusta*)-dominated lowland forest of Eastern Himalaya: Floristic composition, regeneration and conservation. *Current Science* 81: 776–786.

Shannon, C. E. and Weiner, W. (1963). The mathematical theory of communication *Urban University Illinois Press*. 125pp.

3.2.2. Assessment of hydrological budget of Pine-Oak dominated watersheds and future scenarios under a warmer climate

3.2.2.1. Understanding the Role of Land Use-Land Cover in Runoff Generation in the Upper Kosi River Catchment using SWAT Model:

The following sections discuss the sensitivity analysis of the SWAT parameters, the results for calibration and validation of the model, the model performance and the model outputs and hydrological insights.

Sensitivity Analysis

In SWAT, the calculation of surface runoff, sediment erosion, etc., requires a number of parameters, making the calibration process very complex and challenging. Sensitivity analysis is a process of finding out which parameter is more sensitive. Sensitive here refers to a marked change in model output with respect to even a small change in model input. In the present work, SWAT-CUP is used for sensitivity analysis. Having prior information about the sensitive parameters can help us reduce and quantify the uncertainty in model output. The most sensitive parameters were identified as GW_DELAY.gw, CH_N1.sub, GWQMN.gw, and RCHRG_DP.gw. These parameters are described briefly below.

- GW_DELAY.gw: The Time required for water to leave from the bottom of the root zone to the deep aquifer
- CH_N1.sub: Manning coefficient for tributary channels
- GWQMN.gw: Threshold depth of water in the shallow aquifer required for return flow to occur (mm)
- RCHRG_DP.gw: Deep aquifer percolation fraction from the root-zone to deep aquifer

The sensitivity analysis provided the range of the different model parameters, and also the sensitivity rank to help identify the sensitive model parameters.

Calibration and Validation

Calibration can be defined as the process of estimating model parameter values to enable a hydrologic model to match observations such as streamflow. Calibration is the process in which small changes are made in the parameter value to simulate model output much closer to real observed data. Calibration can be done manually and automatically or a mix of both manual and automatic. SWAT-CUP was used to calibrate the SWAT model. After finding the fitted value, this value is used in SWAT-model to run a simulation for the calibration period. Furthermore, the sub-basin output is again checked in the validation part to evaluate the model performance.

Evaluation of model performance

The performance metrics and graphical method are used to see how closely observed data mirrors the expected data. It is an indication of the accuracy and efficiency of any model. Furthermore, all these compare observed values with simulated values and give an indication of well our model performs. In this study, calibration and validation are done on the monthly time steps. The monthly time step is robust enough to characterize long-term trends in water yield and LULC changes.

Performance metrics are defined using three terms given below

1. Nash-Sutcliffe simulation efficiency (NSE)
2. Coefficient of determination (R^2)
3. Percent bias (PBIAS)

Performance of the model in the calibration period

Calibration is done on the monthly time steps for two years, Jan-2014 to Dec-2015. After choosing the best sensitive parameter value, the model returns the simulated time series. A comparison of observed and simulated time series is given in Figure 3. The figure reveals distinct features like peaks, time to peak, and flow behaviour between simulated and observed data. The model captures the overall trend in the dataset but still underperforms in capturing the high flow peaks. For the calibration period, the performance metrics were 0.45 (NSE), 0.37 (R^2), and 2.9 (PBIAS).

Performance of the model in the validation period

In validation processes, we check the simulated value of the model after changing parameters. Validation has also done for a monthly time steps period of two years, from Jan-2016 to Dec-2017, after getting the fitted value in the calibration period. Figure 3 shows a comparison of simulated and observed time series. Model performance in the validation period is better than in the calibration period. Goodness-of-fit values between observed and simulated values are within acceptable limits. during the validation period, performance metrics were 0.60 (NSE), 0.75 (R^2), and 2.07 (PBIAS) There is an increase in the magnitude of all the evaluation metrics (NSE, R^2 , PBIAS), which again indicates better model performance. The results obtained for the performance metrics in the calibration and validation stage indicate that the model is well suited for evaluating the LULC impact on water yield for the Kosi basin. In the next section, we evaluated the model output for quantifying this LULC dependence for water yield.

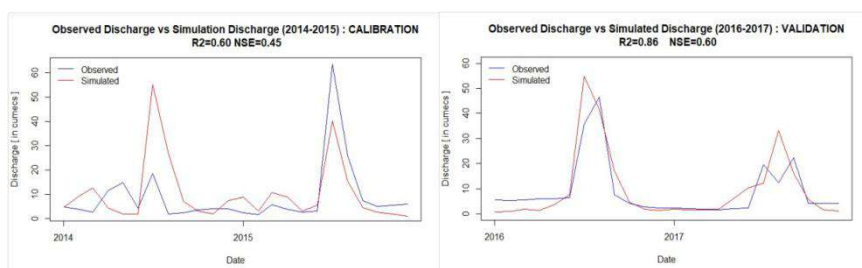


Fig. 3. Monthly observed and simulated discharge during the calibration period.

Analysis of model output

[A] Average annual stream flow rate from the entire basin

The average annual water yield of the whole basin comes out to be in the range of 6 to 12 m³/sec (Fig.11). The yield in 2014 and 2016 was higher than in 2015 and 2017. This indicates a possible oscillatory nature of the water yield dependence. More work can be done to quantify the possible forcing(s) for such marked changes in annual water yield.

[B] Seasonal variation in stream flow rate : The duration is divided into four different temporal windows: Post Monsoon (Rabi) – January to March, Pre-Monsoon – April to June, Monsoon – July to September, Post – Monsoon (Kharif) - Oct to Dec. This helps in quantifying the seasonal variation in the water yield. Figure 4 shows that Monsoon consistently exhibits a higher water yield throughout all the years, and after that, in 2014 and 2015, the Post-Monsoon (Rabi) season gives second higher values. However, this pattern changed in 2016, and in 2017 Pre-Monsoon offered a higher value than the Post-Monsoon (Rabi). Year-wise, we can infer that the total yield in 2014&16 was higher than in 2015&17. The seasonal changes are an indication of altering monsoon and other hydro climatic mechanisms.

[C] Region-wise analysis in the basin

Kosi-basin is divided into the Upstream region, Midstream region, and Downstream region for the sub-basin analysis. Upstream region consists of sub-basin numbers 1,2,3,4,5,6 and 7, the Midstream region consists of sub-basin 8,9,11,12,13,14,15 and Downstream region consist of sub-basin number 16,17,18,19,20,21. The various sub-basins and their regions are depicted in Figure 5. Red denotes the Upstream, green denotes the Midstream, and pink denotes the Downstream regions.

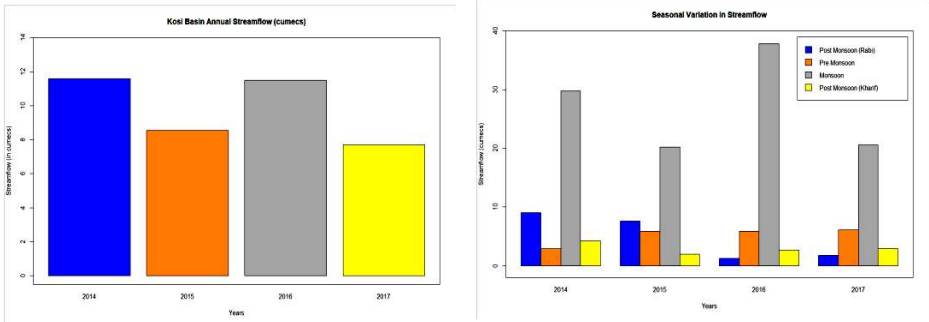


Fig.4. subplot (a) shows average annual streamflow rate in cumecs from the Upper Kosi Basin and subplot (b) Seasonal variation in streamflow rate in upper Kosi basin.

The yield rates for the three regions are shown in Figure 6. We find that the downstream region gives more yield than others, followed by Midstream and the upstream. The yield in Downstream is higher than the Total Average. The water yield depends on the LULC present in the region and precipitation patterns, and many other factors. Next, we try to quantify the LULC impact on water yield.

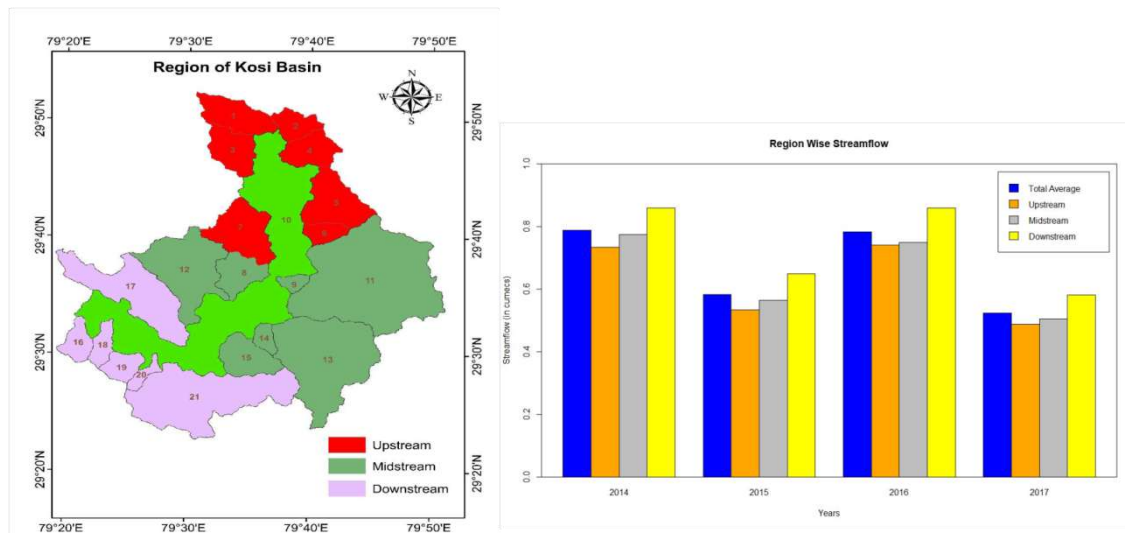


Fig.5 Regions of the upper Kosi basin. And Region-wise streamflow rates for the upper Kosi basin.

[D] Land-use and land-cover impact on water yield

[D1] LULC fraction in different sub-basin

- Kosi region consists of 5 LULCs classes, namely, forest-mixed, forest-evergreen, pastureland, agricultural land, and urban land. The fraction of urban land is less; due to this, it is not considered in the remainder of the analysis.
- Forest-mixed is more in the sub-basin numbers 11,14,15 and 21 in the range of 81-93 % value and medium in the 6,7,8,13,19 and 20 sub-basins in the range of 62-80% and is lowest in the 16,17 sub-basins in the range of 41-49%.
- Forest evergreen is more in the sub-basin numbers 1,2,12, and 16 in the range of 29-46 % value and medium in the 3,4,5,18,19 and 20 sub-basins in the range of 12-28% and is lowest in the 7,8,11,14,15 sub-basins in the range of 0-11%.
- Agricultural land is more in the sub-basin numbers 9, and 17 in the range of 17-42 % value and medium in the 3,5,7,8 and 12 sub-basins in the range of 10-16% and is lowest in the 13,15,16,21 sub-basins in the range of 0-2%.
- Pastureland is more in the sub-basin numbers 7 and 11 in the range of 5-6 % value and medium in the 3,4,8 and 13 sub-basins in the range of 3-4% and less in the 1,2,5,6,12,14,15,16-21 subbasin in the range of 0-2%. These all-land cover values are depicted in figure 6.

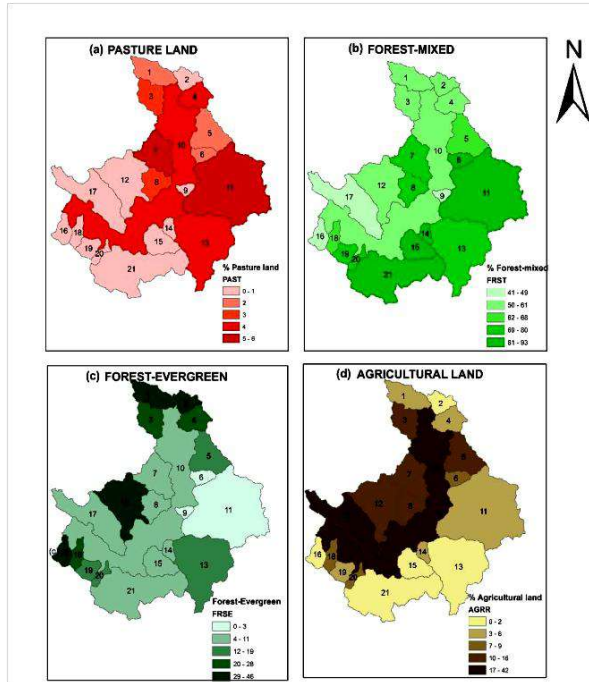
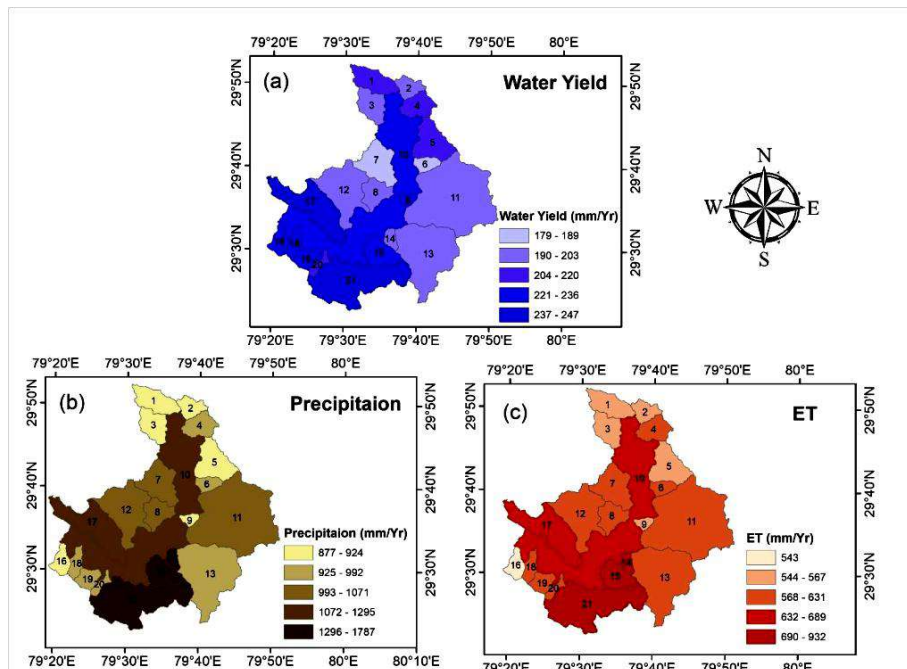


Fig 6 : Percent area covered by LULC classes in different sub-basin

[D2] Water yield, precipitation, and evapotranspiration value in different sub-basin

The water yield of a sub-basin depends mainly on the precipitation and evapotranspiration in this sub-basin.



Values of these are given in Figure 7.

Fig.7 Water yield, precipitation, and Evapotranspiration value in different sub-basin

From the Fig.7, it can be seen Water yield (mm/year) is more in the sub-basin number 17, 21 in the range 237-247 mm/year and medium in the 9,16,18,19 in the range of 221-236 mm/year and lowest in the sub-basin 6-7 in the range of 179-183 mm/year. Precipitation (mm/year) is more in the sub-basin number 14,15,21 in the range 1296-1787 mm/year. And medium in the 11,17 in the range of 993-1295 mm/year and lowest in the subbasin 1,2,3,5 in the range of 877-924 mm/year. Evapotranspiration (mm/year) is more in the sub-basin number 14,15,21 in the range 690-932 mm/year and medium in the 17 in the range of 632-689 mm/year and lowest in the sub-basin 1,2,3,5 in the range of 543 mm/year.

[D3] Relationship between land use-land cover and water yield for different sub-basin

To define a relationship, several sub-basins are selected. The chosen sub-basins compose all the three major classes – High, Medium, and Low. Table 1 shows the water yield values and LULC fractions for the selected sub-basins.

Some of the major observations are:

- ✓ Sub-basin number 21,17 has markedly different precipitation rates for almost the same water yield. A possible reason is seen in examine the relative fraction of different LULC classes. Higher Agricultural land (41%) in sub-basin 17 may be one of the crucial factors for the higher water yield. A similar pattern can also be seen in sub-basin numbers 16 to 19.
- ✓ The similar water yields in Sub-basin numbers 11 and 12 with near equal precipitation rates but different forest evergreen and forest-mixed fraction rates show that both land cover classes are nearly identical from a water yield perspective.
- ✓ Sub-basin number 9, with 31% urban area, has an approximately same yield as subbasin 21 with less precipitation, which means the impact of lesser precipitation is offset by the higher water yield contribution of the urban land cover class.
- ✓ Sub-basin number 9 is further compared with 17, and it shows that the Urban area has a higher yield impact compared to agriculture.

Water yield categories	Sub-basin Number	Water yield range(m m/year)	Precipitation range (mm/year)	Evapotranspiration range(mm/year)	Forest mixed (%)	Forest Evergreen (%)	Agricultural land (%)	Pasture land (%)
High	21	246.7	1736.6	903.5	89.6	8.7	0	0.2
High	17	245.6	1294.6	688.6	48.9	7.5	41.9	0
Medium to high	16	233.2	877.0	543.4	49.1	45.6	0.6	0
Medium to high	19	232.8	963.5	585.3	76.1	17.3	5.5	0
Medium	9	245.6	890.2	543	41.2	0	27.6	0 (31% URBN)
Medium	4	212.5	984.6	594	61.4	27.6	5.3	3.4
Medium	11	198.6	1021.1	615.3	85.1	2.7	5.4	5.7
Medium	12	197.6	1023.7	610.7	52.5	33.9	11.8	0.6
Low	6	188.8	986.1	606.0	89.6	2.5	6.4	1.4
Low	7	179.3	1071.1	631.3	72.6	5.3	16.2	5.2

Table 1. sub-basin wise water yield and land cover values.

Conclusions from modelling studies.

The model was successfully set up, and after calibration and validation, these conclusions can be made from the present work:

- GW_DELAY.gw, CH_N1.sub, GWQMN.gw, and RCHRG_DP.gw were the most sensitive parameter, which indicates that the water yield in the basin is highly sensitive to groundwater parameters.
- The values of performance metrics were $NSE = 0.45$, $R^2 = 0.37$ and $PBIAS = 2.9$ for calibration and $NSE = 0.60$, $R^2 = 0.75$ and $PBIAS = 2.07$ for validation. Though the model was not able to simulate high and low flows very well, but given the limited availability of data, the model could reasonably simulate the water yield.
- SWAT model simulations indicated that the downstream sub-basins contribute more water yield followed by the midstream sub-basin and upstream sub-basin.

After analysing LULC impact on water yield, it is found that urban area contributes more to surface runoff followed by agricultural and forest area. The contribution of mixed forest and Evergreen areas to surface runoff is approximately the same

3.2.2.2. Estimation of water yield of a Pine and a Oak forest dominated micro-watershed of U.K.

Two small experimental watersheds in close areal proximity to the GBPIHED, Kosi-Katarmal, Almora were monitored at its outlet for estimation of water yield. The hydrological assessment was carried out over an altitudinal range of 1400m to 2200m a.s.l. Both watersheds are situated between 1400m and 2200m a.s.l. with Sitlakhth located upward of 1900m while Papoli downslope from 1700m. The two watersheds are almost identical in some geomorphological characteristics, but the vegetation types vary considerably between them. Some characteristics of the Pine and Oak watersheds are tabulated below.

Characteristics of Pine and Oak watershed

Parameters	Pine Watershed	Oak Watershed
------------	----------------	---------------

Watershed identifier	Papoli	Sitlakheth
Latitude	79.5834 °E	79.5520 °E
Longitude	29.6458 °N	29.5861 °N
Altitude (m a.s.l.)		
Maximum	2191	1658
Minimum	1946	1395
Aspect	North	North
Area	90.8 ha	91.2 ha
Soil Texture	Silt Loam	Silt Loam
Gravel (%)	34.32 ± 6.76	3.06 ± 1.43
Sand (%)	33.52 ± 5.43	30.46 ± 5.25
Silt (%)	31.28 ± 2.09	63.09 ± 3.77
Clay (%)	0.88 ± 0.37	3.39 ± 0.94
Volumetric moisture at saturation (%)	37.77 ± 3.38	52.51 ± 4.82
Bulk Density (g/cc)	1.65 ± 0.12	1.10 ± 0.15
Porosity	35.04 ± 3.93	53.83 ± 6.00

The Pine watershed is largely covered by *Pinus roxburghii* followed by *Myrica esculenta* and *Quercus leucotrichophora*, while the Oak watershed is predominantly covered by *Quercus leucotrichophora* followed by *Rhododendron arboreum*, *Lyonia ovalifolia*, *Q. glauca* and others. Remote sensing based LULC map reveal that Papoli has 64% forest cover, while Sitlakheth has 57.6% forest cover. Agriculture on the hillslopes is the next largest LULC class in both watersheds.

The monthly pattern of water yields or discharge from pine and oak watersheds are presented below. The overlapping period of record (January to December 2022) is used for water yield estimates.

Months Year: 2022	Precipitation (mm)	Pine Watershed		Oak Watershed	
		Runoff (mm)	% of annual yield	Runoff (mm)	% of annual yield
January	15.8	3	2.29	22	6.32
February	75	2	1.53	19	5.46
March	0	1	0.76	18	5.17
April	7.2	0	0.00	22	6.32
May	82.8	0	0.00	18	5.17
June	79.6	1	0.76	15	4.31
July	164.4	1	0.76	27	7.76
August	141.8	1	0.76	21	6.03
September	196	6	4.58	34	9.77

October	208.6	94	71.76	81	23.28
November	0	18	13.74	33	9.48
December	1	4	3.05	38	10.92
Totals	972.2 mm	131 mm	100%	348 mm	100%

The total yield in the investigation period (2022) is $131163 \text{ m}^3\text{yr}^{-1}\text{km}^{-2}$ for the Pine watershed and $348365 \text{ m}^3\text{yr}^{-1}\text{km}^{-2}$ for the Oak watershed. The peak streamflow in both watersheds rises sharply in October though rainfall is observed in both pre-monsoon and monsoon months. The total annual yield from Oak watershed is more than two and half times than the Pine watershed. More than 90% of the total yield from the Pine watershed leaves as runoff in the month of October, while only less than 25% leaves as runoff during the peak yield month in the Oak watershed. The yield from the Oak watershed is buffered maintaining almost a constant yield of 5-6% in the months of January through June before the onset of summer monsoon. The hydrograph shows that discharge abruptly increases in October and gradually declines through November and December in the Pine watershed. The outlet stream in the Pine watershed remains almost dry till the next monsoon. In the Oak watershed, the increase in runoff at the outlet is gradual from June through October, and the decline post-monsoon is also gradual.

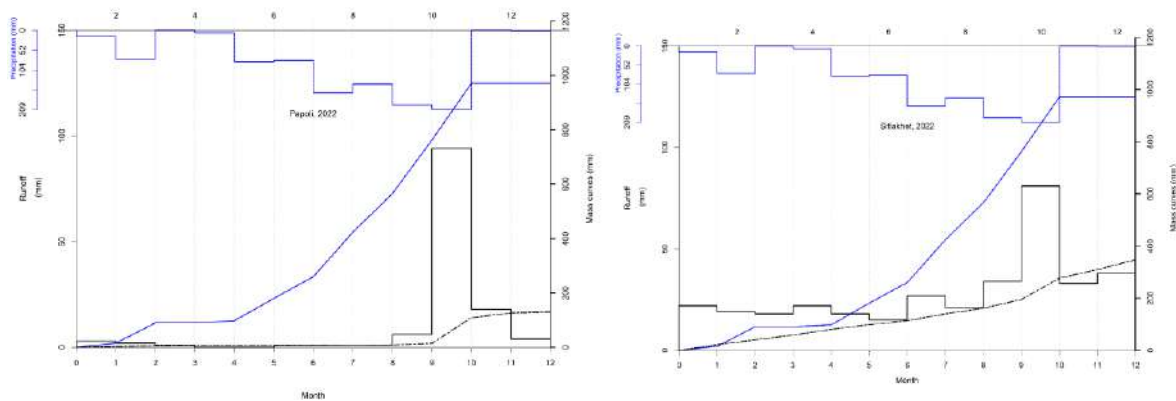


Fig 8. Hydrography of monthly runoff in the Pine watershed (above) and the Oak watershed (below). Concurrent monthly records of rainfall (mm) is also shown. The mass curve of rainfall (blue) and runoff(dot-dash black) is also plotted.

The cumulative precipitation is also plotted alongside the cumulative yield of the watershed. The total rainfall received is 972 mm of which the total annual discharge from the Pine watershed is 131 mm while that from the Oak watershed is 348 mm which is 13.5% and 36% respectively. The higher rainfall runoff conversion rate of the Oak watershed is indicative of lesser losses from precipitation in the Oak watershed.

The daily runoff records from both the Pine and Oak watersheds are shown below. The daily average discharge from the Pine site in the overlapping observational period reaches a maximum of 17065 LPM on 10-October-2022 after a 3 day spell of rainfall. During the same rainfall event the maximum daily average runoff from the Oak site was observed as 14440 LPM. This difference translates to a difference of 3779 m^3 of less runoff from the Oak watershed compared to the Pine watershed over an one day. Though the annual yield from the Pine

watershed is less than the Oak watershed, the daily average runoff reaches a higher value in the Pine watershed compared to the Oak watershed.

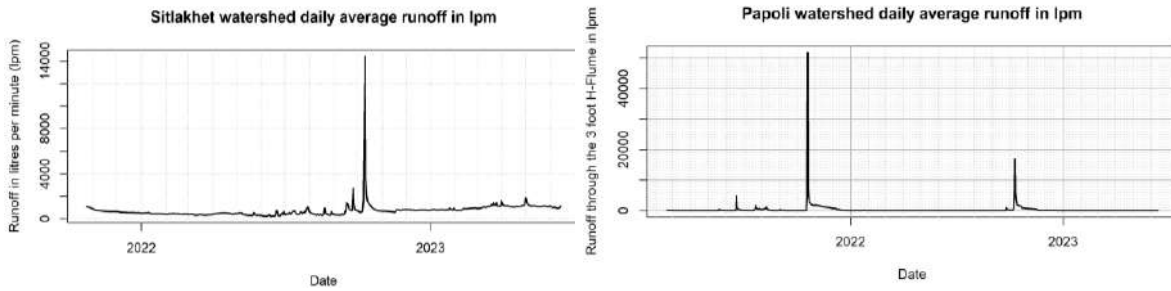


Fig. 9. Time series of daily average runoff measured at the outlet of the (above) Pine (Papoli watershed) and (below) Oak (Sitlakhet watershed).

4.2.2.3. Partitioning of rainfall into throughfall and stemflow in Pine- and Oak-dominated forest stands

In this study, rainfall partitioning into throughfall and stemflow were measured for the observational period, August 2021 - October 2022. Throughfall is measured using throughfall troughs for integrating throughfall over a large area. The throughfall is collected in storage containers, and the volume of collected throughfall is measured periodically before being emptied. In this manner, estimates of total throughfall % are determined at forest stand level for the observational period. Stemflow is collected by diverting water along a spiral type gutter affixed to the tree trunk and diverted to a storage container. Like the throughfall measurement, the storage containers for stemflow were periodically monitored, emptied, and measured for precise volume determination and estimation of stemflow %. which is emptied and measured for volume collected, periodically. This approach provided us with valuable data on the amount of precipitation intercepted and lost by the forest canopy in both Pine and Oak forested watersheds during the observational period. The loss through interception was calculated by subtracting throughfall and stemflow from the bulk precipitation.

The measurements of throughfall and stemflow were made for two forest patches of 30m x 30m of Pine dominated and Oak dominated forest respectively. The volume of water collected is divided by the collection area for the throughfall trough, to give a depth equivalent of throughfall. For stemflow, the volume of water collected is first scaled from sample trees to forest patch. Volume is expressed as volume per m² of basal area. This value multiplied by tree basal area of forest patch then divided by forest area gives depth equivalent of stemflow. The results are scalable to watershed level using estimates of tree canopy cover and site basal area for the watershed. For periodic totals of throughfall and stemflow during the observation period, the average stemflow (%) for the Pine-dominated forest is 0.3 ± 0.1 (13 observations) and for the Oak-dominated forest is 0.6 ± 0.1 (12 observations), while the average throughfall (%) is 67.4 ± 12.8 (11 observations) and 66.3 ± 7.2 (10 observations), respectively.

Assuming the species distribution, canopy cover, tree density and basal area of the watershed is similar to the characteristics of the forest patch where throughfall and stemflow measurements were made, the estimate for interception loss as a percentage of rainfall over the watershed is possible. The stand throughfall is estimated by averaging the throughfall over forested and non-forested areas of the watershed following Loshali and Singh

(1992) and Pathak et al. (1983). The stand throughfall (%) is 80.59 which slightly higher for the Oak forest due to lesser forest cover in Sitlakhet compared to 79.14 for the Pine forest. Overall, the estimates of interception loss is 20.56 % for the Pine dominated forest and 18.81 % for the Oak dominated forest.

Estimates of rainfall partitioning by the Pine and Oak watershed for the year 2022

Forest site	Bulk Precipitation (mm)	Canopy throughfall (mm)	Stemflow (mm)	Stand throughfall (mm)	Stand interception loss (mm)
Chir Pine	972.2	655.3	2.9	769.4	199.9
Banj Oak	972.2	644.6	5.8	783.5	182.9

For the Pine forest stand, higher totals and higher intensity of precipitation results in a higher proportion of throughfall. The relationship was not significant for the Oak stand. In the Pine forest, during high intensity spells, the rain drops penetrate the canopy more easily resulting in higher throughfall %. During winter and pre-monsoon months, the throughfall % recorded in the Pine forest is as low as 34% while during monsoon, it was as high as 96.7%. The lower variability of throughfall between periods and the lack of an evident positive relationship between throughfall and rainfall intensity, or throughfall and total rainfall, for the Oak forest stand is because of the dense canopy structure of the Oak forest, thus constant throughfall % across rainfall totals, and rainfall intensities.

3.2.2.3. Runoff process understanding from runoff plot experiments

Physical characterization of soils in the plot study of Pine and Oak ecosystems:

Soil physical properties such as bulk density, porosity, sorptivity, hydraulic conductivity, and soil moisture retention ability tests were performed to identify the difference between Pine and Oak forest floor in terms of soil physical parameters. The following subsections include summary details of soil physical properties at plot scales and discussions on expected runoff behavior.

Undisturbed Soil Bulk Density and Porosity

Bulk density shows the compactness of the soil and is used for the calculation of porosity. Core samples were weighed in the laboratory and core sample's bulk densities were calculated as the ratio of wet weight of soil and volume of core. To calculate porosity the particle density of soil was considered as 2.6 g/cc and porosity calculated as $[1 - (\text{bulk density of soil} / \text{particle density of soil})]$. The bulk density of the forest floor was marginally higher for the Pine forest (1.554 ± 0.298 g/cc) as compared to the Oak forest (1.442 ± 0.175 g/cc) for the 5 samples considered. Consequently, porosity was lower for the Pine forest (0.40 ± 0.12) as compared to the Oak forest (0.45 ± 0.07) floor. The higher bulk density in the Pine forest is indicative of compaction of the forest floor, and may govern runoff pathways by causing a larger fraction of water to pond and runoff the surface in the Pine forest as compared to the Oak forest.

Hydraulic Conductivity and Sorptivity of Soil

Hydraulic conductivity and sorptivity were measured by establishing a relationship between cumulative infiltration (I) vs. square root of time (t) from the data of hand-held minidisk Infiltrometer experiments. Zhang (1997) developed a two term equation where the first (C_1) and second (C_2) terms characterize water flow out of the disk due to gravity (related to hydraulic conductivity) and capillarity (given directly as sorptivity), respectively.

$$I = C_1 \times t + C_2 \times \sqrt{t}$$

Hydraulic conductivity is estimated by dividing the first term (C_1) by a value relating the van Genuchten parameters for a given soil type to the suction rate and radius of the infiltrometer disk. For the present study, suction was taken -2 cm for both forest ecosystem floors and soil type is considered as sand and loam for Pine and Oak floor, respectively. For the given suction rate and soil type, the values of A are 1.73 and 6.27 for Pine and Oak floor, respectively.

For Pine forest floor the unsaturated hydraulic conductivity ranged from 17.28 cm/d to 49.48 cm/d which was much higher than that of the Oak forest floor (1.86 cm/d to 7.98 cm/d). The lower unsaturated hydraulic conductivity of the Oak forest floor can be attributed to higher soil moisture of the Oak forest (36% as compared to 6% in the Pine forest) floor at the time of the disc infiltrometer field experiment. The mini-disc infiltrometer experiment on the forest floors need to be repeated in the next reporting period to obtain comparable values for the respective ecosystems.

Soil Moisture Retention Curves

The soil moisture retention curve is the relationship between soil matric potential (ψ) and the volumetric moisture content (θ). The matric potential is the suction or negative pressure formed due to meniscus of water droplets at the interface of soil, air and water, and due to the adhesion of water to the soil particles. It is dependent on the pore volume and the texture of the soil. In the pressure plate experiment, at each value of suction, moisture is retained in the soil, determined as gravimetric moisture content which can be converted to volumetric moisture content by multiplying with bulk density of the samples (in g/cc). Preliminary results indicate that for any given pressure, the soils from the Oak forest floor retain much higher water compared to the soils from the Pine forest floor. The laboratory experiment is complete and the results are being analyzed at the time of this report.

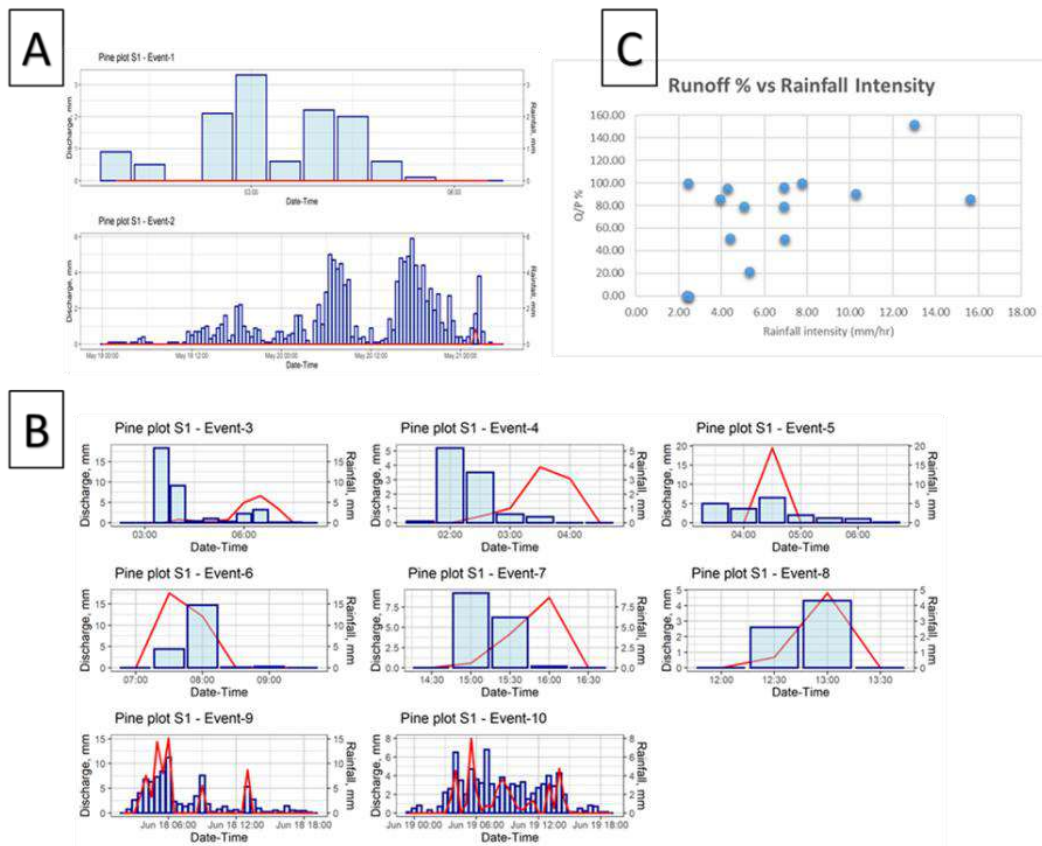


Fig. 10. Rainfall-runoff analysis in Pine plot study; (A) Runoff hydrograph (red line) and rainfall hyetograph (blue bars) in pre-monsoon rainfall events. (B) Runoff hydrograph and rainfall hyetograph in monsoon rainfall events. (C) Relationship between runoff amount and rainfall intensity.

Nutrient content of throughfall, stemflow, soil leachate and plot runoff

A full set of water quality samples was collected in March 2022, and a partial set in February 2021 and September 2021. The analysis of macro- and micro-nutrients of the March 2022 samples are presented in Fig. 2. The data is currently fragmented and further samples in Monsoon 2022 will be needed to identify which components of the forests behave as a source and sink for various nutrients, and how the nutrient content varies with season.

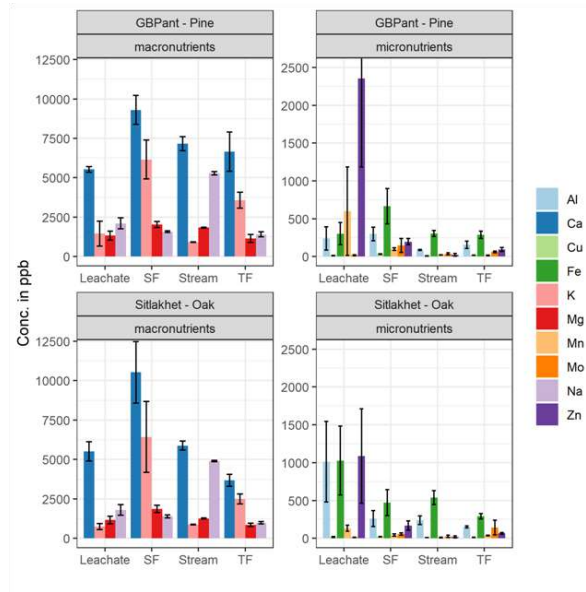


Fig 11. The nutrients content of leachate, stemflow (SF), throughfall (TF) and streamflow in March 2022 at Oak and Pine watersheds.

The traditional perception in the Western Himalayas is that Oak (*Quercus* spp.) forests provide the most effective water conservation. In contrast, Pine (*Pinus roxburghii*) forests are colonizers replacing Oak forests in large areas while consuming excessive water. We conducted field experiments in two forested microcatchments (< 100 hectares each), representing Pine- and Oak-dominated forests, to understand the controls on runoff generation and ecosystem services exerted by soils under both forests in the Western Himalayan headwaters.

The soil under the Pine forest was sandy loam of shallow depth, while that under the Oak forest was silty loam with deep soil profiles. The field capacity and residual moisture of soils under Pine (Oak) forests are 8% (34%) and 4% (14%), respectively, corresponding to 0.33 bar and 15 bar soil water potential on the soil moisture characteristic curves constructed using the pressure plate experiment.

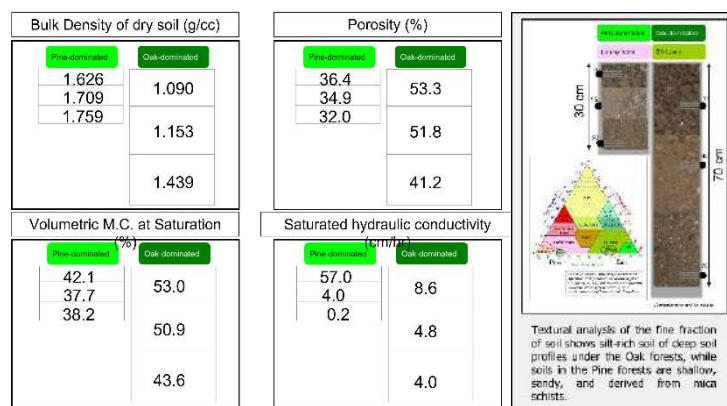


Fig. 12 (Left and middle) Soil physical characteristics measured in the laboratory from undisturbed soil samples extracted at 3 depths adjacent to the runoff plots. (Right) Soil texture of fine fraction of soils show silt-rich soils of deep soil profiles adjacent to runoff plots under Oak canopy, while soils in the Pine forests are shallow, sandy, and derived from Mica schists.

Based on the water retention characteristics, we expect the Oak forests with deeper soils to behave like sponges with moisture stored in the soil profile during wet seasons and gradually released throughout the year to the streams. Observational evidence indicates this to be the case with the first-order streams draining the Pine forest drying up during the summer months while the streams in the Oak forest headwaters remain perennial.

Measurement of field saturated hydraulic conductivity (K) showed large spatial variability, yet consistently higher values in Pine forests (~24 cm d⁻¹) as compared to Oak forests (~8 cm d⁻¹). The high K values in the Pine forest indicate that surface runoff under Pine stands will primarily be saturation-excess runoff during the wet season. The Oak forest with a large water holding capacity will take longer for soils to reach saturation, and runoff will be primarily by infiltration-excess. Runoff was measured at the outlet of each runoff plot concurrently with soil moisture to validate this understanding based on the soil properties. A total of 41 and 34 rainfall events were identified during the year 2022 for further analysis runoff generation. A rainfall record is considered as a rainfall event if it is preceded by at least 2.5 rainless hours.

Month	Pine runoff plot					Oak runoff plot				
	Event ID	Time of onset of rainfall	Total rainfall mm	Total runoff mm	Q/P %	Event ID	Time of onset	Total rainfall mm	Total runoff mm	Q/P %
May	c51	5/12/2022 18:30	12.8	0	0					
	c54	5/23/2022 07:00	17.3	2.4	13.9					
June	c59	6/29/2022 13:30	40	19.1	47.8	o02	6/20/2022 17:00	75.4	0.0	0.0
						o10	6/30/2022 0:45	42.9	0.0	0.0
July	c60	7/02/2022 15:00	33.6	12.8	38.1	o08	7/29/2022 9:00	57.2	26.6	46.5
	c69	7/30/2022 14:00	22.9	0.1	0.44	o09	7/30/2022 11:00	43.7	31.8	72.8
Aug	c71	8/14/2022 14:30	41.3	17.4	42.1	o05	8/19/2022 23:15	56.9	8.5	14.9
						o11	8/14/2022 14:15	30.0	0.3	1.0
Sep	c82	9/24/2022 19:00	62.2	0.4	0.64	o32	9/24/2022 21:30	74.6	0.0	0.0
						o30	9/16/2022 21:30	53.8	1.6	3.0
Oct	c85	10/07/2022 2 23:00	195.5	27.5	14.1	o34	10/7/2022 20:30	283.8	108.8	38.3

The wet spell in October 2022 generated a large response in both the Pine and Oak watersheds, and so will be described first at plot scale. The event id is c85 for the Pine site and o34 for the Oak site.

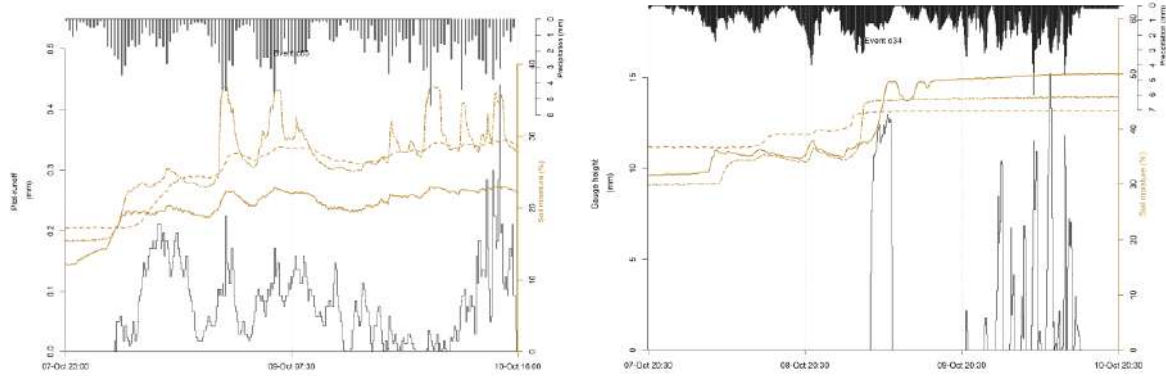


Fig 13. Rainfall hyetograph and runoff hydrograph for event recorded on 07 October to 10 October 2022 at G B Pant Campus (Pine site) and Shitlakhet (Oak site)

At the Pine site, rainfall records show that a total rainfall of 283.8 mm was received in 66.5 hours with an average rainfall intensity of 4.3 mm/hr. There were 33 record (half-hourly) out of 130 observations when the rainfall exceeded the 4.3 mm/hr, and just 5 instances when the rainfall intensity was twice the average intensity i.e., 2022-10-08 21:30, 2022-10-08 22:00, 2022-10-09 05:00, 2022-10-10 03:30, 2022-10-10 08:00. At these instances the soil moisture sensor at 15cm depth (dot-dash profile) shows sharp peaks that exceed the moisture at saturation for the Pine Forest soil at that depth (37.7 %). At these instances, the rainfall intensity exceeding the vertical saturated hydraulic conductivity of the soil horizon at 15cm depth (determined as 4 mm/hr in the laboratory). Runoff at the outlet though happening continuously throughout the rainfall spell is actually happening in trickles with maximum gauge height not exceeding 4mm, and the median of gauge height over 3 days only 1.1 mm. The trace of the peak runoffs generally follows the trace of the soil moisture readings at 15cm, partially because underlying the second horizon is a layer of low saturated hydraulic conductivity. When the flow is not able to be routed through subsurface drainage pathways, the runoff emerges at the surface. In the Oak site, the wet spell in October is identified as event 34. One immediate observation is that all soil layers is saturated on the evening of 09-October. The capacitance probe seems to have recorded continuous flow upward of 1cm above the flume bottom. Once the topsoil is saturated, the runoff is mimicking the pattern of rainfall falling on the surface.

Additional: Innovation in low-cost hydrological monitoring instrumentation

The collection of Throughfall and Stemflow currently involves a pipe and gutter system that directs the water into holding drums. After a specified time, the quantity of collected water is measured. However, this method lacks the ability to provide time-resolved data for a comprehensive analysis of throughfall and stemflow at the scale of rainfall events. To address this limitation, a tipping bucket flow gauge was developed as an alternative to manual measurement. The cost of commercially available tipping bucket solutions was found to be prohibitive, leading to the conception of a low-cost tipping bucket flow gauge. This gauge was designed and developed using the Open-Source Arduino framework with a focus on modular electronics (Figure 1 & 2).

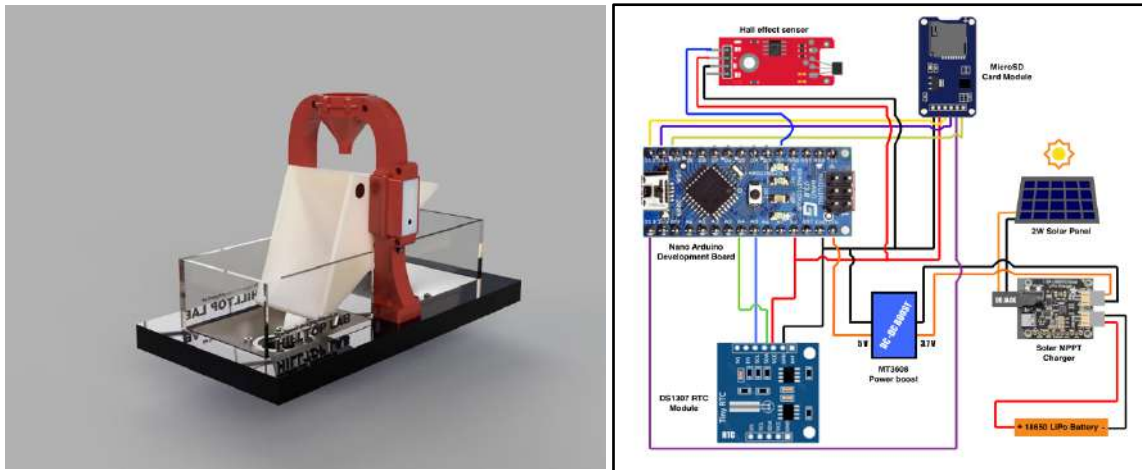


Fig1. (Left) 3D model render of the essential parts of the tipping bucket flow gauge. (Right) Circuit diagram of the Data logger.

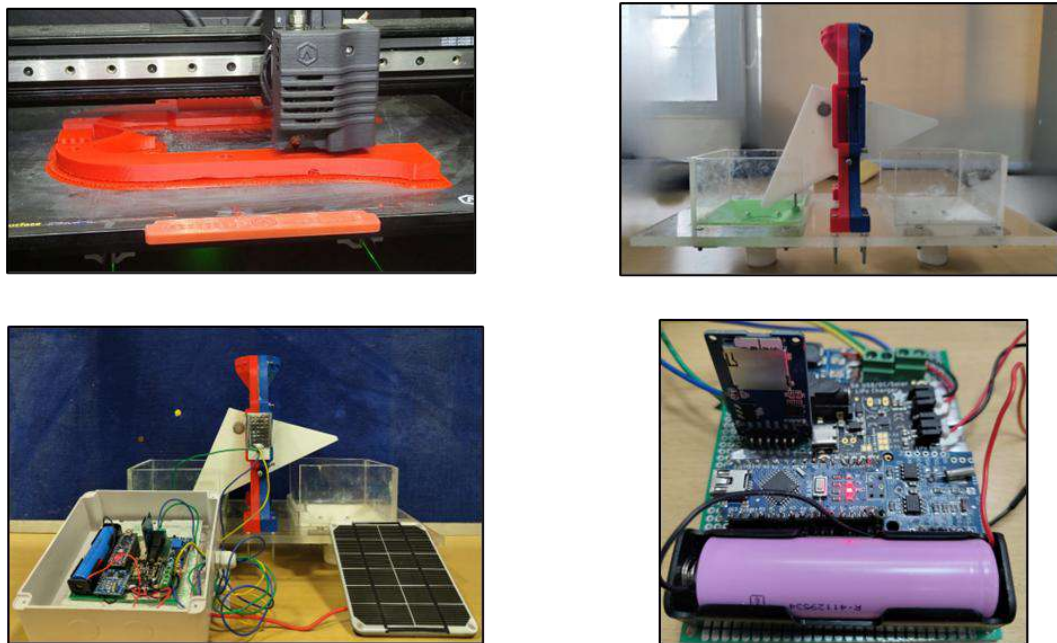


Fig 2 (clockwise from top-left) FDM 3D printing of tipping bucket flow gauge hardware; Completed assembly of the tipping bucket flow gauge physical components; Completed data logger; Completed tipping bucket flow gauge without protective enclosure.

The instrument was fabricated at IIT Roorkee using FDM 3D printing technology, enabling rapid prototyping and simplified assembly (Figure 21). It intelligently utilizes the Arduino's sleep mode during idle periods to optimize battery performance, and its solar-powered functionality allows for remote operation. To ensure accurate data logging, a hall effect sensor was incorporated, avoiding the potential errors associated with Reed sensors. The low-cost flow gauge was compared favourably with similar devices available in the market, demonstrating an 86% efficiency during preliminary testing. Currently, a total of 5 prototypes are being assembled, but they are yet to undergo comprehensive testing both in laboratory and field conditions. The

tipping bucket flow gauge once deployed will improve our understanding on the influence of seasons, rainfall and stand characteristics on throughfall under different forest canopies.

Key findings:

1. The total yield in the overlapping investigation period (2022) is 131163 m³yr⁻¹km⁻² for the Pine watershed and 348365 m³yr⁻¹km⁻² for the Oak watershed.
2. The rainfall-surface runoff conversion is 13.5% and 35.8% in the Pine and Oak watersheds respectively.
3. More than 90% of the total yield from the Pine watershed leaves as runoff in the month of October, while only less than 25% leaves as runoff during the peak yield month in the Oak watershed.
4. The peak daily average discharge is higher for the Pine watershed compared to Oak watershed by more than 25%.
5. The estimates of interception loss is 20.56% ± 8.3 for the Pine dominated forest and 18.81% ± 4.2 for the Oak dominated forest.
6. For the Pine forest stand, higher totals and higher intensity of precipitation results in a higher proportion of throughfall. The relationship was not significant for the Oak stand.
7. The runoff behaviour on the Pine runoff plot is indicative of large subsurface flows interrupted by surface runoff due to infiltration excess during high intensity rainfall spells.
8. The runoff process observed on the Oak runoff plot can be predominantly attributed to infiltration excess, mainly due to the presence of deep soil profiles. As the soil layers become fully saturated, the mechanism then shifts to saturation excess runoff.

References

- Gorelick, N., Hancher, M., Dixon, M., Ilyushchenko, S., Thau, D., & Moore, R. (2017). Google Earth Engine: Planetary-scale geospatial analysis for everyone. *Remote Sensing of Environment*.
- Zhang, R. (1997), Infiltration Models for the Disk Infiltrometer. *Soil Science Society of America Journal*, 61: 1597-1603. <https://doi.org/10.2136/sssaj1997.03615995006100060008x>
- Loshali, D. C., & Singh, R. P. (1992). Partitioning of rainfall by three Central Himalayan forests. *Forest ecology and management*, 53(1-4), 99-105.
- Pathak, P. C., Pandey, A. N., & Singh, J. S. (1983). Partitioning of rainfall by certain forest stands in Kumaun Himalaya. *Tropical Plant Science Research*, 1(2), 123-126.

3.2.3. Comparison of Pine and Oak ecosystem exchange and transpiration using sap flow observations under limiting meteorological conditions for two sites of watersheds.

3.2.3.1. Diurnal pattern of sap flux density:

Fig. 1 shown diurnal variation of sap flux density estimated over 1 hour interval and it is denoted by J_p ($\text{ml}/\text{cm}^2/\text{min}$). It can be noted from the diurnal pattern of sap flux densities that J_p was found to vary between 0 to 10 J_p ($\text{ml}/\text{cm}^2/\text{min}$) for *Pinus roxburghii*, 0 to 5 ($\text{ml}/\text{cm}^2/\text{min}$) and 0 to 8 ($\text{ml}/\text{cm}^2/\text{min}$) for *Quercus leucotrichophora* and *Quercus glauca*. Further, it can be concluded from the analysis that *Pinus roxburghii* has higher water loss than *Quercus leucotrichophora* and *Quercus glauca*. Diurnal pattern of J_p was similar for all three species. The variation in J_p is largely associated with variation in VPD and net radiation. Typically, J_p rapidly increased and reached to a maximum around mid-day (12:00 noon) and a gradual decline was observed after 15:00 hours. A more gradual decline in the sap flux density was observed after sunset in all the species. During the entire study period the *Pinus roxburghii* trees found to have higher water loss than *Quercus leucotrichophora* and *Quercus glauca*.

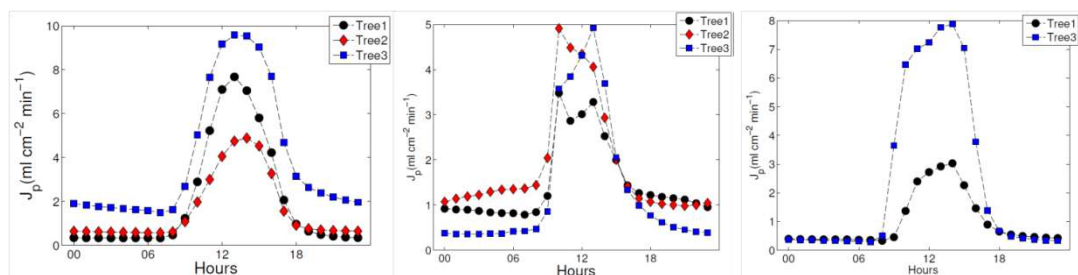


Figure 1: Diurnal pattern of sap flux density of *Pinus roxburghii* (a), *Quercus leucotrichophora* (b) and *Quercus glauca* (c).

Sapwood area estimation

Both the studied tree species showed a strong (linear) relationship between their functional xylem area (A_x , cm^2) and stem cross-sectional area (A_s , cm^2), with correlation coefficients of consistently above 0.8. The Pine trees (25-30 years old at the time of measurement) were much larger (mean DBH 35.9 cm) than the Oak trees (mean DBH = 25.5 cm). The average Lsw was higher for *P.roxburghii* (9.0 cm) than *Q.leucotrichophora* (5.64 cm). Average A_x was also higher for *P.roxburghii* ($171.9 \pm 66.3 \text{ cm}^2$) than *Q.leucotrichophora* ($127.02 \pm 58.2 \text{ cm}^2$). Despite the similarity in Lsw among tree species in the natural forest, the variation in tree sapwood area was much larger due to the differences in tree size occurring in the plot (Table 1). There was a 1.35-fold difference in Lsw and A_x between *P. roxburghii* and the *Q. leucotrichophora* suggesting potentially large differences in transpiration between the two forest types.

Species	DBH	Sapwood depth (cm)	Sapwood area (cm ²)
<i>Pinus roxburghii</i>	35.9(±6.21)	9.77(±4.22)	170.9(±66.3)
<i>Quercus leucotrichophora</i>	24.5(±66.3)	5.64(±66.3)	127.02(±58.2)

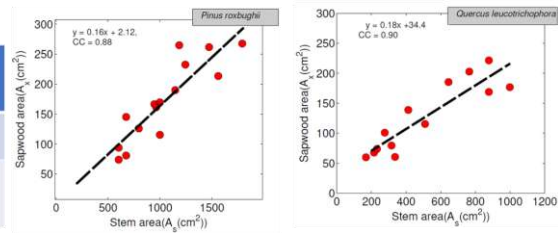


Table 1: provides information about DBH, sapwood depth and sapwood area and Fig 1. Relationship between sapwood area and stem area for Chir-Pine and Banj-Oak trees

Stand level transpiration dynamics

Daily stand transpiration (E_t) showed distinct seasonal variation in both the Pine and Oak forest. Although the seasonal patterns of E_t were significantly different, the Pine forest E_t was higher than that of the Oak forest throughout the study period even when allowing for the inferred difference in short-wave radiation inputs due to the difference in site exposure. Both sites showed higher E_t rates during the pre-monsoon season months (March–May) compared to the wet season months (June–September).

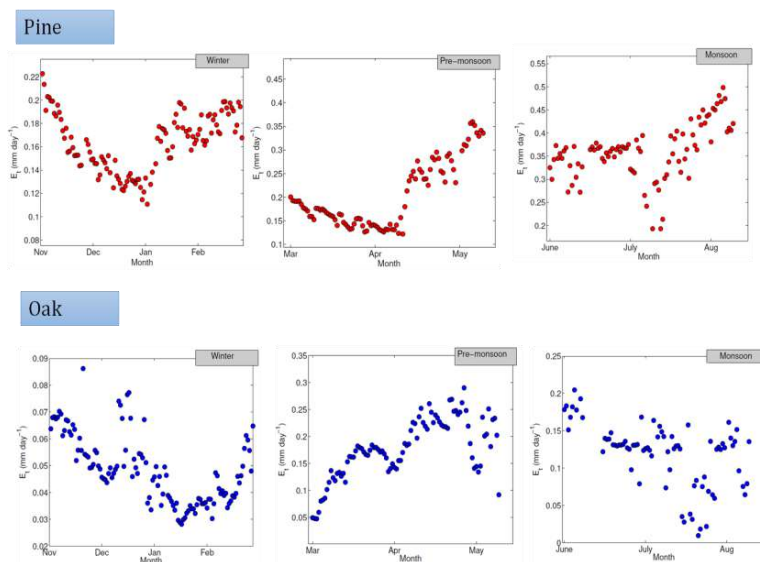


Fig 2. Seasonal pattern of stand level transpiration of Chir-Pine and Banj-Oak trees.

Micro-meteorological controls affecting Pine-Oak transpiration:

Relationship of different micro-meteorological (Air-temperature, relative humidity and net radiation) was established with Pine-Oak stand level transpiration was established. Transpiration was found to increase with increasing air-temperature, relative humidity and net radiation in case of Pine. However, in case of Oak, no statistically significant relationship was observed with relative humidity. Furthermore, a thorough quantification is required in order to establish relationship between transpiration and rainfall.

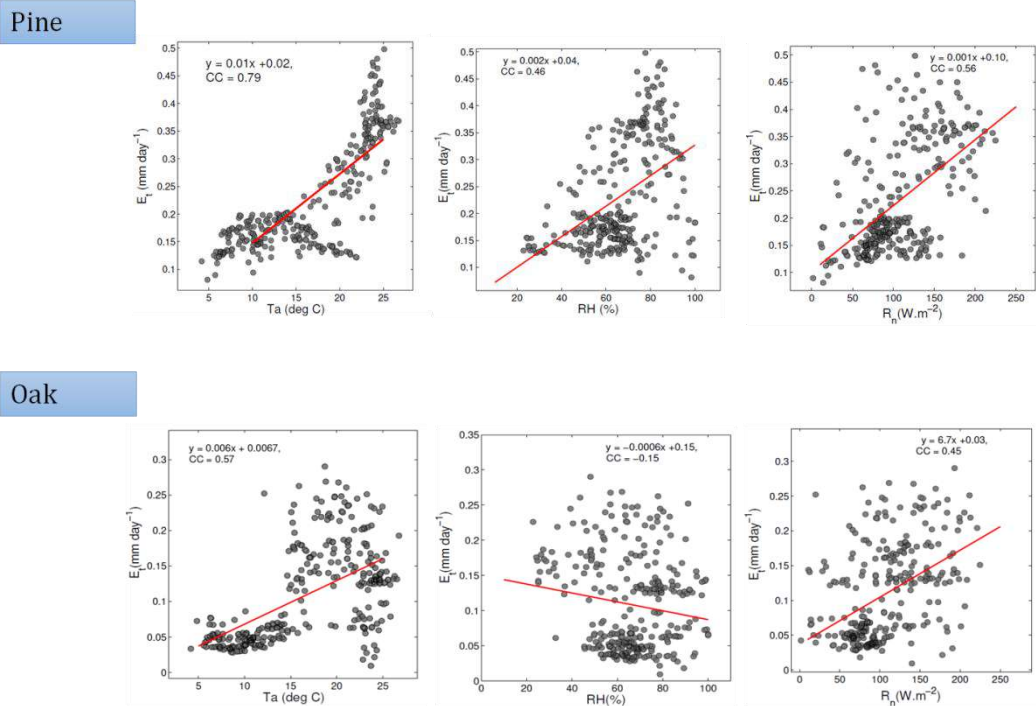


Fig 3: relationship between micro-meteorological controls and transpiration.

Conclusion:

For the first time, tree transpiration was quantified for *Pinus roxburghii* (deciduous needle leaf) and *Quercus Spp.* (ever green broadleaf) over central Himalayn region. In this study, we reported sub-daily to seasonal dynamics of the sap flux densities of *Pinus roxburghii* and *Quercus Spp.*, and their responses to environmental variable in daily scale. The daily average sap flux density of *Pinus roxburghii* was found higher (1.5-2 times) for both winter and pre-monsoon seasons than *Quercus Spp* indicating higher water loss by Pine stands. Seasonal variations of sap flux densities were consistent with meteorological parameters during winter season. However, pre-monsoon season was found to have negative relationship between sap flux density and VPD, as higher VPD conditions cause stomata closure in most of the plants which further reduces the transpiration by plants. These are the initial results of the analysis. Further, sap flow derived ET would be estimated using these measurements.

3.2.3.2. Comparison of Pine and Oak ecosystem fluxes under limiting meteorological conditions for two sites

The monthly values of NEE, GPP and RE for Pine and Oak sites were compared and presented in **Fig below**. We found that both Pine and Oak systems were sink of carbon through out the year as the average NEE for the period of observations (2016-17) was $-2.99 (\pm 0.05) \text{ gC.m}^{-2}.\text{day}^{-1}$ for the Pine, whereas NEE of $-2.14 (\pm 0.05) \text{ gC.m}^{-2}.\text{day}^{-1}$ was observed for Oak ecosystem. Similarly, when the average GPP values of 2016-17 were compared between the Pine and Oak systems, we found that average GPP of Pine, $5.38 (\pm 0.03) \text{ gC.m}^{-2}.\text{day}^{-1}$, was higher than the Oak, $3.76 (\pm 0.03) \text{ gC.m}^{-2}.\text{day}^{-1}$, ecosystem. Values in parenthesis are standard errors. Hence, Pine sequestered almost 1.4 times higher carbon than the evergreen broadleaf Oak ecosystem of

Himalaya considering both GPP and NEE. The average NEE values of both ecosystems were found to be marginally lower than the NEE of a mixed forest at the Himalayan foothill of Uttarakhand, India, ($NEE = -3.24 \text{ gC.m}^{-2}.\text{day}^{-1}$), as reported by Watham et al. (2014). The GPP values of Pine and Oak systems of this study was marginally lower than that of temperate coniferous forests ($GPP = 5.7 - 6.84 \text{ gC.m}^{-2}.\text{day}^{-1}$) as reported by Falge et al. (2002). When the RE values were compared, we found average RE of Oak system, $3.26 (\pm 0.01) \text{ gC.m}^{-2}.\text{day}^{-1}$ was almost 1.8 times higher than the Pine system, $1.78 (\pm 0.008) \text{ gC.m}^{-2}.\text{day}^{-1}$. The low RE value of Pine ecosystem can be attributed to the rather acidic nature of top-soil having relatively smaller thickness under the Pine stands of Himalaya restricting the microbial activity. Such low total respiration from the acidic soils of *Pinus roxburghii* vegetations of Himalaya are already reported in Joshi et al. (1991), indicated top soil under *Pinus roxburghii* stand respired $37.6 - 192 \text{ mg.CO}_2.\text{m}^{-2}.\text{s}^{-1}$ with pH of 5.7. The higher RE values Oak system could also be attributed to higher leaf-litter assisted microbial activities (Pant and Tiwari, 2021).

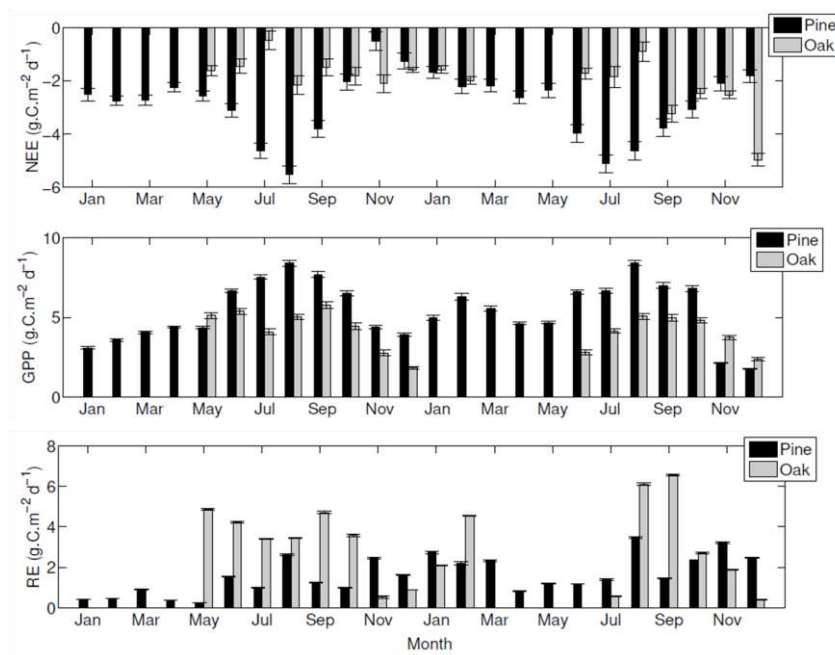


Fig. 4 Monthly variation of (a) NEE, (b) GPP and (c) RE over Chir-Pine and Oak dominated ecosystems. The vertical lines are standard errors.

In order to quantify the amplitude of rainfall triggering the highest change in the ecosystem fluxes, the continuous wavelet spectra of NEE, GPP and RE were produced using 2016-17 daily values of monsoon season and are provided in Fig.4(a and b). It can be clearly observed from the wavelet spectra of NEE that compressed high frequency variations having smaller scales (2-4 scales) were present in the Chir-Pine dominated ecosystem, which signified abrupt changes in the NEE for the system; whereas stretched wavelet with larger scale (4-8 scales) variation of NEE of Banj-Oak dominated ecosystem signified slow varying changes. The high frequency variations in the Chir-Pine dominated ecosystem could be linked to higher response of the ecosystem to the environmental changes in comparison to the Banj-Oak dominated ecosystem. However, unlike NEE, comparison of RE wavelet spectra between Chir-Pine and Banj-Oak dominated ecosystems showed high frequency variation with smaller scales (2-4 scales) for Banj-Oak dominated

ecosystem indicating abrupt changes in the terrestrial ecosystem respiration. The low variation in RE values over Chir-Pine dominated ecosystem was associated to low soil moisture availability and microbial activities Joshi et al (1991).

To understand relationships between ecosystem fluxes and rainfall in different time-frequency spaces during monsoon seasonal variation, cross wavelet spectra were produced (Fig.5). In the cross wavelet spectra, the red area enclosed by the thick solid line represented statistically significant local correlation (i.e., 95% confidence level) between two variables i.e. NEE/GPP/RE and rainfall that signifies ecosystem fluxes are more sensitive to changes in rainfall. Darker coloured contour in the cross wavelet spectra indicated higher local correlation in the time-frequency space. Phase (lag-lead) relationships are shown by the arrows, a positive correlation is represented by an arrow pointing to the right, a negative correlation is represented by one to the left. Leadership of the first variable is shown by a downwards pointing arrow and if it lags, the relationship is represented by an upward pointing arrow (Mukherjee et al, 2018).

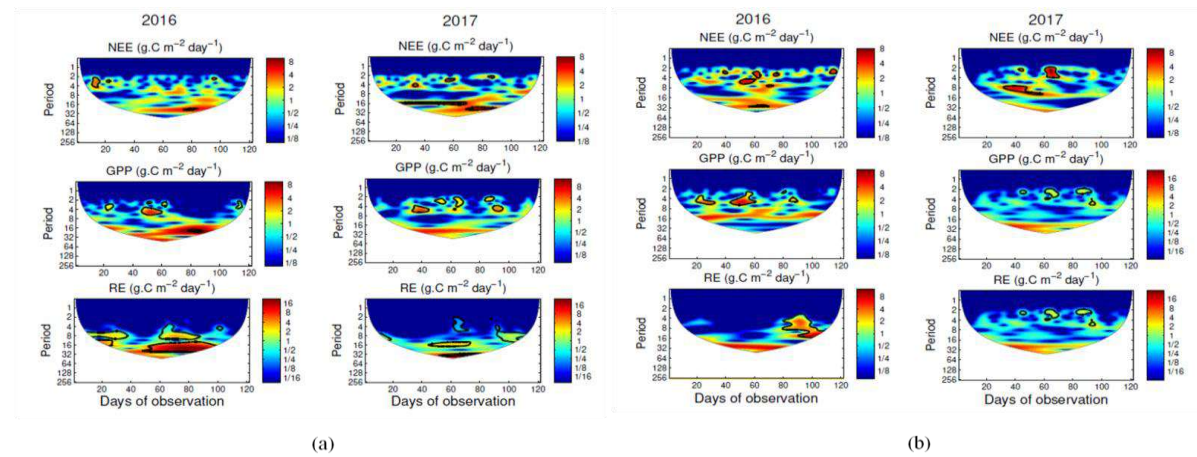


Fig. 5 Power spectra of daily average ecosystem fluxes (NEE, GPP and RE) for the (a) Chir-Pine and (b) Banj-Oak dominated ecosystems.

Seasonal common powers with respect to rainfall and all three fluxes can easily be identified from Fig.5(a and b) with periods varying significantly between 2–16 days for Chir-Pine dominated ecosystem and 2–8 days for Banj-Oak dominated ecosystem having intermittent phase-locked relationship was observed for a limited time period in the Banj-Oak dominated ecosystem. The cross wavelet spectra of GPP with rainfall (Fig.5c, d) indicated marginally different behaviour than NEE–rainfall scalograms as arrows were pointing marginally downward, indicating the GPP of Banj-Oak dominated ecosystem had restrained responses to rainfall than the Chir-Pine dominated ecosystem. The comparison of RE–rainfall scalogram (Fig. 5 e, f) indicated increasing rainfall leading to enhancing RE over Banj-Oak dominated ecosystem, however, no such signatures were observed over Chir-Pine dominated ecosystems.

Response of the ecosystem fluxes to rainfall spell

The three important rainfall parameters that control ecosystem exchanges are spell duration, amount and threshold (Yuhui et al,2018). As indicated in the method section, dissimilarities in the ecosystem fluxes of Chir-Pine and Banj-Oak dominated ecosystems due to varying rainfall spell were quantified using the monsoon

season data. Subsequently, successive rainy days of a monsoon season were considered upto 10-day from 0-day of initiation where 0-day and 'rainfall event + 01-day' implied no rain. Total rainfall spell was calculated for each monsoon season of 2016 and 2017 for Chir-Pine and BanjOak dominated ecosystems (Table1), and it can be noted that, irrespective of sites and observation years, a total of 31 and 42 rainfall spells were recorded for Chir-Pine and Banj-Oak dominated ecosystems, respectively. Additionally, 02-day rainfall spells were found to have maximum occurrence (09) at Chir-Pine site, whereas 01-day rainfall spells (17) were maximum at the Banj-Oak site. To identify the impact of rainfall spell on carbon assimilation scatter diagram of the average NEE and associated length of rainfall spell was produced (Fig.6a and b). It was noted from the Fig.6(a and b) that 01-day rainfall spell within the monsoon period had resulted lowest average carbon sequestration amongst all the rainy days ($-2.98 \text{ g.C.m}^{-2}.\text{day}^{-1}$) by the Chir-Pine dominated ecosystem while 3-day consecutive rainfall spell had the lowest carbon sequestration amongst all the rainy days ($-1.93 \text{ g.C.m}^{-2}.\text{day}^{-1}$) by the Banj-Oak dominated ecosystem. However, with increasing successive rainy days within a monsoon season, enhanced carbon sequestration by the Chir-Pine dominated ecosystem having maximum carbonassimilation ($-5.17 \text{ g.C.m}^{-2}.\text{day}^{-1}$) for a continuous rainfall spell of 09-day was observed.

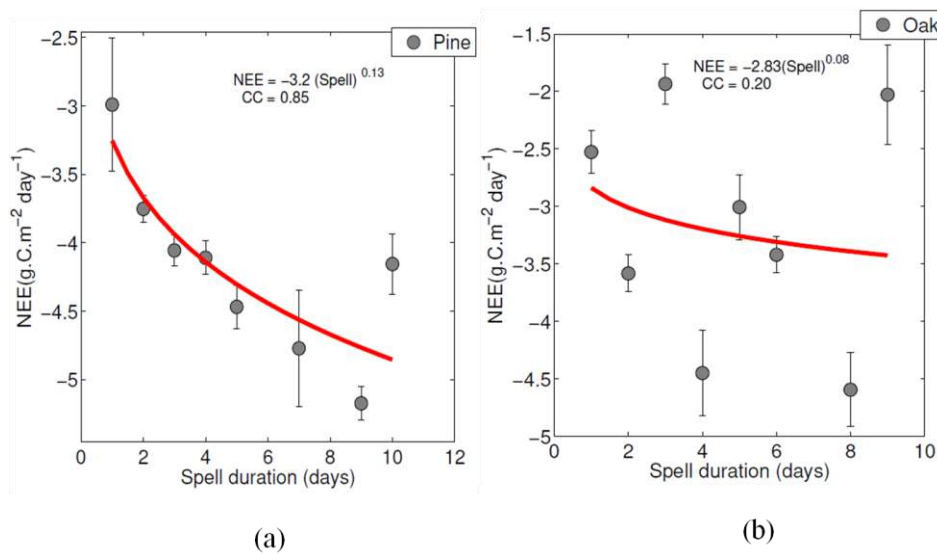


Fig. 6 Subplots show average net ecosystem exchange (NEE) of the monsoon seasons of 2016-2017 for length of rainfall spell where '0-day' and 'rainfall+1 day' implied no rain.

On the contrary to Chir-Pine dominated ecosystem, no statistically significant relationship was observed between NEE and rainfall spell for Banj-Oak dominated ecosystem. The solid line in the Fig.6(a and b) depicts the fitted curve of $NEE = aS^b$, where S is the rainfall spell. The comparison of power-law relationships between Chir-Pine and Banj-Oak dominated ecosystems indicated the Chir-Pine dominated ecosystem had systematic response to rainfall spell ($NEE = -3.2S^{0.13}$ with correlation coefficient of 0.85 at p -value < 0.001); whereas the Banj-Oak dominated ecosystem did not systematically respond to rainfall spell ($NEE = -2.83S^{0.08}$ with correlation coefficient of 0.20 with no statistical significance).

Response of the ecosystem fluxes to rainfall amount

In general, plants are highly sensitive to variation in rainfall amount (Yuhui et al,2018), and over the Himalayan terrain, monsoon seasonal precipitation has larger impact on the carbon assimilation than any other seasons (Deb Burman et al,2021). To assess the impact of maximum rainfall within a rainfall spell on carbon assimilation, boxplots were used to identify the highest carbon assimilation by an ecosystem after the maximum rainfall irrespective of rainfall spells (Fig.7). It can be clearly observed from the Fig.7 that both Chir-Pine and Banj-Oak dominated ecosystems were sequestering highest amount of carbon (-4.65 and -4.91 $\text{g.C.m}^{-2}.\text{day}^{-1}$, respectively) just after the day having maximum rainfall. Subsequently, it can be inferred that maximum rainfall within a spell increased the ecosystem responses of both Chir-Pine and Banj-Oak sites resulting increased productivity. Our observations corroborates well with the earlier of observations of Austin et al (2004) and Schwinning and Sala (2004) who illustrated that water uptake by the plants in water limiting conditions accelerated after a large precipitation event through increased photosynthesis capacity.

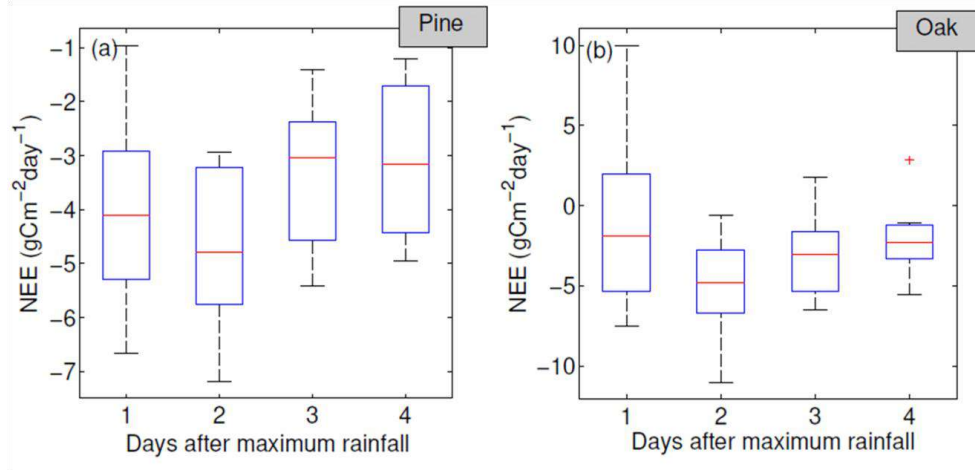


Fig. 7 Box plots show net ecosystem exchange (NEE) for each r_d , $r_d + 1$, $r_d + 2$ and $r_d + 3$ days .

To identify the rainfall threshold that had maximum carbon assimilation for Chir-Pine and Banj-Oak dominated ecosystems, scatter diagram of the average NEE and associated rainfall amount, irrespective of the rainfall spells, was produced (Fig. 8). However, rainfall threshold was quantified by only considering 5-day consecutive rainfall events as more than 5 consecutive rainfall days could be considered as ‘heavy rainfall spell’ as of Tang et al (2018). The rainfall thresholds resulting highest carbon assimilations in Chir-Pine and Banj-Oak dominated ecosystems are easily noticeable from Fig. 8, and the thresholds were $10(\pm 0.7)$ mm and $17(\pm 1.2)$ mm amount of rainfall for Chir-Pine and Banj-Oak dominated ecosystems having highest carbon assimilation of -4.46 and -4.44 $\text{g.C.m}^{-2}.\text{day}^{-1}$, respectively. The fitted quadratic models for Chir-Pine and Banj-Oak dominated systems were found to be $NEE = 0.03R_m^2 - 0.85R_m - 0.04$ for Chir-Pine having $r^2=0.82$; and $NEE = 0.03R_m^2 - 1.02R_m + 4.28$ for Banj-Oak having $r^2=0.87$.

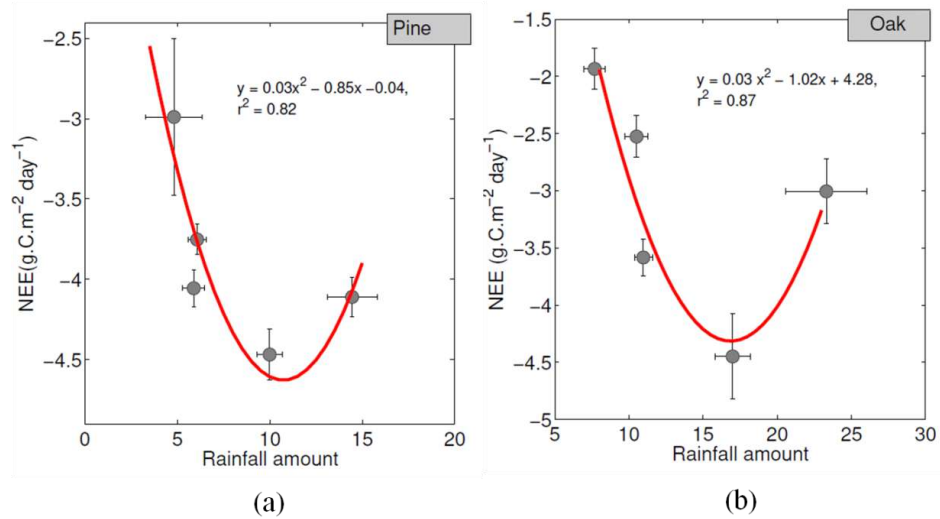


Fig. 8 Subplots represent the variation of net ecosystem exchange (NEE) with rainfall amount. The vertical and horizontal lines represent standard errors. The red lines indicate fitted quadratic equation where 'y' is NEE and 'x' is rainfall amount.

(a) General comparison of WUE w.r.t Pine and Oak ecosystem

Results of the analyses indicate that both Pine and Oak dominated ecosystems efficiently use water during photosynthesis activity. However, the Pine dominated ecosystem has marginally higher annual WUE (1.35 ± 3.18 gC.Kg⁻¹H₂O) than Oak (1.10 ± 2.08 gC.Kg⁻¹H₂O) dominated ecosystem. No Statistically significant relationship between WUE and air-temperature and PPFD are also observed for both Pine and Oak dominated ecosystems during pre-monsoon and monsoon seasons; whereas a positive relationship is observed between WUE and VPD for Pine dominated ecosystems during post-monsoon, and Oak dominated ecosystem during pre-monsoon seasons. Furthermore, WUEs of both Pine and Oak dominated ecosystems decreases with increasing rainy days of monsoon period and the decreasing rate is higher for the Oak dominated ecosystem. The general inference of the study indicates that Oak has higher resilience to micro-climatic fluctuations than Pine dominated ecosystem.

Response of the water use efficiency to environmental factors:

During pre-monsoon, the daily GPP, ET had a strong positive linear relationship with air-temperature and photon flux density. However, GPP, ET and WUE did not hold any relationship VPD over both the ecosystem. compared to the pre-monsoon season, the WUE is smaller in the monsoon and post-monsoon seasons. The photosynthesis and evapo-transpiration are mostly coupled in pre-monsoon and post-monsoon season.

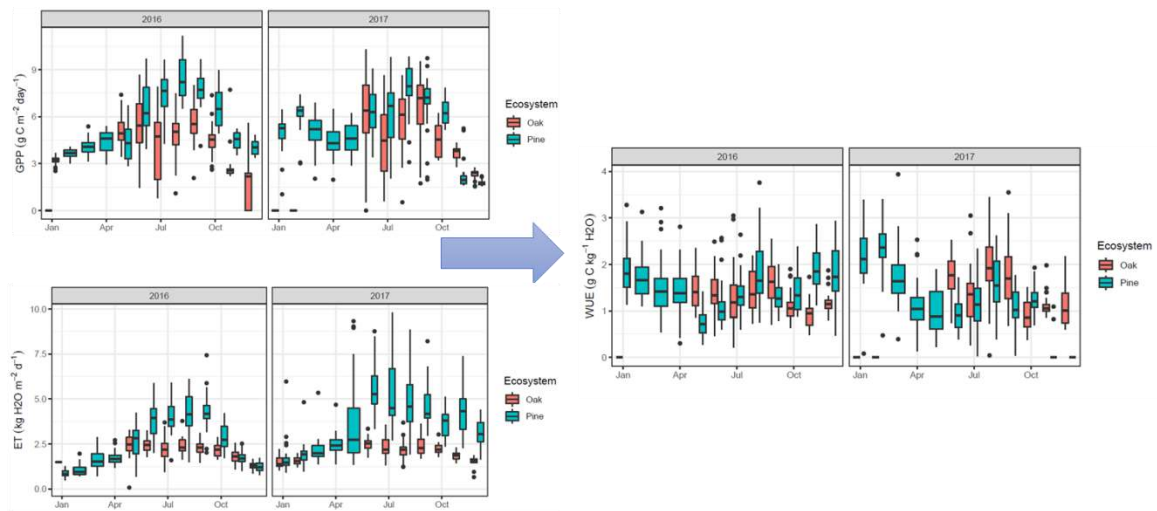


Fig. 9 General dynamics of Pine-Oak water use efficiency.

Water use efficiency in different season

The relationship between GPP and ET during different seasons is plotted in Fig. 1. Additionally, to quantify the rates of increase of GPP with ET, linear relationship was fit to scatter plot. Slope in the equation denotes WUE for different seasons. Irrespective of the season, the highest water use efficiency was recorded for post-monsoon season Pine (1.62 $\text{gC.Kg}^{-1}\text{H}_2\text{O}$) and Oak (2.14 $\text{gC.Kg}^{-1}\text{H}_2\text{O}$) ecosystem. Further, GPP was found to increase linearly with ET in pre-monsoon and post-monsoon season. However, in monsoon season less coupling was observed between GPP and ET.

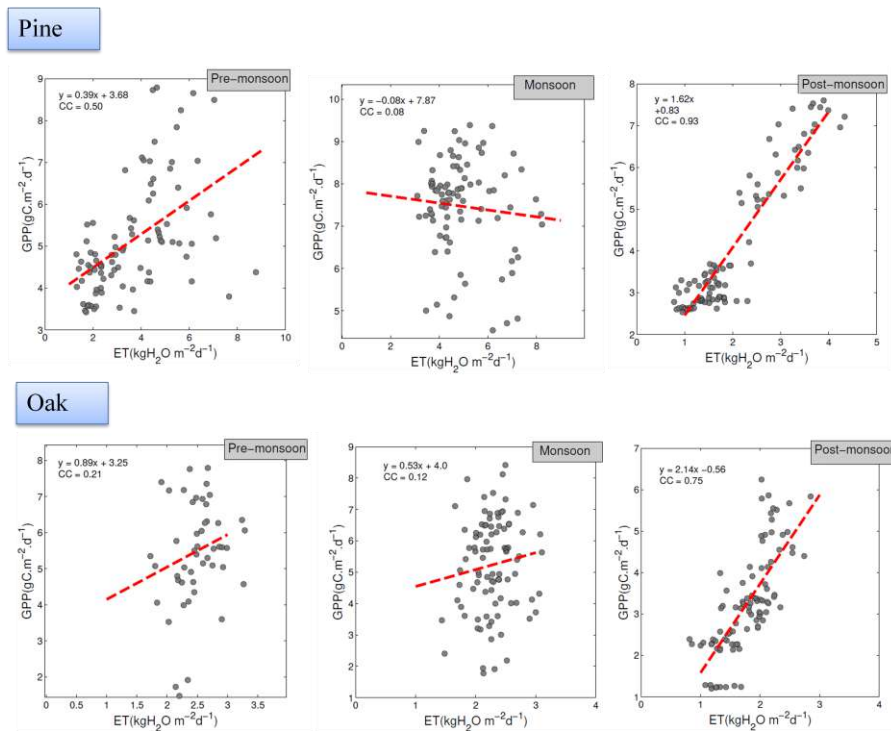
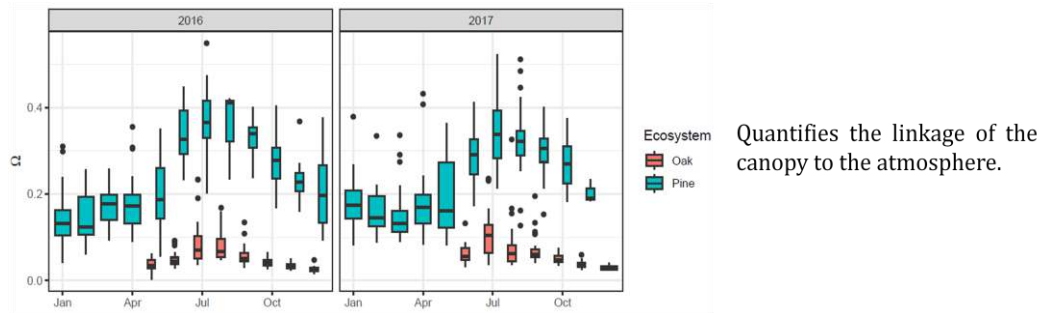


Fig 10: Relationships between GPP and ET are presented for Pine and Oak ecosystem during pre-monsoon, monsoon and post-monsoon season.

Variation of decoupling coefficient: Pine and Oak ecosystem

- Both Pine and Oak dominated ecosystem found to be well coupled with atmosphere during monsoon (July-September) season while gradual decreasing trend was observed during post-monsoon season.
- It can be inferred from the analysis that the physiological controls impose stronger constraint to the surface atmospheric layer over Oak dominated ecosystem than Pine dominated ecosystem.



Note: Values close to 0 indicate well coupled conditions characterized by high physiological (i.e. stomata) control on transpiration (Jarvis and McNaughton.,1986)

(b) Impact of air temperature on Pine and Oak ecosystem exchange

Many studies have highlighted that precipitation, air temperature, vapour pressure deficit and radiation are the major influencing factors of the ecosystem growth at regional and global scale (Law et al. 2002; Renaud and Rebetez 2009; Renaud et al. 2011; Grossiord et al. 2020; Hao et al. 2020). Therefore, attempts are made in this study to quantify seasonal-scale relationships between these meteorological parameters and NEE of the Pine-Oak system. In general, air temperature increases gradually in the pre-monsoon season in the sites till the end of May, however, when this air temperature trend was evaluated with respect to NEE of the Pine system, no statistically significant correlation was observed for Pine, although it can be clearly noticed from the figure that carbon uptake rate of the vegetation decreases under high temperature of pre-monsoon season. Similarly, in the monsoon season, no statistically significant relationship was observed between NEE and air temperature. However, in the post-monsoon season, due to less surface heating, the air temperature was noted to decline, and this declining air temperature was statistically correlated to the NEE values of the Oak system.

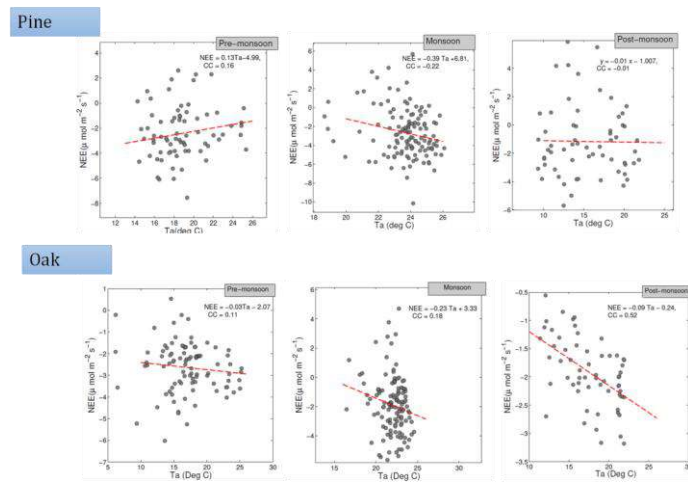


Fig. 11: Relationship between air-temp and NEE

(c) Impact of net radiation on Pine and Oak ecosystem exchange

The Light use efficiency for varying length of rainfall spell (LRS) was quantified and plotted to comprehend the role of radiation in plant productivity. The general dynamics of the LUE for Chir-Pine and Banj-Oak dominated ecosystems can be seen in the figure below.

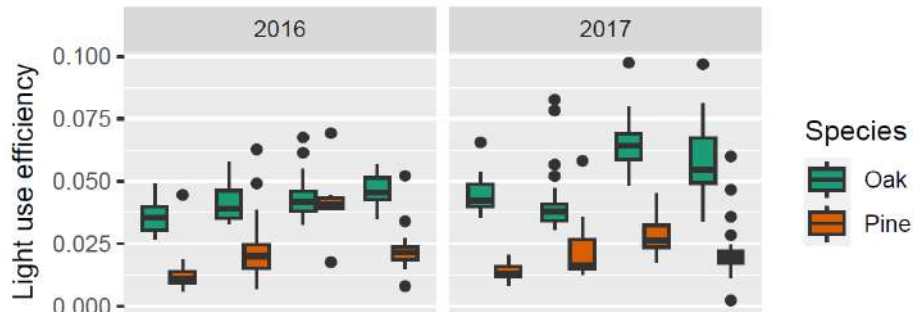


Fig 12. Light use efficiency during monsoon season.

In order to get more clarity on this, a separate analysis was carried out by segregating Light use efficiency of rainy days and rain free days for the period of the study (Fig:12). Almost identical pattern of light use efficiencies during rain free and rainy days were observed for the period of the study which indicate that more rainy/cloudy days could not directly alter the carbon fixation capacity of both Chir-Pine and Banj-Oak dominated ecosystems. This significant change could be due to daily scale analysis of the data which corresponds to the changes in the light level.

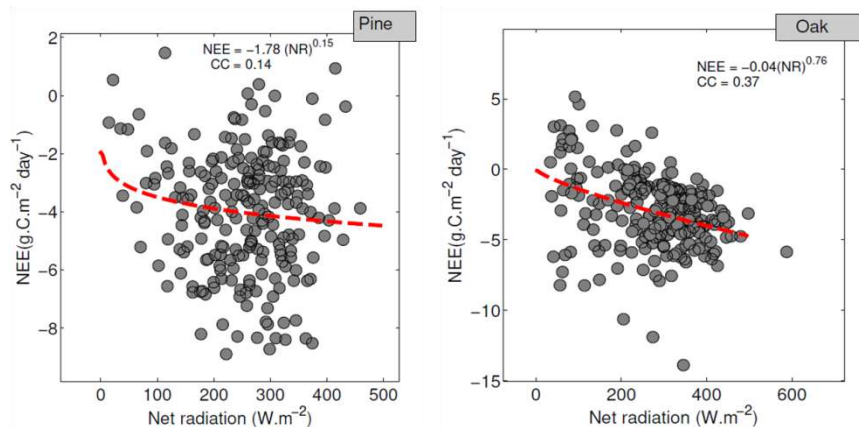


Fig 13. Relationship between net radiation and Pine-Oak ecosystem exchange for monsoon season.

(d) Impact of VPD on Pine and Oak ecosystem exchange

The plants are highly responsive to variation in the VPD leading to stomata closure which further reduces the carbon uptake (Cowan 1977; Farquhar and Sharkey 1982). In actuality, higher VPD values can reduce the carbon assimilation and an inverse relation can be observed between NEE and VPD (Zhou et al 2014; Zhang et al 2016). Stomatal conductance observed to decline under high VPD condition which further increases the transpiration in most plants up until a given VPD threshold, subsequently, photosynthesis and growth are reduced. In order to quantify the impact of VPD on NEE, a power law relationship between NEE and VPD was evaluated by plotting daily average values of VPD against NEE. It can be noted from Figure 6 (g-i) that the NEE-VPD relationship of Banj-Oak system, irrespective of seasons, was moderately strong. The power law

relationship $NEE = -1.96VPD^{0.59}$ of post-monsoon season was noted to have the highest correlation coefficient of 0.48 ($p\text{-value} < 0.001$), followed by the pre-monsoon season ($NEE = -1.86VPD^{0.40}$) correlation coefficient of 0.41 ($p\text{-value} < 0.001$). The monsoon season relationship was noted to be $NEE = -1.58VPD^{0.42}$ having correlation coefficient of 0.23 with no statistical significance. The higher NEE-VPD coupling of post-monsoon and pre-monsoon seasons could be linked to lesser rainfall activities resulting limited changes in the relationships between radiation and VPD, i.e. correlation coefficients between VPD and PPFD were 0.88 and 0.72 ($p\text{-value} < 0.001$), respectively; whereas the rainfall events of monsoon season had significantly modulated the VPD fluctuations through changes in PPFD, i.e. correlation coefficient between VPD and PPFD was 0.62 at a $p\text{-value} < 0.001$.

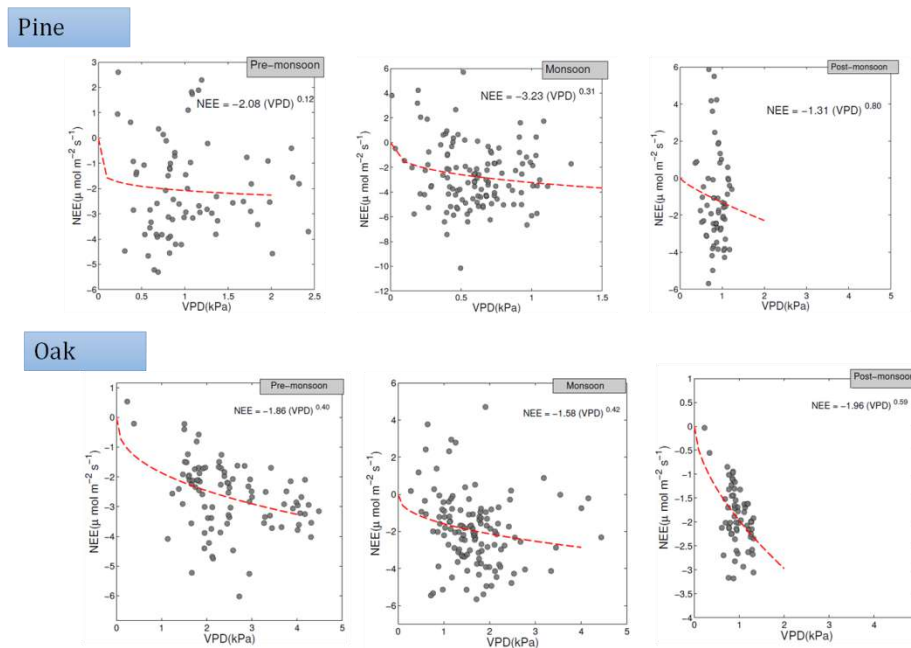


Fig 14. Relationship between VPD and Pine-Oak ecosystem exchange for monsoon season.

3.2.3.3. Comparison of soil CO₂ effluxes: Pine and Oak ecosystem (*manuscript under preparation*)

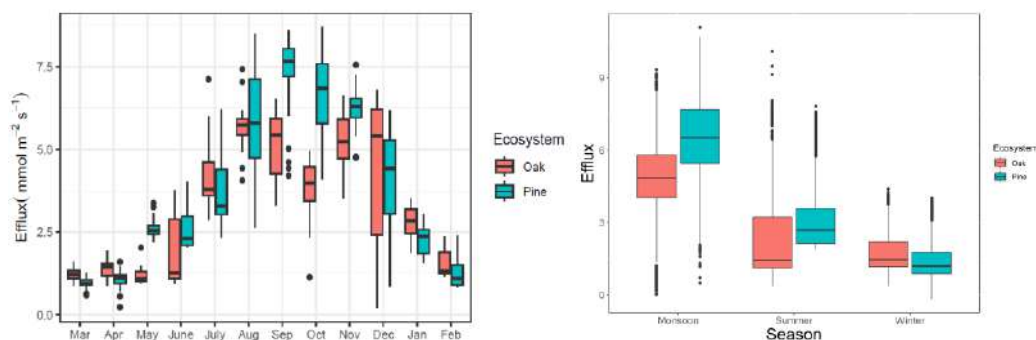
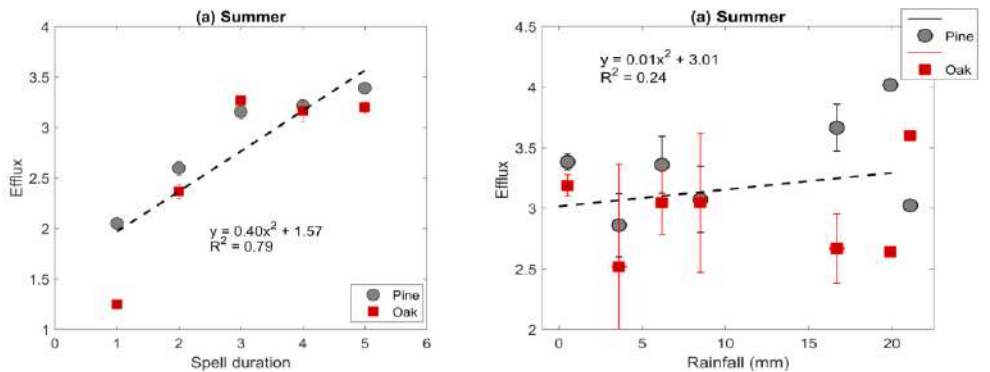


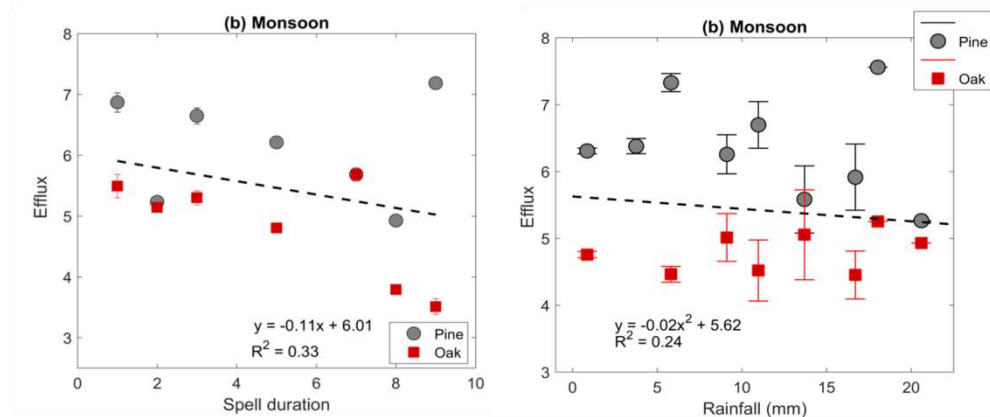
Fig 15. General variation of Pine-Oak soil CO₂ effluxes during 2021-2022.

The mean soil effluxes of Chir-Pine and Banj-Oak dominated ecosystems were found to be $3.71(\pm 2.36) \mu\text{mol.m}^{-2}.\text{s}^{-1}$ and $3.23(\pm 2.23) \mu\text{mol.m}^{-2}.\text{s}^{-1}$ during the period of observation, respectively. Both Chir-Pine and Banj-Oak dominated ecosystems have notably high soil effluxes (6.49 ± 1.28 and $4.90\pm 1.11 \mu\text{mol.m}^{-2}.\text{s}^{-1}$) during monsoon season.

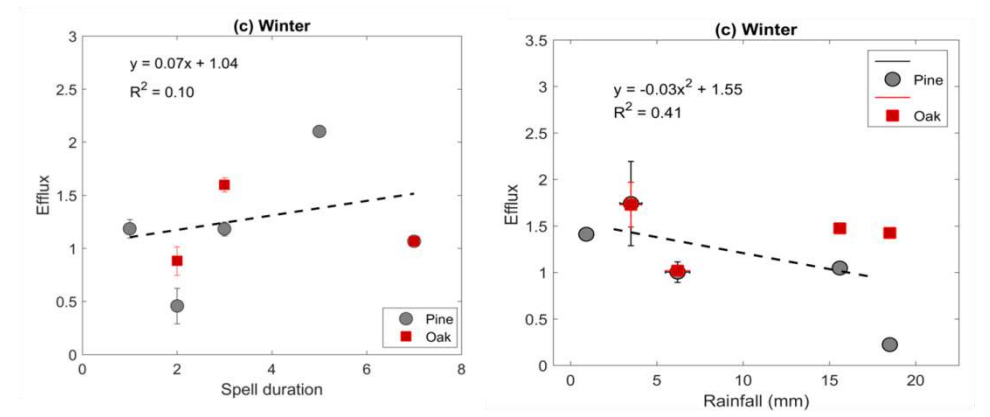
Relationships between daily rainfall spell and amount with soil CO₂ effluxes: Summer, monsoon and winter



During Summer period, due to the prevalent drier condition in the atmosphere and soil, spell duration and amount of rainfall is noted to have **positive relationship** with soil CO₂ effluxes at both sites.



During **Monsoon** period, the moisture condition in the atmosphere and soil is exactly opposite to Summer season, hence, saturated soil moisture prohibits auto and heterotrophic respiration resulting **Negative Relationship** with soil CO₂ effluxes at both sites. A decreasing trend could be observed during monsoon season due to the reason that the soil microbes need optimum moisture level whereas too high or too low moisture can limit soil CO₂ efflux rate.



During winter period, a contrasting effect was observed for spell and amount. Soil CO₂ efflux found to increase with increasing rainfall spell, however, a decreasing trend was observed as the amount of rainfall increases. This could be due to the reason that a larger amount rainfall could be detrimental to microbial activities.

Summary

- Transpiration dynamics indicate higher water loss by Pine stands than Oak stands.
- Results of the study indicate that the Pine vegetation is having 1.5 times higher carbon uptake than Oak vegetation and 20 times higher deciduous broadleaf forest.
- It can be concluded from the wavelet analysis that Pine system are responsive to rapid changes where as Oak systems adapt changes slowly.
- Both Pine and Oak dominated ecosystems efficiently use water during photosynthesis activity. However, the Pine dominated ecosystem has marginally higher annual WUE ($1.35 \pm 3.18 \text{ gC.Kg}^{-1}\text{H}_2\text{O}$) than Oak ($1.10 \pm 2.08 \text{ gC.Kg}^{-1}\text{H}_2\text{O}$) dominated ecosystem.

References:

Gaira, K., Rawal, R. S., Rawat, B., Bhatt, I. D. (2014). Impact of climate change on the flowering of *Rhododendron arboreum* in central Himalaya, India. *Current Science*, 106(12), 1735–1738.

Grinsted, A., Moore, J., Jevrejeva, S. (2004). Application of the cross wavelet transform and wavelet coherence to geophysical time series. *Nonlinear Processes in Geophysics*, 11, 561–566.

Hao, G., Hu, Z., Di, K., Li, S. (2020). Rainfall pulse response of carbon exchange to the timing of natural intra-annual rainfall in a temperate grass ecosystem. *Ecological Indicators*, 118, 106730.

Hao, Y. B., Kang, X. N., Wu, X., Cui, X. Y., Liu, W. J., Zhang, H., Zhao, H. T. (2013). Is frequency and amount of precipitation more important in controlling CO_2 fluxes in the 30 year old fenced and moderately grazed temperate steppe agriculture? *Agriculture, Ecosystem and Environment*, 171, 63–71.

Hao, Y. B., Zhou, C. T., Liu, W. J., Li, L., Kang, X. N., Jiang, L. L., Xu, C. Y. (2017). Above ground net primary production and carbon balance remain stable under extreme precipitation events in a semi-arid steppe ecosystem. *Agricultural and Forest Meteorology*, 240, 1–9.

Huntely, B. (1991). How plants respond to climate change: migration rates, individualism and the consequences for plant communities. *Annals of Botany*, 67, 15–22.

Huxman, T. E., Snyder, K., Tissue, D., Leffler, A. J., Ogle, K., Pockman, W., Sandquist, D., Potts, D., Schwinning, S. (2004). Precipitation fluxes and carbon fluxes in semi-arid and arid ecosystem. *Oecologia*, 141(2), 254–268, <https://doi.org/10.1007/s00442-004-1682-4>.

Joshi, B., Rawal, R. S., Chandra Sekar, K., Pandey, A. (2019). Quantitative ethnobotanical assessment of woody species in a representative watershed of west Himalaya, India. *Energy, Ecology and Environment*, 4, 56–64, <https://doi.org/10.1007/s40974-019-00114-9>

Joshi, B., Rawal, R. S., Chandra Sekar, K., Tewari, A. (2020). Assessment of fuel wood resource preference in representative watershed of west Himalaya, India: conservation and management implications. *Environment, Development and Sustainability*, 22, 1617–1632.

Joshi, G., Negi, G. C. S. (2011). Quantification and valuation of forest ecosystem services in the western Himalayan region of India. *International Journal of Biodiversity Science, Ecosystem Services & Management*, 7(1), 2–11, <https://doi.org/10.1080/21513732.2011.598134>.

Joshi, M., Mer, G., Singh, S., Rawat, Y. (1991). Seasonal pattern of total soil respiration in undisturbed and disturbed ecosystems of Central Himalaya. *Biology and Fertility of Soils*, 11, 267–272.

Joshi, V. C., Bisht, D., Sundriyal, R. C., & Pant, H. (2022). Species richness, diversity, structure, and distribution patterns across dominating forest communities of low and mid-hills in the Central Himalaya. *Geology, Ecology, and Landscapes*, 10(4):1-10

Khanduri, V. P., Sharma, C. M., Singh, S. P. (2008). The effect of climate change on plant phenology. *The Environmentalist*, 28, 143–147.

Lasslop, G., Reichstein, M., Papale, D., Richardson, A., Arneeth, A., Barr, A., Stoy, P., Wohlfahrt, G. (2010). Separation of net ecosystem exchange into assimilation and respiration using a light response curve approach: critical issues and global evaluation. *Global Change Biology*, 16(1), 187–208, <https://doi.org/10.1111/j.1365-2486.2009.02041.x>.

Lohani, P., Mukherjee, S. (2021). Impact of terrain complexity on the turbulence drag coefficient: a case study from the Indian Himalayan region. *Dynamics of Atmospheres and Oceans*, 93C, 101201, <https://doi.org/10.1016/j.dynatmoce.2021.101201>.

Mukherjee, S. (2021). Nonlinear recurrence quantification of the monsoon-season heavy rainy-days over the northwest Himalaya for the baseline and future periods. *Science of The Total Environment*, 789, 147754, <https://doi.org/10.1016/j.scitotenv.2021.147754>.

Mukherjee, S., Sekar, K. C., Lohani, P., Kumar, K., Patra, P. K., Ishijima, K. (2018). Investigation of scale interaction between rainfall and ecosystem carbon exchange of Western Himalayan Pine dominated vegetation. *Biogeosciences Discussion*, <https://doi.org/10.5194/bg-2018-299>.

Mukherjee, S., Hazra, A., Kumar, K., Nandi, S., Dhyani, P. (2019). Simulated projection of ISMR over Indian Himalayan region: assessment from CSIRO-CORDEX South Asia experiments. *Meteorology and Atmospheric Physics*, 131(1), 63–79, <https://doi.org/10.1007/s00703-017-0547-4>.

Mukherjee, S., Lohani, P., Kumar, K., Chowdhuri, S., Prabhakaran, T., Karipot, A. (2020). Assessment of new alternative scaling properties of the convective boundary layer: application to velocity and temperature spectra. *Boundary-Layer Meteorology*, 176, 271–289, <https://doi.org/10.1007/s10546-020-00525-w>.

Mukherjee, S., Lohani, P., Tiwari, A., Sturman, A. P. (2021). Characteristics of convective surface layer turbulence over central Himalaya with an emphasis to monin-obukhov similarity theory. *Journal of Atmospheric and Solar Terrestrial Physics*, 225, 105748, <https://doi.org/10.1016/j.jastp.2021.105748>.

3.2.4. Regional scale climate modeling for IHR including three sites of two watersheds including high resolution data assimilation.

3.2.4.1. Future precipitation extremes over base Himalayan Uttarakhand region: analysis using the statistically downscaled, bias-corrected high-resolution NEX-GDDP datasets.

To understand the fidelity of the model simulations, we have examined the annual cycles in the precipitation (mm day^{-1}) over the Uttarakhand state from 1976 to 2005, as shown in Figure 1. The figure represents monthly mean precipitation from the APHRODITE (black line) and MMM (red line). The visual inspection shows that the model simulations could reasonably capture the seasonal rainfall. The mean monthly precipitation patterns obtained from the MMM are the same as that of APHRODITE. The maximum peak exhibited by APHRODITE is 9.7 mm day^{-1} in July and lowest in November, 0.3 mm day^{-1} whereas, the MMM peaked in August (7.9 mm day^{-1}) and a minimum of 0.2 mm day^{-1} in November. The variability in the MMM precipitation increases with rainfall quantity.

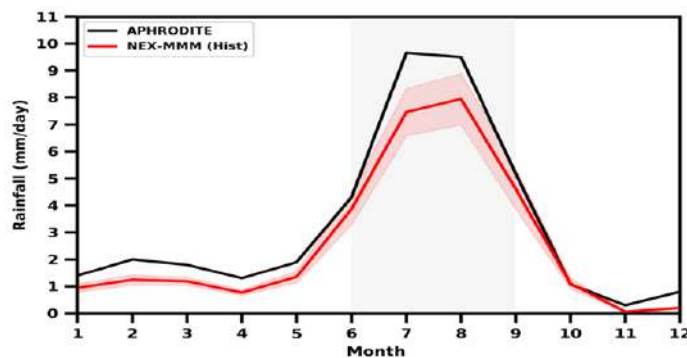


Figure 1: Annual cycle of monthly precipitation (mm/day) over Uttarakhand during 1976–2005 from APHRODITE (black) and NEX–GDDP MMM (red line). Red-color shading denotes \pm standard deviation of 20 NEX–GDDP models. Shaded gray region denotes the SW-monsoon season (JJAS).

Figure 2 shows the contribution of the monsoon rainfall to the annual rainfall of Uttarakhand as obtained from APHRODITE and MMM. As revealed from MMM, southern parts of Uttarakhand receive about 75-90%, and northern parts receive 60-70% of the annual rainfall (Fig. 4b). On the other hand, most of the Uttarakhand region receives $\sim 75\%$ of the annual rainfall in the monsoon season.

The projected precipitation (%) change's spatial distribution from the MMM is presented for the near and far future with reverence to the model baseline period (Figure 3). Figure 4a and b show an increase in the near future of about 10% in RCP 4.5 and 18% in the RCP 8.5 scenario. At the same time, it may increase by 21% and 42% in the far-future from RCP 4.5 and RCP 8.5 scenarios, respectively (Figure 3c and d). A substantial increase in rainfall percentage has been noticed in the high emission scenario (RCP 8.5) to the end of the 21st century (Figure 3d). The projected changes in precipitation vary across Uttarakhand, but overall, a significant increase in the future rainfall is noticed.

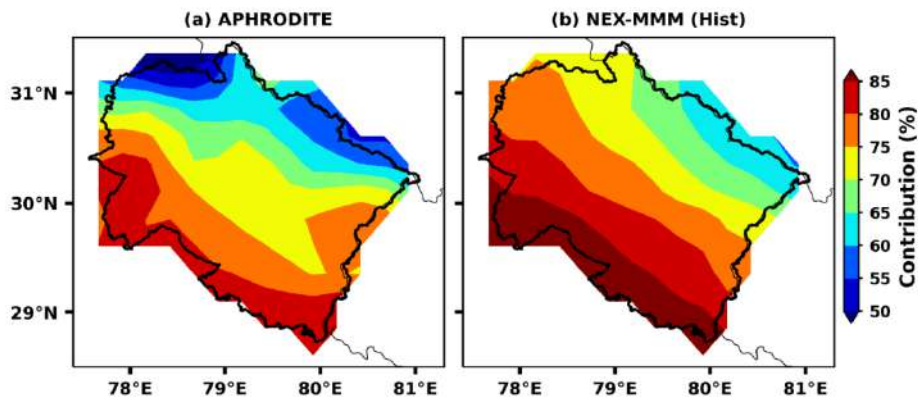


Figure 2: The contribution of SW monsoon (JJAS) rainfall to annual rainfall from APHRODITE and NEX–GDDP MMM.

The spatial analysis further reveals that maximum precipitation change may be seen in the northern parts of Uttarakhand under lower and higher emission scenarios to the end of the century. Sharma et al. (2015) also presented increasing rainfall patterns of Uttarakhand in the future using multiple linear regression analysis and artificial neural networks.

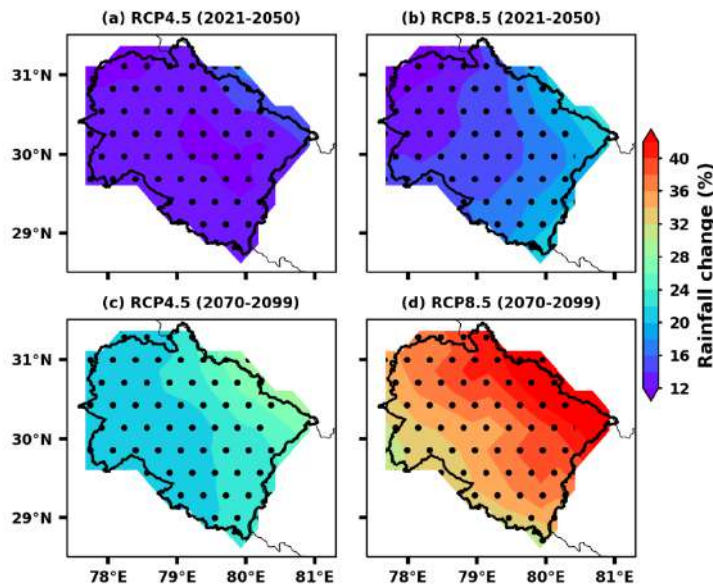


Figure 3: Projected changes in MMM of rainfall in the near (2021-2050) and far future (2070-2099) under RCP4.5 and RCP8.5 scenarios relative to 1976-2005. The black dots represent regions of 90% significance level.

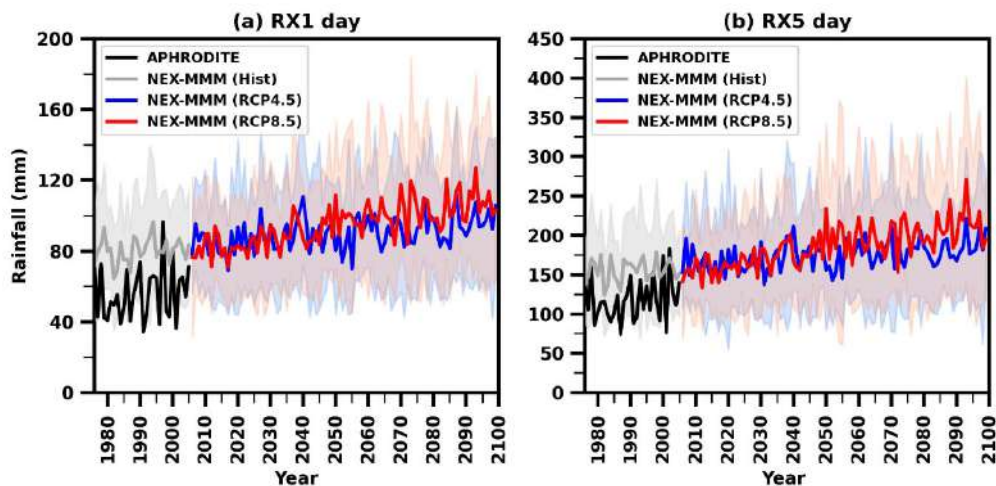


Figure 4 Future projections a) RX1DAY, and b) RX5DAY (area averaged over Uttarakhand state). Solid lines show the MMM, and shading regions indicate the range of the standard deviation each model.

Figure 4 shows the relative projections in the highest ONE-day (RX1DAY) and Five-day (RX5DAY) precipitation in the Uttarakhand state. The solid lines represent the projection of RX1DAY and RX5DAY, and shaded regions indicate the individual models standard deviation. Results show an increase in RX1DAY and RX5DAY rainfall from the middle of the 21st century. RX1DAY increases by 1.4 mm decade⁻¹ and 3.3 mm decade⁻¹ under RCP 4.5 and RCP 8.5 scenarios. However, the RX5DAY precipitation increases by 2.7 mm decade⁻¹ and 7 mm decade⁻¹ under RCP 4.5 and RCP 8.5 scenarios. Increasing extreme precipitation intensity is expected to be the primary cause of total precipitation increase. 21st century projected intense rainfall, RX1DAY, and RX5DAY consistently indicate increased precipitation over the Uttarakhand region. Thus, future flood risk is expected to grow with extreme precipitation (Gu et al. 2018).

Conclusion

The NEX-GDDP MMM shows an increase in rainfall over Uttarakhand in the near future, and it is likely to increase further towards the end of the 21st century. Projected change in mean rainfall infers a modest increase in precipitation in the near future and a considerable increase in the far future. A study by Kulkarni et al. (2020) also reported rainfall in India is increasing in the future due to the response of global warming. The change in rainfall in the northern parts of Uttarakhand is relatively higher than in the southern parts of the state. RX1DAY and RX5DAY precipitation under the RCP 8.5 scenario increase more than the RCP 4.5 scenario. This could be the reason for intense downpours occurring over the Uttarakhand region. According to this study, the mean and extreme precipitation events would change during the monsoon season over Uttarakhand in the future. In the future, the intensity of precipitation and the extreme event frequency in Uttarakhand are likely to increase under global warming conditions.

3.2.4.2. Projected changes in precipitation and temperature extremes using bias corrected NEX-GDDP6 simulations over Hindu Kush Himalaya

The models do a much better job in simulating daily maximum and minimum temperature over HKH. The RMSE values are very low and the models are very close to the observation point (Figure 6). The models are spread around the dotted line and hence, have similar standard deviation as the CRU data. It can be observed that the correlation is also very high in figures 6 a, b, d, e and f (above 0.9) and it is high in Figure 6c (0.7 to 0.9). Thus the NEX-GDDP6 models are able to capture the daily minimum and maximum temperatures over HKH region well.

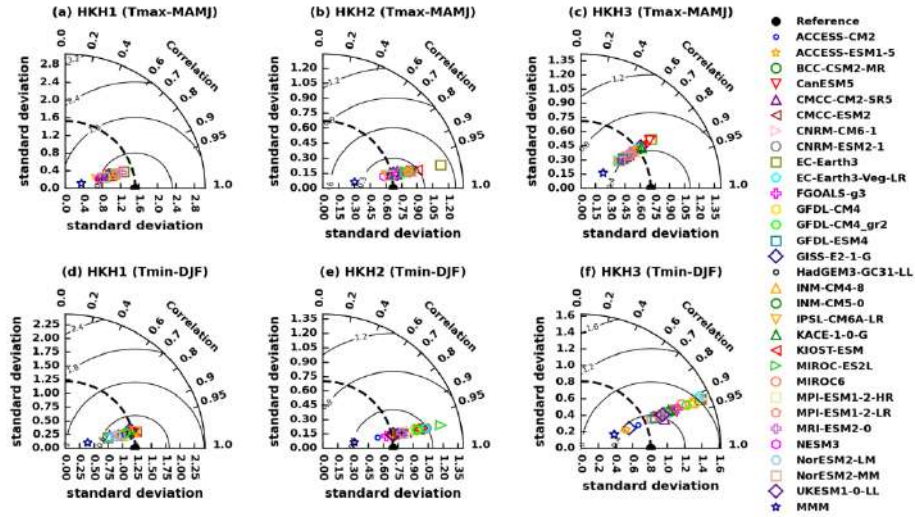


Figure 6: Taylor diagrams for maximum (MAMJ) and minimum (DJF) temperatures comparing with CPC with NEX-GDDP6 models for HKH1, HKH2, and HKH3 region for the 1985-2014. Here multi model mean (MMM)

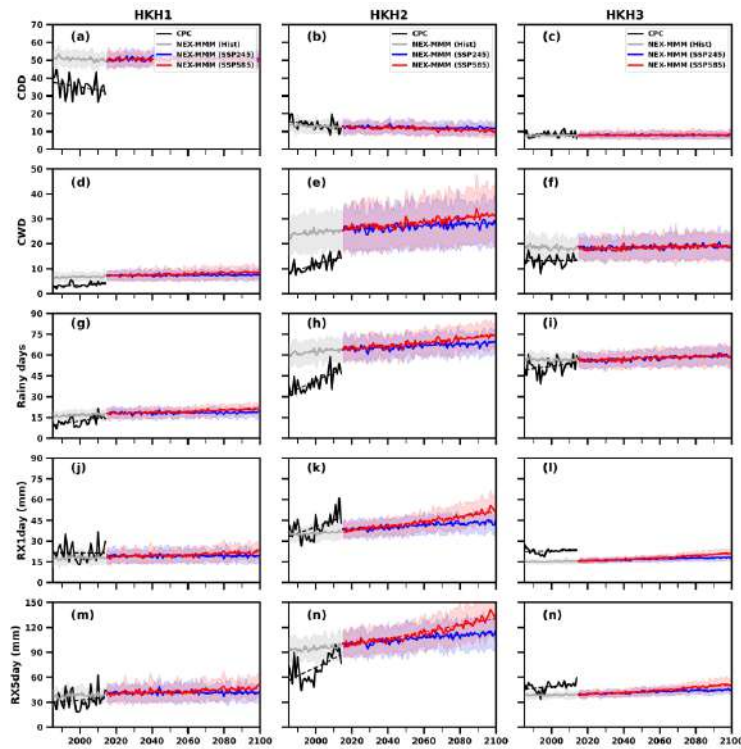


Figure 7: Time series plots of seasonal monsoon (JJAS) season in various extreme precipitation extremes over HKH1, HKH2 and HKH3 such as CDD (a-c), CWD (d-f), Rainy days (g-i), RX1 day (j-l), RX5 day (m-n) during 1985-2100.

Figure 7 shows the temporal evaluation of projected changes of extreme precipitation indices (refer Table 3). The number of days with rainfall and how the total rainfall over HKH might change by the end of the century. The models project a slight decrease in the number of CDD and an increase in the number of CWD and rainy days over the region. The rate of increase in rainy days is estimated to be 0.07 days and 0.4 days per decade in HKH1, 0.5 days and 1.1 days per decade in HKH2, and 0.4 days and 0.46 days per decade in HKH3 regions under the SSP245 and SSP585 scenarios, respectively. The values of RX1Day and RX5Day are also projected to increase

over the regions. RX1Day rainfall is projected to increase by 0.02 mm and 0.41 mm per decade in HKH1 under the SSP245 and SSP585 scenarios, 0.7 mm and 1.8 mm per decade in HKH2, and 0.3 mm and 0.7 mm per decade in HKH3 regions, respectively. According to the models, RX5Day rainfall can also be expected to increase by 0.06 mm and 0.85 mm per decade in HKH1, 1.7 mm and 4.1 mm per decade in HKH2, and 0.74 mm and 1.55 mm per decade in HKH3 regions, under the SSP245 and SSP585 scenarios respectively. It's worthy of notice that the patterns are consistent with all these indices, with the increase being more under SSP585 compared to SSP245.

This decrease is consistent with the projected increase in temperatures under the SSP245 and SSP585 scenarios in the HKH1, HKH2, and HKH3 regions (Figure 8). The rate of decrease in TX10p is estimated to be 0.64 and 0.83 days per decade in HKH1, 1.1 and 1.2 days per decade in HKH2, and 0.62 and 0.75 days per decade in HKH3 regions under the SSP245 and SSP585 scenarios, respectively. Similarly, the percentage of TN10p is projected to decrease by 0.67 and 0.87 days per decade in HKH1 under the SSP245 and SSP585 scenarios, 0.67 and 0.85 days per decade in HKH2, and 0.62 and 0.80 days per decade in HKH3 regions. On the other hand, the percentages of TX90p and TN90p are projected to significantly increase under the SSP245 and SSP585 scenarios. The trend shows an increase of 4.0 and 8.4 days per decade in TX90p in HKH1, 5.13 and 9.21 days per decade in HKH2, and 4.31 and 8.58 days per decade in HKH3 regions under the SSP245 and SSP585 scenarios, respectively. Similarly, TN90p are projected to increase by 4 and 8.4 days per decade in HKH1, 5.1 and 9.2 days per decade in HKH2, and 4.3 and 8.58 days per decade in HKH3 regions under the SSP245 and SSP585 scenarios. These findings are consistent with previous studies that have also observed a decrease in cold events and an increase in warm events in most parts of the Himalaya region (Rao et al., 2022; Krishnan et al., 2019). The number of SU is projected to likely increase in the HKH1, HKH2, and HKH3 regions under the SSP245 and SSP585 scenarios. The increase is estimated to be 0.47 and 0.16 days per decade in HKH1, 0.69 and 1.37 days per decade in HKH2, and 0.005 and 0.02 days per decade in HKH3 regions under the SSP245 and SSP585 scenarios respectively.

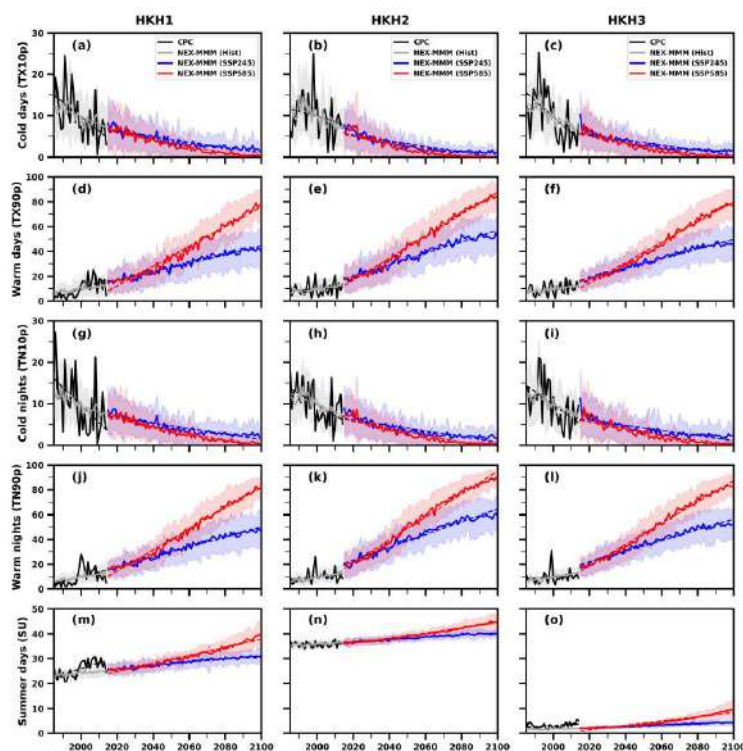


Figure 8: Time series plots of seasonal various extreme temperature extremes over HKH1, HKH2 and HKH3 such as cold days (TX10p) (a-c), warm days (TX90p) (d-f), cold nights (TN10p) (g-i), warm nights (TN90p) day (j-l), summer days (SU) (m-n) during 1985-2100.

Conclusions:

- 1) Increasing the RX1day, RX5day and rainy days are increasing over HKH region
- 2) Cold days and cold nights are decreasing and warm days, warm nights and summer days are increasing over HKH region.
- 3) The study findings highlight the need for considering more extreme precipitation and temperature over HKH climate resiliency planning.

3.2.4.3. Development of regional land surface model and assessment of Pine and Oak forest dominated region

(a) Land Surface characteristics based on 1D Noah-MP LSM: Sensitivity to vegetation and Evaluation. [Under Review: JGR Atmospheres]

The LHF and evapotranspiration (ET) have been verified at Gangolihat station against *in-situ* observation, and the mean errors in diurnal variation are shown in Figure 9. The ERA5-Land and MERRA2 errors are slightly higher (~20 to 60 W m⁻²) compared to IMDAA and GLDAS (0 to 30 W m⁻²) in winter (Figure 9a). During the monsoon season, the daytime LHF errors vary from -25 to 170 W m⁻² in IMDAA and -40 to -110 W m⁻² in GLDAS and MERRA2 (Figure 9c). The Noah-MP EXP3 exhibits much lesser errors between -31 to 64 W m⁻². The EXP1 simulates the highest error -225 to -1 W m⁻² against observations in all seasons at Gangolihat (Figure 9a-d). During the monsoon season, LHF is greater than SHF at Kosi-Katarmal, Kantali, and Gangolihat locations (not shown). The partitioning of surface fluxes from Noah-MP simulations and global reanalysis indicates the influence of the monsoon on the surface energy components (Krishnamurti and Biswas, 2006).

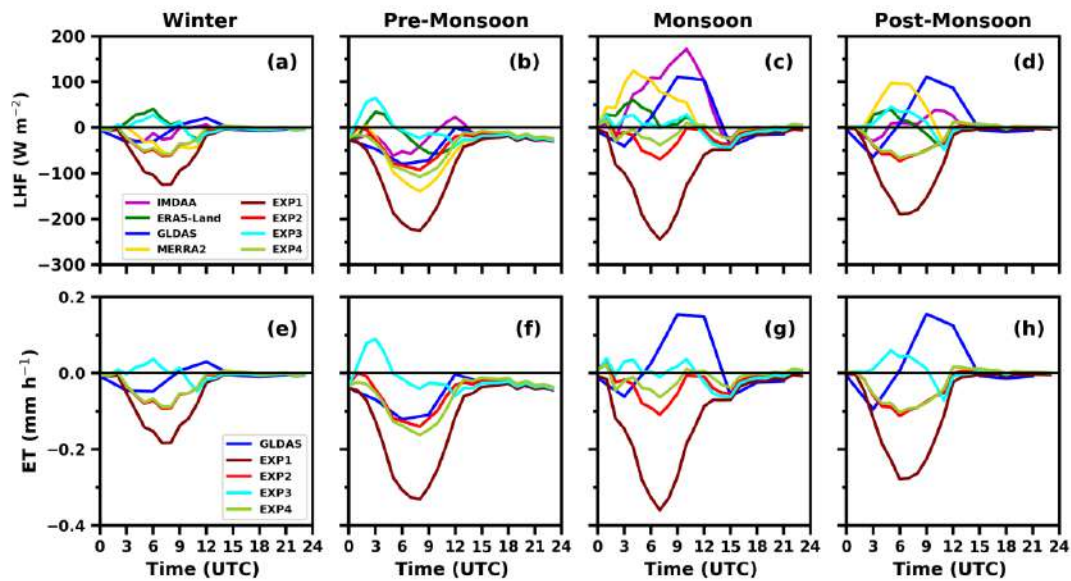


Figure 9: Mean errors of diurnal cycle of latent heat flux (LHF) from Noah-MP experiments and reanalysis against *in-situ* observation for (a) winter (b) pre-monsoon (c) monsoon, and (d) post-monsoon seasons. (e-h) is same as (a-d) but for Evapotranspiration (ET) errors. All these analyses are done at Gangolihat station from 2016-2018.

Similar to LHF, the ET is maximum in monsoon and pre-monsoon seasons and minimum in winter (not shown). The mean error in diurnal patterns at Gangolihat station is shown for the Noah-MP individual simulations and GLDAS (Figure 9e-h) for all seasons. It is observed that the ET error from Noah-MP experiments is more during noon (6–8 UTC) compared to the rest of the day in all seasons. Compared to GLDAS, EXP3 appears to be better (error close to zero) than EXP2 and EXP4 (64 to 92 $W m^{-2}$) in all seasons. However, EXP1 highly underestimates ET against observation and analyses (Figure 9e-h). The maximum errors of EXP3 in winter, pre-monsoon, monsoon, and post-monsoon seasons are about -0.05, 0.09, -0.06, and -0.07 $mm h^{-1}$, respectively. The GLDAS showed the opposite bias in monsoon and post-monsoon seasons. The ET errors in the nighttime are almost zero in all the seasons except pre-monsoon (Figure 9f). It can conclude that the Noah-MP simulations can provide better diurnal variation, unlike the GLDAS in most of the seasons.

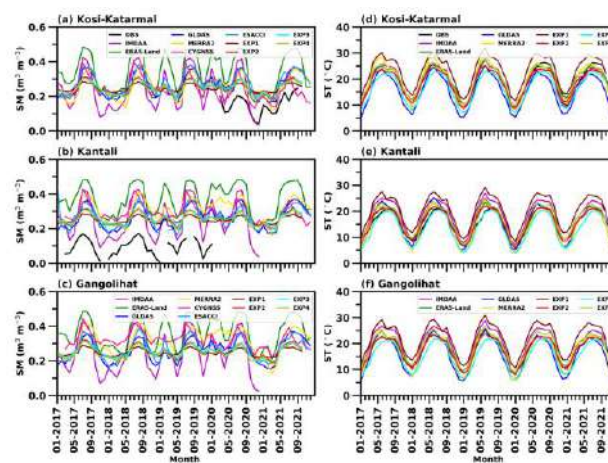


Figure 10. Monthly wise variation of soil moisture (SM) at (a) Kosi-Katarmal, (b) Kantali, and (c) Gangolihat stations. (d-f) are same as (a-c) but for soil temperature (ST).

The SM and soil temperature (ST) impact regional climate by controlling the distribution of available energy at the ground surface into sensible and latent heat fluxes with the atmosphere (Wei, 1995). Monthly variations of SM and ST obtained from Noah-MP individual experiments and other analyses are analysed at Kosi-Katarmal, Kantali, and Gangolihat stations for the period 2017-2021 (Figure 10). Rainfall has a significant impact on SM on various temporal scales, particularly in the shallow levels (Nayak et al., 2019; Wang et al., 2010). The regional, global analysis, satellite derived (CYGNSS and ESACCI) overestimate the SM compared to the observation. ERA5-Land overestimates the SM compared to the observed, CYGNSS and ESACCI throughout the period, however, the monthly variations are maintained. The ERA5-Land shows higher SM throughout the year varying 0.2 to 0.5 $m^3 m^{-3}$, showing maximum in the monsoon and minimum in winter season (Figure 10a-c). IMDAA underestimates SM between October to December months compared with other global and satellite analysis. The SM simulated from Noah-MP individual experiments show less standard deviations and the monthly mean is comparable with CYGNSS, ESACCI, GLDAS and MERRA2 at Kosi-Katarmal and Kantali locations, and ESACCI and GLDAS at Gangolihat station. Simulated SM also identifies the monthly variations as observed (Figure 10a-c), especially in the monsoon where the increase in precipitation causes the SM to increase (Osuri et al., 2020). All the analyses could show maximum variation of SM between monsoon and the Post-monsoon/winter seasons. Note that the performance of LSM in SM simulation over complex regions may be differed when compared with abundant of *in-situ* SM observations.

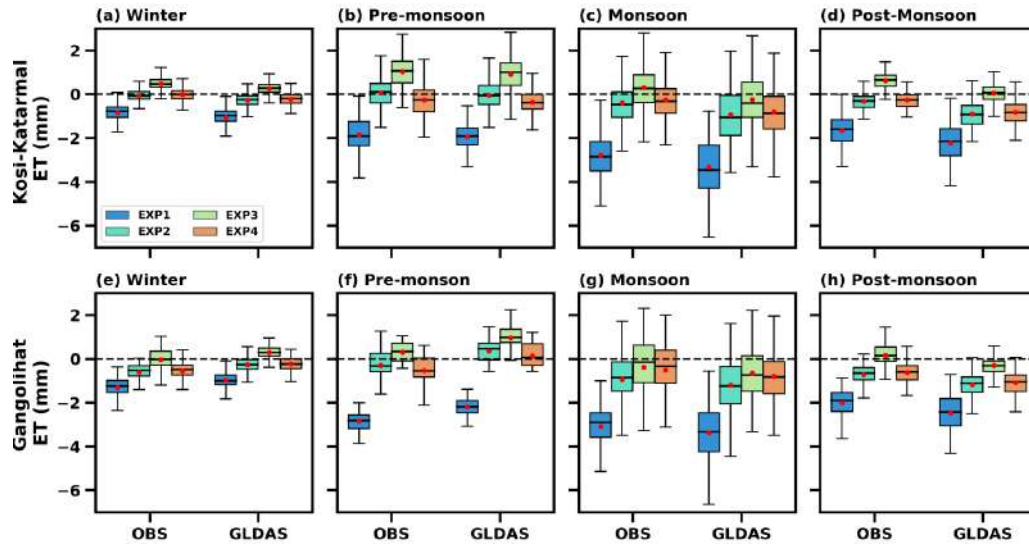


Figure 11. Box plot of ET errors estimated against in-situ observation and GLDAS for (a) winter, (b) pre-monsoon, (c) monsoon, and (d) post-monsoon seasons at Kosi-Katarmal station. (e-h) are same as (a-d) but at Gangolihat station. The red marker shows the mean value.

The monthly variations of ST from Noah-MP simulations and reanalyses data sets indicate the observed patterns satisfactorily (Figure 10d-f). The Noah-MP EXP1 ST is highly overestimates 1.7-5 °C, EXP2, EXP3 and EXP4 slightly underestimated (-4.2 to -0.4 °C) in June to September at Kosi-Katarmal (Figure 10d). The GLDAS overestimates (by 0-6 °C) from April to August and underestimates (by 0-3 °C) from October to January in Kantali (Figure 10e). IMDAA overestimated (by 0-5 °C) from April to August at Kantali location. EXP2 ST is closely to the observation compared to EXP1, EXP3 and EXP4 at Kosi-Katarmal and Kantali. Noah-MP simulations except EXP1 are close to the ERA5-Land, GLDAS and MERRA2 at Gangolihat (Figure 10f). While the individual experiments monthly mean resembles the observed patterns are closely to Kosi-Katarmal and Kantali (Figure 10d, e). However, EXP1 ST is highly overestimated thought the period compared with observation and reanalyses at these 3 locations (Figure 10d-f).

Figure 11 provides the seasonal mean errors of simulated ET from Noah-MP experiments against *in-situ* observation and GLDAS. In winter, the simulations show mean errors between -1 to 0.47 mm with observation, and GLDAS (Figure 11a). Similarly, the mean errors lie near zero in other seasons except for EXP1 (Figure 11b-d). The EXP2 appears consistently better when compared with observations in all the seasons (Figure 11a-d). However, it exhibits slightly higher errors in monsoon and post-monsoon seasons at Kosi-Katarmal station when compared with GLDAS (Figure 13c-d). The simulated ET error from EXP3 is the minimum (0.4 to 0.3 mm) against observation in all the seasons at the Gangolihat location (Figure 11e-h). The error against GLDAS is -0.7 to 0.3 mm except pre-monsoon at the Gangolihat location (Figure 13e-h). From the above analyses, it could conclude that the realistic vegetation information in the LSM improves the simulation of land conditions as seen at Kosi-Katarmal and Kantali stations (from EXP2 with Deciduous Needleleaf forest) and Gangolihat station (from EXP3 with Evergreen Broadleaf forest). Thus, the study highlights the importance of defining the vegetation type for improved land surface conditions.

Conclusion

1. The Noah-MP LSM could reproduce the diurnal, monthly, and seasonal evolution of land conditions such as ST, SM, heat fluxes, and ET and reasonably agrees with the *in-situ* observations. However,

Noah-MP products appear to be better than the global analysis datasets most of the time in different seasons.

2. The SM simulated from the Noah-MP model is comparable with satellite analyses (CYGNSS, ESACCI), while overestimating against *in-situ* observations. Similarly, the ST has been simulated well compared to *in-situ* and reanalyses products, with mostly warm (positive) bias.
3. The Noah-MP simulations could represent correct surface energy balance terms (NR, SHF & LHF) and ET close to the *in-situ* observations.
4. Individual experiments show that the SM simulated from Noah-MP does not show noticeable changes from experiment to experiment and could be similar vegetation properties across the stations. However, the ST and surface fluxes are noticeably different among the experiments in different seasons. Analyses of surface flux terms indicate that the Noah-MP experiment with correct vegetation index (for ex., EXP2 at Kosi-Katarmal and Kantali stations and EXP3 at Gangolihat station) could produce land surface processes close to observations and better or comparable with the global analyses.

3.2.4.4. Development of regional land surface model and assessment of Pine and Oak forest dominated region using 3-dimensional High-Resolution Land Data Assimilation System

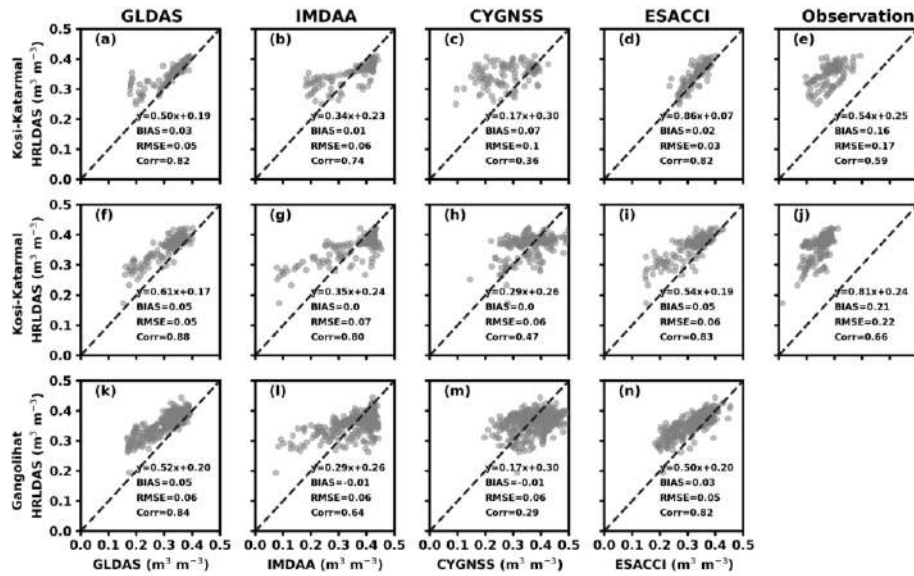


Figure 12. HRLDAS SM verification with a) GLDAS, b) IMDAA c) CYGNSS, d) ESACCI, and e) ESACCI analyses with respect to *in-situ* observations at Kosi-Katarmal station. f-j are the same as a-e but over Kantali station, k-n are the same as a-d but over Gangolihat station

The *in-situ*, global, regional and satellite derived (CYGNSS and ESACCI) products of SM in the top layer compared with HRLDAS at Kosi-Katarmal, Kantali and Gangolihat stations during the monsoon season in Figure 12. HRLDAS perform well, with the highest correlation coefficient (CC) of ~ 0.82 , less root mean square error (RMSE) ($0.02 - 0.06 \text{ m}^3 \text{ m}^{-3}$) and bias ($0.02 - 0.05 \text{ m}^3 \text{ m}^{-3}$) with ESACCI at Kosi-katarmal, Kantali and Gangolihat stations. HRLDAS comparable with the IMDAA and GLDAS reanalysis. HRLDAS is reasonable agree with the CYGNSS analysis, less bias at Kantali, and Gangolihat stations (Figure 12 h, m). HRLDAS is highly overestimated (0.16 and $0.21 \text{ m}^3 \text{ m}^{-3}$) with the observation and high RMSE (0.17 and $0.22 \text{ m}^3 \text{ m}^{-3}$) at Kosi-Katarmal and Kantali (Figure 12 e, j). However, HRLDAS SM exhibits better performs with the ESACCI than reanalysis and *in-situ* observations.

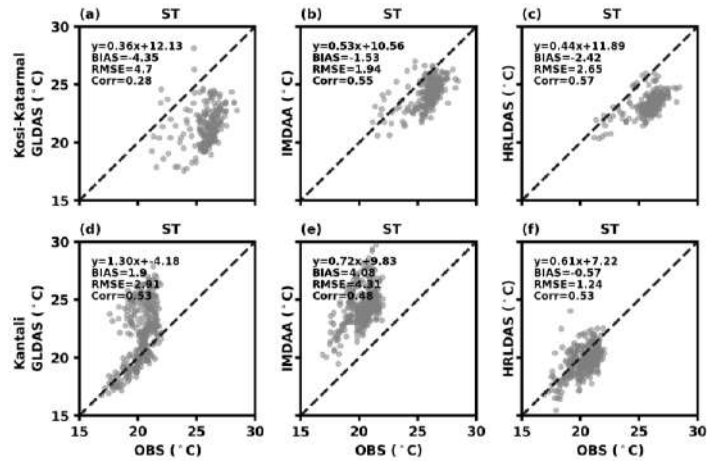


Figure 13. Scatter plots of ST (°C) analyses of GLDAS, IMDAA and HRLDAS with respect to *in-situ* observations at Kosi-Katarmal (a-c) and Kantali (d-f).

Figure 13 shows the scatter diagram of ST analyses and *in-situ* observations along with basic statistics at Kosi-Katarmal and Kantali stations during the monsoon season. Based on the analyses, it has been found that GLDAS underestimates the ST by approximately 4.35 °C, and the RMSE is the highest (4.75 °C), with the lowest CC of 0.28, at the Kosi-Katarmal station (Figure 13a). IMDAA shows the reasonable agree with the observation and underestimates the ST by 1.75 °C and CC (0.55) (Figure 13b). GLDAS overestimates the ST by 1.9 °C, and the RMSE is 2.91 °C at Kantlai (Figure 13d). IMDAA highly overestimated the ST (4.08 °C) and high RMSE (4.31 °C) (Figure 13e). The ST with high CC (0.57), low bias (-2.42 °C), and low RMSE (2.65 °C) at the Kosi-Katarmal station (Figure 13c). However, at Kantali the HRLDAS has even lower bias (-0.57 °C), RMSE (1.24 °C) (Figure 13f). The ST of HRLDAS consistently performs better than the IMDAA and GLDAS in bias, RMSE, and CC. Point observations provide valuable information for assessing the accuracy and reliability of global and regional analyses. In general, the SM in a particular geographic region is primarily influenced by precipitation. The difference in the spatial distribution of SM top (0-10 cm) layer between the GLDAS, IMDAA, CYGNSS, and ESACCI datasets are examined (Figure 14).

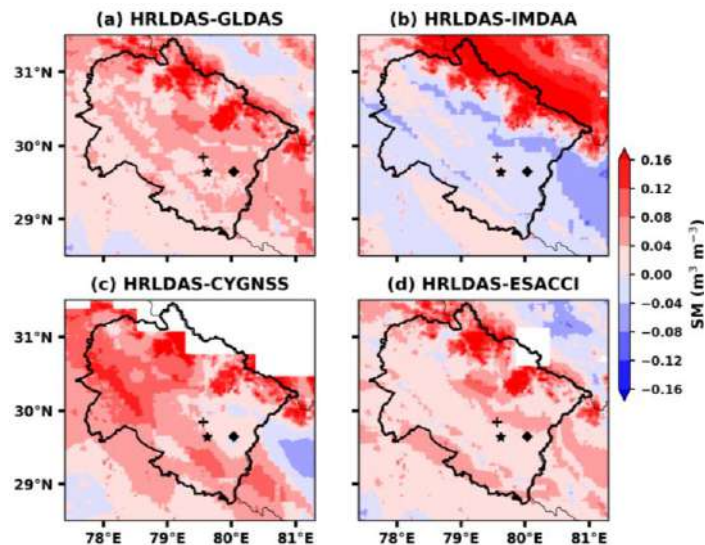


Figure 14. Monsoon season SM bias from GLDAS, IMDAA, CYGNSS and ESACCI from 2017 to 2020. Location of observational sites, Kosi-Katarmal marked by black star, Kantali marked Red Cross, and marked by diamond.

The HRLDAS model exhibited positive bias and similar patterns with GLDAS and ESACCI analysis. High elevation regions bias is 0.12 to $0.16 \text{ m}^{-3} \text{ m}^{-3}$ and low elevations regions bias if 0 to $0.04 \text{ m}^{-3} \text{ m}^{-3}$ with GLDAS and ESACCI. The HRLDAS model SM is dry bias (0 to $-0.08 \text{ m}^{-3} \text{ m}^{-3}$) in most of the regions and high elevations regions wet bias ($>0.12 \text{ m}^{-3} \text{ m}^{-3}$) with IMDAA. The comparison between the HRLDAS with the CYGNSS shows the most of the regions wet bias (0.04 to $0.12 \text{ m}^{-3} \text{ m}^{-3}$). Nevertheless, the ESACCI and GLDAS datasets exhibit lower bias compared to IMDAA and CYGNSS. The HRLDAS model performance relatively better with ESACCI and GLDAS than IMDAA and CYGNSS. These results are consistent with previous studies (Ankur et al., 2021).

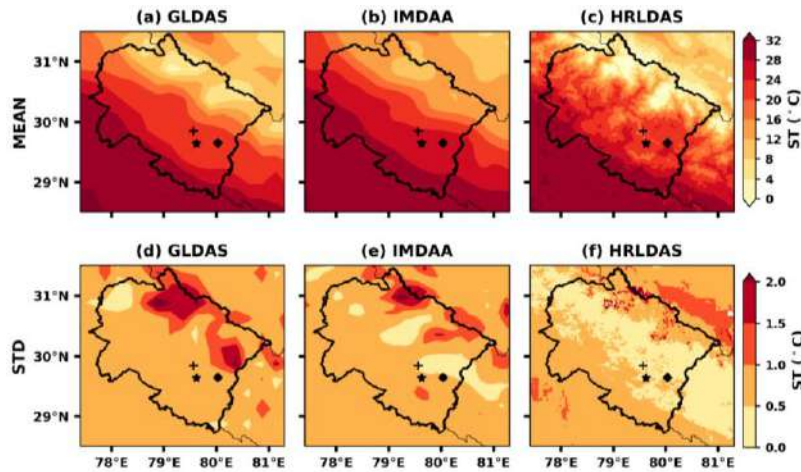


Figure 15. Seasonal distribution of mean ST from GLDAS, HRLDAS and HRLDAS (a-c). d-f same as a-c but the standard deviation (STD) from 2011-2020.

Figure 15 depicts the spatial distribution of seasonal mean ST and standard deviation (STD) derived from GLDAS, IMDAA and HRLDAS. The spatial distribution of ST in monsoon season significant variations from south to northern parts among the all products (Figure 15a-c). The GLDAS, IMDAA and HRLDAS analysis indicates similar temperatures in southern part of Uttarakhand. The northern parts of Uttarakhand experience lower ST compared to the central and southern parts, as shown in GLDAS, IMDAA and HRLDAS. The surface temperature of a specific geographic region varies based on altitude and location relative to geographical features like water bodies (such as lakes, rivers, or seas) and mountains (Banerjee et al., 2020). The GLDAS, IMDAA and HRLDAS show minimum ST of $0-8 \text{ }^{\circ}\text{C}$, $8-12 \text{ }^{\circ}\text{C}$ and $-4-4 \text{ }^{\circ}\text{C}$ respectively (Figure 15a-c). The maximum whereas the peak ST value in these datasets are around 28 to $32 \text{ }^{\circ}\text{C}$ in southern part of foot hills of Himalaya region (Figure 15a-c). The patterns of STD in monsoon season are similar between GLDAS, IMDAA and HRLDAS, as shown in Figure 15c-d. The maximum STD in the northern parts of Uttarakhand region is around 1 to $2.5 \text{ }^{\circ}\text{C}$ in GLDAS and IMDAA, and 0.5 to $1.5 \text{ }^{\circ}\text{C}$ in HRLDAS. HRLDAS performs better in capturing the spatial patterns of ST, especially in areas with complex terrain and heterogeneous land cover. Additionally, HRLDAS exhibits better agreement with observed soil temperature at individual site levels than GLDAS.

Conclusions

The HRLDAS has shown a reasonable skill in simulating SM, ST over the Uttarakhand region. High resolution could provide realistic heterogeneity in the land surface conditions, which are important to trigger atmospheric convection.

References

Ankur, K., Nadimpalli, R., & Osuri, K. K. (2021). Evaluation of Regional Land Surface Conditions Developed Using The High-Resolution Land Data Assimilation System (HRLDAS) with Satellite and Global Analyses Over India. *Pure and Applied Geophysics*, 178(4), 1405-1424. <https://doi.org/10.1007/s00024-021-02698-y>.

Basistha, A., Arya, D. S., & Goel, N. K. (2009). Analysis of historical changes in rainfall in the Indian Himalayas. *International Journal of Climatology*, 29(4), 555-572. <https://doi.org/10.1002/joc.1706>.

Charusombat, U., Niyogi, D., Garrigues, S., Olioso, A., Marloie, O., Barlage, M., et al, (2012). Noah-GEM and Land Data Assimilation System (LDAS) based downscaling of global reanalysis surface fields: Evaluations using observations from a CarboEurope agricultural site. *Computers and electronics in agriculture*, 86, 55-74. <https://dx.doi.org/10.1016/j.compag.2011.12.001>.

Chen, F., & Dudhia, J. (2001). Coupling an advanced land surface–hydrology model with the Penn State–NCAR MM5 modeling system. Part I: Model implementation and sensitivity. *Monthly weather review*, 129(4). [https://doi.org/10.1175/1520-0493\(2001\)129<0569:CAALSH>2.0.CO;2](https://doi.org/10.1175/1520-0493(2001)129<0569:CAALSH>2.0.CO;2).

Chen, L., Li, Y., Chen, F., Barlage, M., Zhang, Z., & Li, Z. (2019). Using 4-km WRF CONUS simulations to assess impacts of the surface coupling strength on regional climate simulation. *Climate Dynamics*, 53(9), 6397-6416. <https://doi.org/10.1007/s00382-019-04932-9>.

Chew, C. C., & Small, E. E. (2018). Soil moisture sensing using spaceborne GNSS reflections: Comparison of CYGNSS reflectivity to SMAP soil moisture. *Geophysical Research Letters*, 45(9), 4049-4057. <https://doi.org/10.1029/2018GL077905>.

Dimri, A. P. (2012). Wintertime land surface characteristics in climatic simulations over the western Himalayas. *Journal of earth system science*, 121(2), 329-344. <https://doi.org/10.1007/s12040-012-0166-x>.

Ek, M. B., Mitchell, K. E., Lin, Y., Rogers, E., Grunmann, P., Koren, V., et al. (2003). Implementation of Noah land surface model advances in the National Centers for Environmental Prediction operational mesoscale Eta model. *Journal of Geophysical Research: Atmospheres*, 108(D22). <https://doi.org/10.1029/2002JD003296>.

Gelaro, R., McCarty, W., Suárez, M. J., Todling, R., Molod, A., Takacs, L., et al. (2017). The Modern-era retrospective analysis for research and applications, version 2 (MERRA-2). *Journal of Climate*, 30(14), 5419–5454. <https://doi.org/10.1175/JCLI-D-16-0758.1>.

Hong, S., Yu, X., Park, S. K., Choi, Y. S., & Myoung, B. (2014). Assessing optimal set of implemented physical parameterization schemes in a multi-physics land surface model using genetic algorithm. *Geoscientific Model Development*, 7(5), 2517-2529. <https://doi.org/10.5194/gmd-7-2517-2014>

- Huffman, G. J., Bolvin, D. T., Braithwaite, D., Hsu, K., Joyce, R., Xie, P., & Yoo, S. H. (2015). NASA global precipitation measurement (GPM) integrated multi-satellite retrievals for GPM (IMERG). Algorithm Theoretical Basis Document (ATBD) Version, 4(26).
- Koster, R. D., Dirmeyer, P. A., Guo, Z., Bonan, G., Chan, E., Cox, P., et al. (2004). Regions of strong coupling between soil moisture and precipitation. *Science*, *305*(5687), 1138-1140.
- Li, H., Chen, R., Han, C., & Yang, Y. (2022). Evaluation of the Spatial and Temporal Variations of Condensation and Desublimation over the Qinghai–Tibet Plateau Based on Penman Model Using Hourly ERA5-Land and ERA5 Reanalysis Datasets. *Remote Sensing*, *14*(22), 5815.
- Liu, Y. Y., Dorigo, W. A., Parinussa, R. M., de Jeu, R. A., Wagner, W., McCabe, M. F., et al. (2012). Trend-preserving blending of passive and active microwave soil moisture retrievals. *Remote Sensing of Environment*, *123*, 280-297. <https://doi.org/10.1016/j.rse.2012.03.014>
- Liu, Y. Y., Parinussa, R. M., Dorigo, W. A., De Jeu, R. A., Wagner, W., Van Dijk, A. I. J. M., et al. (2011). Developing an improved soil moisture dataset by blending passive and active microwave satellite-based retrievals. *Hydrology and Earth System Sciences*, *15*(2), 425-436. <https://doi.org/10.5194/hess-15-425-2011>.
- Ma, N., Niu, G. Y., Xia, Y., Cai, X., Zhang, Y., Ma, Y., & Fang, Y. (2017). A systematic evaluation of Noah-MP in simulating land-atmosphere energy, water, and carbon exchanges over the continental United States. *Journal of Geophysical Research: Atmospheres*, *122*(22), 12-245.
- Mukherjee, S., Joshi, R., & Kumar, K. (2018a). Meteorological monograph: Compendium of meteorological data 2012-2016 of Kosi-Katarmal, Almora, Utrakhand, field station: Part I, GBPNIHESD, pp70, ISBN: 978-93-5346-136-2.
- Mukherjee, S., Lohani, P., Kumar, K., Chowdhuri, S., Prabhakaran, T., & Karipot, A. K. (2020). Assessment of new alternative scaling properties of the convective boundary layer: application to velocity and temperature spectra. *Boundary-Layer Meteorology*, *176*(2), 271-289. <https://doi.org/10.1007/s10546-020-00525-w>.
- Mukherjee, S., Sekar, K. C., Lohani, P., Kumar, K., Patra, P., & Ishijima, K. (2018b). Investigation of scale interaction between rainfall and ecosystem carbon exchange of Western Himalayan Pine dominated vegetation. *Biogeosciences Discussions*, 1-23. <https://doi.org/10.5194/bg-2018-299>.
- Muñoz-Sabater, J., Dutra, E., Agustí-Panareda, A., Albergel, C., Arduini, G., Balsamo, G., et al. (2021). ERA5-Land: A state-of-the-art global reanalysis dataset for land applications. *Earth System Science Data*, *13*(9), 4349-4383. <https://doi.org/10.5194/essd-13-4349-2021>.
- Nair, A. S., & Indu, J. (2019). Improvement of land surface model simulations over India via data assimilation of satellite-based soil moisture products. *Journal of Hydrology*, *573*, 406-421.
- Nayak, H. P., Osuri, K. K., Sinha, P., Nadimpalli, R., Mohanty, U. C., Chen, F., et al. (2018). High-resolution gridded soil moisture and soil temperature datasets for the Indian monsoon region. *Scientific data*, *5*(1), 1-17. <https://doi.org/10.1038/sdata.2018.264>
- Osuri, K. K., Nadimpalli, R., Ankur, K., Nayak, H. P., Mohanty, U. C., Das, A. K., & Niyogi, D. (2020). Improved simulation of monsoon depressions and heavy rains from direct and indirect initialization of soil

moisture over India. *Journal of Geophysical Research: Atmospheres*, 125(14), e2020JD032400. <https://doi.org/10.1029/2020JD032400>

Osuri, K. K., Nadimpalli, R., Mohanty, U. C., Chen, F., Rajeevan, M., & Niyogi, D. (2017). Improved prediction of severe thunderstorms over the Indian Monsoon region using high-resolution soil moisture and temperature initialization. *Scientific Reports*, 7(1), 1-12. <https://doi.org/10.1038/srep41377>

Pielke Sr, R. A., Pitman, A., Niyogi, D., Mahmood, R., McAlpine, C., Hossain, F., et al. (2011). Land use/land cover changes and climate: modeling analysis and observational evidence. *Wiley Interdisciplinary Reviews: Climate Change*, 2(6), 828-850. <https://doi.org/10.1002/wcc.144>

Rajesh, P. V., Pattnaik, S., Rai, D., Osuri, K. K., Mohanty, U. C., & Tripathy, S. (2016). Role of land state in a high resolution mesoscale model for simulating the Uttarakhand heavy rainfall event over India. *Journal of Earth System Science*, 125(3), 475-498. <https://doi.org/10.1007/s12040-016-0678-x>

Rani, S. I., Arulalan, T., George, J. P., Rajagopal, E. N., Renshaw, R., Maycock, A., et al. (2021). IMDAA: High-resolution satellite-era reanalysis for the Indian monsoon region. *Journal of Climate*, 34(12), 5109-5133. <https://doi.org/10.1175/JCLI-D-20-0412.1>

Rawat, R., Lepcha, S., Pande, D., Bhatt, N., and Pant, M.: Uttarakhand Forest Statistics 2012-13, Department of Forest: Uttarakhand, 2011.

Rodell, M., Houser, P. R., Jambor, U. E. A., Gottschalck, J., Mitchell, K., Meng, C. J., et al. (2004). The global land data assimilation system. *Bulletin of the American Meteorological society*, 85(3), 381-394. <https://doi.org/10.1175/BAMS-85-3-381>

Singh, J. S., & Singh, S. P. (1987). Forest vegetation of the Himalaya. *The Botanical Review*, 53(1), 80-192. <https://doi.org/10.1007/BF02858183>

Vinodhkumar, B., Jose, A. M., Rao, K. K., Osuri, K. K., Bhaduri, R., & Dimri, A. P. (2022). Future precipitation extremes over base Himalayan Uttarakhand region: analysis using the statistically downscaled, bias-corrected high-resolution NEX-GDDP datasets. *Theoretical and Applied Climatology*, 1-15. <https://doi.org/10.1007/s00704-022-04111-7>

Wagner, W., Dorigo, W., de Jeu, R., Fernandez, D., Benveniste, J., Haas, E., & Ertl, M. (2012). Fusion of active and passive microwave observations to create an essential climate variable data record on soil moisture. *ISPRS Annals of the Photogrammetry, Remote Sensing and Spatial Information Sciences (ISPRS Annals)*, 7, 315-321. [10.5194/isprsannals-I-7-315-2012](https://doi.org/10.5194/isprsannals-I-7-315-2012).

Wei, M. Y. (Ed.). (1995). *Soil moisture: Report of a workshop held in Tiburon, California, 25-27 January 1994* (Vol. 3319). NASA Headquarters.

Xue, Y., Fennessy, M. J., & Sellers, P. J. (1996). Impact of vegetation properties on US summer weather prediction. *Journal of Geophysical Research: Atmospheres*, 101(D3), 7419-7430.

Xue, Y., Houser, P. R., Maggioni, V., Mei, Y., Kumar, S. V., & Yoon, Y. (2019). Assimilation of satellite-based snow cover and freeze/thaw observations over high mountain Asia. *Frontiers in earth science*, 7, 115. <https://doi.org/10.3389/feart.2019.00115>

You, Y., Huang, C., Yang, Z., Zhang, Y., Bai, Y., & Gu, J. (2020). Assessing Noah-MP parameterization sensitivity and uncertainty interval across snow climates. *Journal of Geophysical Research: Atmospheres*, 125(4). <https://doi.org/10.1029/2019JD030417>

Zhang, Z., Li, Y., Chen, F., Barlage, M., & Li, Z. (2020). Evaluation of convection-permitting WRF CONUS simulation on the relationship between soil moisture and heatwaves. *Climate Dynamics*, 55(1), 235-252. <https://doi.org/10.1007/s00382-018-4508-5>.

3.2.5. Assessment of eco-hydro-climatological processes with information theory-based process network and understanding resilience under shock.

Micrometeorological drivers affecting the variability of carbon uptake in the Himalayan Oak and Pine dominated ecosystems: An assessment of causal relationships (Under review, *Journal of hydrology*)

The present study investigates the carbon uptake potentials of the Oak and Pine ecosystems of the Himalayas and their linkages to micro-meteorological variables by generating process networks using half-hourly flux tower data considering the maximum memory of 06 hours. We considered the memory of 6 hours to account for the four different phases of the diurnal cycle. The selection of the study period (Table 1C) is based on the continuously available data of all variables obtained from the flux tower (Fig. 1). The networks are generated for the monsoon and post-monsoon seasons of 2016-17, i.e., JJA- 2016, SO - 2016, JJA - 2017, and SO - 2017 (7 weeks/season i.e., 49 days/season i.e., 2352 data points/season).

Variability amongst eco-hydro-meteorological variables

Initially, the sub-daily scale variability of carbon uptake and its impact on weekly and seasonal scale fluctuation is investigated. Fig. 1 illustrates the sub-daily scale variations of NEE for Oak and Pine ecosystems for four selected seasons. We visually observed through the vertical spread of the data points that, in JJA, the NEE variations for Oak are higher than for Pine. During post-monsoon (SO), the variations of NEE are not very different among the ecosystems. The variability contribution (VC) of sub-daily scale processes significantly controls the within-week variability; therefore, the present study generates the process networks on a weekly scale using half-hourly data. Fig. 1 (c, d) represents the VC (within 6 hours) of NEE and LH to the intra-week variability for 7 weeks of every season. During VC estimation, first, we generated the new time series of the 6-hour moving mean. Further, we subtracted the newly generated time series from the original data to get the high-frequency variations. Then we calculated the ratio of the variance of these high-frequency variations to the variance of original data to obtain the VC within each week. The VC from sub-daily to sub-weekly varies between 25-80 % (Fig.1c) for NEE, and 20-70% (Fig.1d) for LH. Most of the time, the NEE of Pine has high VC than Oak. On the contrary, LH shows opposite patterns.

The weekly variations of NEE, TA, SH, WS, P, NSR, VPD, LH, and RH for the Oak (blue) and Pine (red) ecosystems of the Himalayas for four seasons are presented in Figs. 2 (a to i). The negative values of NEE imply carbon absorption by the ecosystem, whereas the positive NEE denotes the carbon released by the ecosystem.

Fig.2a shows that in JJA 2016, the maximum NEE (carbon uptake) corresponding to Oak and Pine are $-2.95 \mu \text{ mol/m}^2/\text{s}$ and $-5.67 \mu \text{ mol/m}^2/\text{s}$, respectively. Besides, in JJA 2017, the maximum NEE associated with Oak and Pine were $-6.06 \mu \text{ mol/m}^2/\text{s}$ and $-7.99 \mu \text{ mol/m}^2/\text{s}$, respectively. On the other hand, no clear demarcation was observed regarding the carbon uptake in Oak and Pine ecosystems in SO 2016 and SO 2017. Hence, the results highlight the higher carbon absorption potential of Pine as compared to Oak in the monsoon season. This is because Pine trees have a higher photosynthetic capacity and can grow faster, which leads to greater carbon sequestration. Additionally, Pine forests are more efficient in terms of water use and can tolerate drier conditions than Oak forests. However, Oak forests are also important carbon sinks and have been found to have significant carbon sequestration potential. Interestingly, the TA of Pine is consistently more in JJA of both years, whereas in post-monsoon (SO), the TA of both ecosystems are more or less the same (Fig.1b). The Oak and the Pine sites are located only 43 km apart; hence, there is no major difference in the synoptic meteorological variables across the sites (Fig.1b, i). High TA in the Pine system increases the NEE during the monsoon (Fig.1b). Variables such as SH, P, NSR, VPD, WS, LH and RH vary depending on the seasons. Their individual and collective influences on the ecosystem dynamics are unclear from the weekly time-series (Fig.1c, e, f, g, h, i).

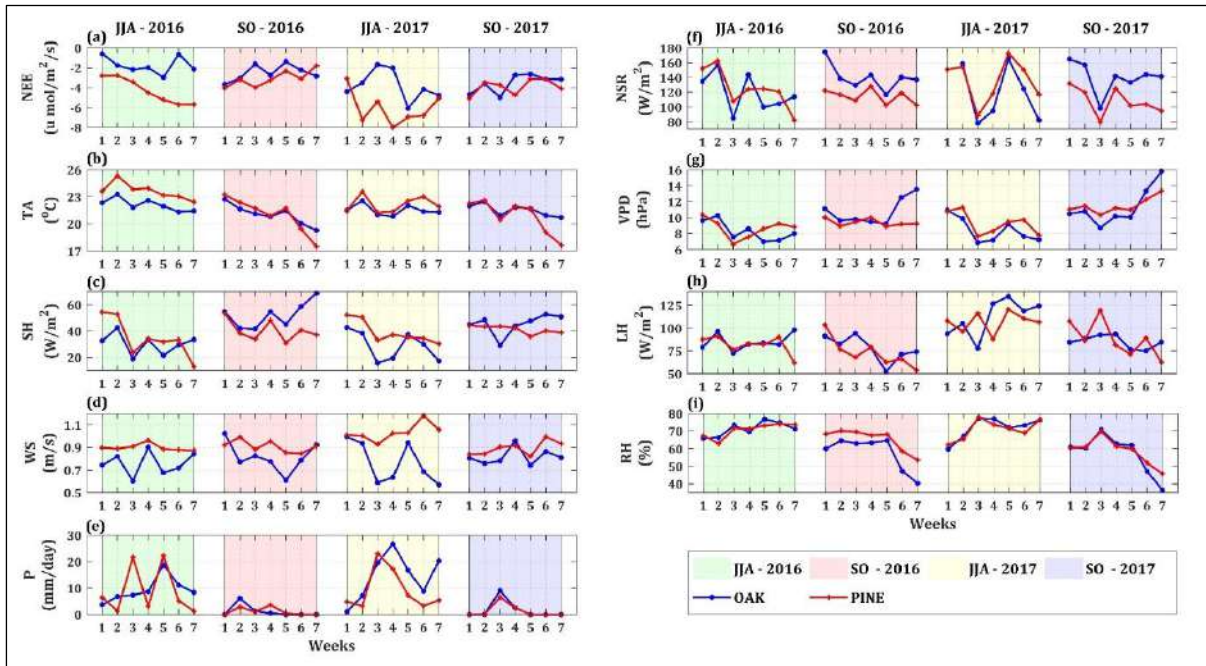


Fig. 1. Weekly time series of Oak and Pine ecosystems for NEE, TA, SH, WS, P, NSR, VPD, LH, and RH. The X-axis indicates the weeks (7 weeks/season), and Y-axis implies the quantity accompanying the corresponding variable. Blue and red color lines denote the time series of Oak and Pine. The color fill indicates the study seasons as green – JJA 2016, red – SO 2016, yellow – JJA 2017, and blue – SO 2017

Mutual information (MI) and transfer entropy (TE)

The MI denotes the real-time interaction among the eco-hydro-meteorological variables without the direction of information transfer. To capture the sub-daily scale variations, we generated the process networks at a weekly scale. The MI of consistent links (appearing $>60\%$ i.e. >4 out of 7 weeks in a season) appear for Oak and Pine in JJA and SO of 2 years (supplementary Fig.4). We observed that the P and NEE consistently interacted with each other in the Oak ecosystem, in JJA of 2016 and 2017. Besides, links between RH and NEE are present in SO of

2016 - 2017, showing the importance of VPD during the post-monsoon season. Overall, the strong and consistent connections (> 60% i.e. > 4 out of 7 weeks) among, P, RH, SH, VPD, TA, and NSR consistently appeared in the Oak network. On the other hand, P is not sharing consistent links with NEE in the Pine ecosystem at 06-hour memory. There is a possibility that the ecosystem may be experiencing the influence of P at higher memory beyond 06 hours (Lohani et al., 2023).

The transfer entropy (TE) indicates the uni-directional flow of information transferred from source to target variables representing a possible causal flow. In Fig.2, the lower hemisphere represents the source variables, and the upper hemisphere denotes the targets. The TE links in the subplots appear more than 60% in a season for the Oak and Pine ecosystems. The TE network of Oak (Fig.2a) illustrates the links originating from P, RH, VPD, TA, and NSR towards the target NEE and LH. It has been observed that P is sending consistent links to NEE and LH in JJA of both years at the Oak site, indicating the impact of P within the memory of 06 hours. The consistent links from P show the immediate effect of the variability of P on the Oak ecosystem dynamics. The consistent 06 hourly links between P and NEE for the Oak ecosystem could be attributed to the higher production of fine roots in the Oak trees leading to faster response to rainfall moisture gain (Usman et al. 1997). The RH played a dominant role in SO 2016, JJA 2017, and SO 2017, representing atmospheric moisture's role in controlling the NEE. RH can be considered a proxy for VPD because of their inverse relationship. Hence, links generated from RH to NEE show the role of VPD. Additionally, the TA shows the TE link in SO 2016, which also reflects the role of VPD in the ecosystem. The role of VPD is prominent from the direct links generated from it. Overall, the Oak ecosystem network shows the dominance of moisture within a short memory as it establishes significant connections in the presence of moisture-governing variables.

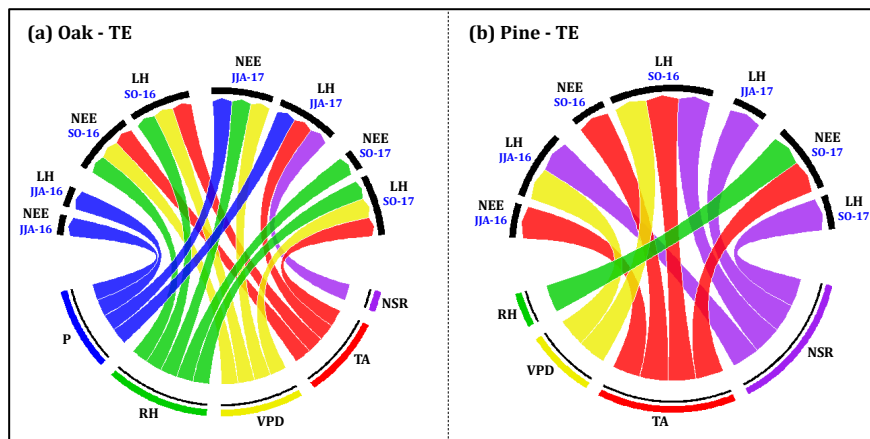


Fig. 2. Transfer entropy (TE), Unique (U), and Synergistic (S) information networks considering the consistent links occurring more than 60% of times in one season. Figure 3 (a) and (b) imply the TE networks in which the bottom semicircle indicates the panel of source variables and the top semicircle denotes the set of target variables. The blue, green, yellow, red, and purple color links refer to the links shared by source variables P, RH, VPD, TA, and NSR.

The consistently appearing TE links (> 60%) in the Pine ecosystem networks are represented in Fig.2b. RH, VPD, TA, and NSR are the active variables that significantly impact the Pine ecosystem. In all seasons of 2016,

and 2017, the TA and NSR are the highly active variables in which the TA influences the target NEE, and NSR impacts the LH. Such links from TA and NSR are expected. Surprisingly the role of VPD and P on NEE is not evident from the network of Pine ecosystems (Fig.2b), probably suggesting that the two major vegetation stressors, low P and high VPD do not have their impacts on Pine vegetation within a short memory of 6 hours. Their impacts are probably visible when a long memory is considered. VPD has its impacts only on LH in JJA and SO in 2016. These observations indicate that the Pine ecosystem is heat-dominating because TA and NSR generate significant and consistent TE links towards NEE in the seasons considered.

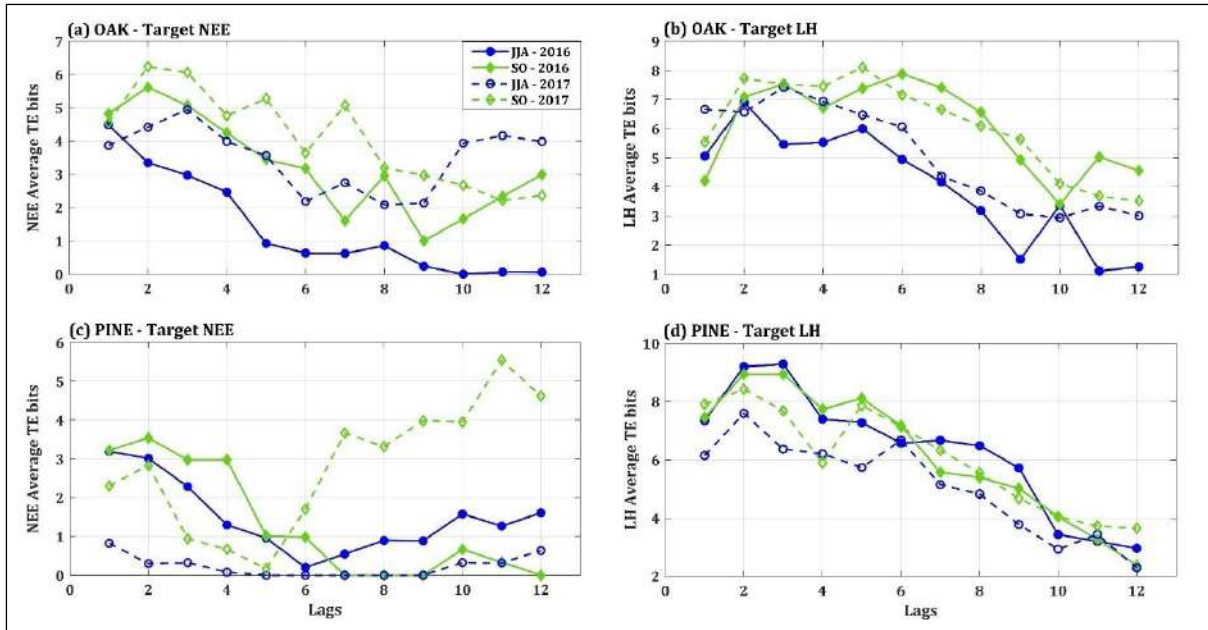


Fig.3. Average TE bits information of Oak and Pine networks at different lags for NEE (a, c) and LH (b, d). The blue color indicates the JJA season, and the green color denotes SO. The Solid and dashed lines represent 2016 and 2017, respectively

To assess the role of system memory in directing the variation of TE at different lags (till 12 lags – 06 hours), we plotted the average TE bits information of Oak and Pine networks. Fig. 3(a, c, and b, d) shows the TE bits from different source variables to NEE and LH at different lags, respectively. The TE bits reaching NEE and LH reduce with increasing lags for the Oak ecosystem (Fig.3a, b) suggesting that the Oak ecosystem variables are more real-time connected. For the Pine ecosystem, such a clear association between TE bits and lags is not prominent. In general, the TE bits reaching NEE increase after 5 lags, i.e., 2.5 hours, signifying the dominant role of memory (Fig. 3c). Chauhan and Ghosh (2021) also reported that memory-based connections of ecohydrological networks are higher for ecosystems of the western Himalayas in comparison to the entire Indian Himalayan Region. Additionally, the study showed that monsoon season is mostly driven by real-time associations and post-monsoon is dominated by memory-based connection. Our results also show a significant number of lagged links in the post-monsoon season which depicts the role of memory-based association. In the case of LH, the NEE TE bits reduce with the lag (Fig. 3d). This shows that LH receives mostly real-time links in the Pine ecosystem like the Oak ecosystem.

Rainfall sensitivity of Oak and Pine ecosystem

Studies across many ecosystems have established that rainfall spell and amount within a season can control the exchanges of carbon and water between the biosphere and atmosphere (Hao et al., 2013, 2017; Huxman et al., 2004; Potts et al., 2006), however, nature of causal linkages between ecosystem carbon exchange and rainfall are rarely investigated at sub-daily scale and for dry and wet spells. Here, we illustrate the rainfall sensitivity experienced by the Oak and Pine-dominated ecosystems by generating the TE networks of maximum and minimum/zero rainfall week (Fig. 4a, b, c, d). The bottom hemisphere denotes the source variables, and the top hemisphere indicates the target NEE and LH.

The seasonally representative networks based on link appearance help identify the consistent/dominant links in the ecosystem, whereas the independent/weekly networks represent the dynamics involved in the corresponding week. Figure 4 provides the general impression that under moisture-stressed dry conditions, the ecosystem generates more links among hydrometeorological and vegetation variables to resist stresses. Such observations were also found in Budakoti et al., (2020) and Scheffer et al., (2012). For both dry and wet weeks, links do not generate from P to NEE for the Pine ecosystem within 6 hours of memory. We observed links from P to NEE for the Oak ecosystem, but not consistently for both high and low rainfall weeks in all seasons. For the Oak ecosystem, VPD plays a major role in the low rainfall weeks, whereas its role is not prominent in high rainfall weeks. VPD results in increased atmospheric water demand, hence, stress on plants for low rainfall and water-limiting conditions. It is not so prominent for Pine, which could be because of lesser fine roots. The other reason could be that such anomalies were detected through the links generated from TA, not from VPD for Pine. In dry weeks, TA generates a significant number of links to LH. It is imperative to note that P, RH, WS, VPD, and TA significantly influence a generation of variations in the NEE of the Oak system. On the other hand, RH, WS, SH, VPD, TA, and NSR are primary contributors to the network formation during the dry condition of the Pine network. The results show that the dry/stressed state forms more TE links than the wet condition of both ecosystems, representing significant interactions amongst ecosystem variables.

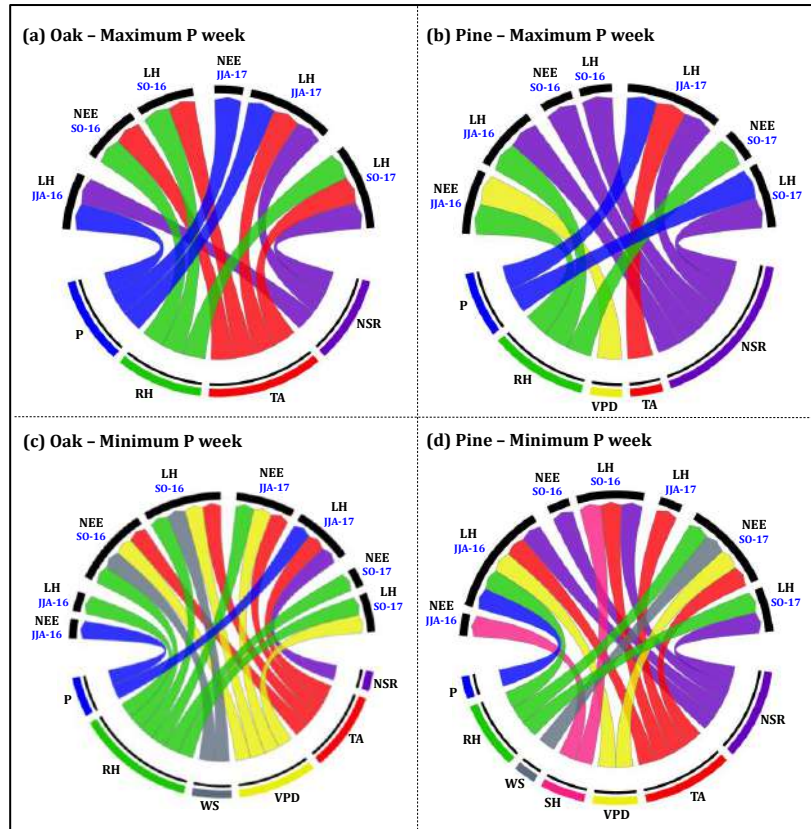


Fig.4. Rainfall sensitivity by considering the wet and dry weeks. Figures (a) and (b) indicate TE links generated in the maximum, and figures (c) and (d) implies the minimum P weeks of the Oak and Pine ecosystem. The links generated from variables P, RH, WS, SH, VPD, TA, and NSR are blue, green, grey, pink, yellow, red, and purple.

In Fig. 4 bars show the number of links received by target NEE (Fig. 4a, b) and LH (Fig. 4c, d) and the line plot indicates the P variation in corresponding weeks. The number of links received by the target NEE is high when the Oak ecosystem experiences less P in JJA of 2016 and 2017 (Fig. 5a). This indicates that the Oak networks are generating more TE links in water-stressed conditions. In Pine networks, this observation is valid only in JJA 2017; however in JJA 2016 we could find a significant number of links irrespective of the amount of P received (Fig. 4b). This attributes to high variability in the causal meteorological factors across weeks with a lack of consistency in the season. The variation in the number of TE links received by the target LH and P is not well followed (Fig. 4c, d) for both ecosystems. In both ecosystems, a significant number of links are generated in all seasons. The total TE bits information presents the sum of TE generated in both ecosystems' networks in all seasons (right panel - Fig. 4). Whenever the bits information in the network is high, the corresponding number of TE links is also higher (left panel, Fig. 4). Overall, in Oak ecosystem, P creates a significant impact in generating TE links, however, this pattern is not well followed in Pine ecosystem. This indicates higher dependence of the Oak ecosystem on P at a sub-daily scale.

Conclusions

The Himalayan ecosystems are susceptible to increasing weather extremes and show high sub-daily scale variability. Using an information theory-based TIPNet framework, we identified the dominant causal drivers of

NEE in the Himalayan Oak and Pine-dominated ecosystems. We used the half-hourly flux tower data to develop the weekly process networks for the monsoon and post-monsoon seasons. The key conclusions are:

1. In the monsoon (JJA) season P, RH, and VPD are the main causal variables driving NEE in the Oak ecosystem, however, in post-monsoon (SO) the NEE is driven mostly by RH. Whereas, the Pine ecosystem is primarily modulated by TA which controls the ecosystem processes. Hence, we conclude that the Oak is moisture-driven and Pine is heat dominating ecosystem.
2. The Oak and Pine forests are important carbon sinks, however, Pine trees have more carbon sequestration than Oak. It is because Pine forests can tolerate drier conditions.
3. P is an important causal variable in the Oak, however, its impact is not visible in the Pine ecosystem within a short memory of 06 hours. This could be attributed to Oak trees having high annual fine-root production and these fine roots accelerate the extraction of water. Therefore, the Oak ecosystem responds to P faster than Pine ecosystems on a 6-hourly scale. Nevertheless, P might be sharing the links in the Pine ecosystem at higher memory and such signatures are reported by Lohani et al. (2023) when the impact of daily rainfall spells and amount on NEE of the Pine ecosystem was investigated.
4. In moisture-stressed/dry weeks, we observed more TE links than in wet weeks for both ecosystems. The causal variables such as TA, RH, WS, and VPD prominently influence the ecosystems in dry weeks.

References

Chauhan, T. and Ghosh, S., 2020. Partitioning of memory and real-time connections between variables in Himalayan ecohydrological process networks. *Journal of Hydrology*, 590, p.125434. <https://doi.org/10.1016/j.jhydrol.2020.125434>

Das, S., Deb, S., Sahoo, S.S. and Sahoo, U.K., 2023. Soil microbial biomass carbon stock and its relation with climatic and other environmental factors in forest ecosystems: A review. *Acta Ecologica Sinica*. <https://doi.org/10.1016/j.chnaes.2022.12.007>

Gao, Y., Jia, J., Lu, Y., Yang, T., Lyu, S., Shi, K., Zhou, F. and Yu, G., 2021. Determining dominating control mechanisms of inland water carbon cycling processes and associated gross primary productivity on regional and global scales. *Earth-Science Reviews*, 213, p.103497. <https://doi.org/10.1016/j.earscirev.2020.103497>

Goodwell A E and Kumar P 2017a Temporal Information Partitioning Networks (TIPNets): A process network approach to infer ecohydrologic shifts. *Water Resources Research*, 53(7), pp.5899-5919. <https://doi.org/10.1002/2016WR020218>

Goodwell A E and Kumar P 2017b Temporal information partitioning: Characterizing synergy, uniqueness, and redundancy in interacting environmental variables. *Water Resources Research*, 53(7), pp.5920-5942. <https://doi.org/10.1002/2016WR020216>

Goodwell A E, Kumar P, Fellows A W and Flerchinger G N 2018 Dynamic process connectivity explains ecohydrologic responses to rainfall pulses and drought. *Proceedings of the National Academy of Sciences*, 115(37), pp.E8604-E8613. <https://doi.org/10.1073/pnas.1800236115>

Grossiord, C., Buckley, T.N., Cernusak, L.A., Novick, K.A., Poulter, B., Siegwolf, R.T., Sperry, J.S. and McDowell, N.G., 2020. Plant responses to rising vapor pressure deficit. *New Phytologist*, 226(6), pp.1550-1566. <https://doi.org/10.1111/nph.16485>

Naudiyal, N. and Schmerbeck, J., 2017. The changing Himalayan landscape: pine-oak forest dynamics and the supply of ecosystem services. *Journal of Forestry Research*, 28, pp.431-443. <https://doi.org/10.1007/s11676-016-0338-7>

3.3. Conclusion of the study (max. 500 words in bullets)

The overall inference of this study indicates that *P. roxburghii* dominated ecosystems are better sink of carbon at the cost of higher loss of surface and ground water, consequently, *Q. leucotrichophora* dominated ecosystems are better for soil and water conservation as envisaged by the traditional knowledge. The initial findings of the project would be useful in providing scientific basis to the plantation and conservation strategies for Pine-Oak forests of central Himalaya. Moreover, the novel research insights would provide the baseline data to undertake qualitative/quantitative analyses of water-climate-biodiversity dynamics in the Central Himalayan Pine-Oak system. Furthermore, long term monitoring and conservations of identified Oak forests in near future would be useful in combating the climate change impact on carbon and water of the region.

4. OVERALL ACHIEVEMENTS – supporting documents to be attached.

4.1. Achievement on Project Objectives/ Target Deliverables (max. 500 words)

Quantifiable Deliverables*	Monitoring Indicators*	Quantified Output/ Outcome achieved	Deviations, if any, & Remarks thereof:
Assessment reports on Pine and Oak transpiration rates of Himalaya linking with water balance and recharge of ground water/springs (3 representative sites)	Database on Pine and Oak transpiration rates (Nos.)	Transpiration data for Pine (Particularly, <i>Pinus roxburghii</i>) and 2 Oak species (Particularly, <i>Quercus leucotrichophora</i> and <i>Quercus glauca</i>) is available from Nov, 2020 to 31 st , March, 2023.	A manuscript on comparative estimates of transpiration and their links with micro-met parameters is under preparation.
New hydro-meteorological database of two (02) watersheds in three (03) IHR States in GIS format;	Hydro-meteorological database (No.) Number of spring Geo-tagged (nos.)	<ul style="list-style-type: none"> • 10 Hz carbon and water flux data is available for the duration of 1-Jan-2014 to dec, 2022 for Pine dominated forest. • 10 Hz carbon and water flux data is available for the duration of 22-April-2016 to till date for Oak dominated forest in Gangolihat, Pithoragarh, Uttarakhand with data gaps. • A total of 18 springs are geo-tagged at Shiltakhet region. 	Hydro-met watershed is developed for Kosi and Hat-Kalika watersheds.
High-resolution land and climate model products (1970 - 2099);	Climate Model products (Nos.)	<ul style="list-style-type: none"> • Noah-MP, a new generation of LSM, simulations are 	NA

		<p>generated for ST, SM, and energy fluxes and compared with the <i>in-situ</i> observations for 2011-2021.</p> <ul style="list-style-type: none"> High-resolution land data assimilation system (HRLDAS) derived land surface products, including SM and ST, are prepared, such data are not currently available for the Himalaya region. 	
Technical reports on Ecological integrity of two dominant forests;		<ul style="list-style-type: none"> Ecological integrity assessment for two dominant forest types is under progress. 	NA
At least 08 Knowledge products: 04 quality research publications including journal articles, 02 book chapters, and 03 policy briefs.	Reports/Research articles/Policy documents prepared and published (Nos.)	<p>Journal articles:</p> <p>03-published; 02-submitted; 02- under preparation.</p> <p>Book chapters:</p> <p>01-published. 01- Conference abstract compendium.</p> <p>Conference publication:</p> <p>07 - National 04 - International</p> <p>Policy briefs:</p> <p>Under preparation.</p>	NA

4.2. Interventions (max. 500 words)

Dissemination of the knowledge products (Research article and policy brief) generated from the project would be helpful in providing the scientific understanding on water use and carbon sequestration pattern of Himalayan Pine-Oak systems and their responses under changing climate scenario.

4.3.On-field Demonstration and Value-addition of Products, if any (max. 500 words) : A

training cum demonstration programme was organised at GIS, Hawalbagh for school students on the occasion of world water day, 22 march, 2022. The training was organised for on-field demonstration of augmented sensors for water budget estimation and transpiration calculation.

4.4.Green Skills developed in State/ UT (max. 500 words): NIL

4.5.Addressing Cross-cutting Issues (max. 200 words)

The project objectives are aligned with three national missions, namely National Mission on Sustaining Himalayan Ecosystem (NMSHE), National Mission of Himalayan Studies (NMHS) and The National Water Mission (NWM). As The NWM has identified five broad goals related to (i) Comprehensive water data base in public domain and assessment of the impact of climate change on water resource, (ii) Promotion of citizen and state actions for water conservation, augmentation and preservation (iii) Focused attention to vulnerable areas including over-exploited areas, (iv) increasing water use efficiency by 20%, and (v) promotion of basin level integrated water resources management, this project has address most of these goals either explicitly or implicitly.